Investigating the Role of PCSK9 C-terminal Domain in the Regulation of Low-Density Lipoprotein Receptor and Cholesterol Metabolism

by

Shijun Deng

A thesis submitted in partial fulfillment of the requirements for the degree of

Doctor of Philosophy

Medical Sciences - Pediatrics

University of Alberta

Abstract

Atherosclerotic cardiovascular disease (CVD) is the leading cause of death worldwide. Hypercholesterolemia and long-term elevated low-density lipoprotein cholesterol (LDL-C) levels are the major risk factors for the development of atherosclerotic lesions, which can eventually lead to myocardial infarction and many strokes, as well as disabling peripheral artery disease. Lowering LDL-C levels remains the cornerstone of the management of CVD. The LDL receptor (LDLR) in the liver is mainly responsible for the removal of LDL-C from the blood. Proprotein convertase subtilisin/kexin type 9 (PCSK9) regulates cholesterol metabolism by promoting LDLR degradation. An array of pharmaceutical companies has created therapeutic agents to inhibit PCSK9 and block its interaction with LDLR, including PCSK9 monoclonal antibodies and small interfering RNAs. These PCSK9 inhibitors, in combination with existing cholesterol-lowering drug statins, have been shown to significantly reduce circulating LDL-C levels and the risk of CVD in a wide variety of subjects. However, we still face considerable challenges in providing equitable access to this PCSK9 therapy. Studies of the cellular and molecular biology of PCSK9 can provide considerable insight into the development of novel PCSK9 inhibitors with efficacy and cost-effectiveness. This thesis aims to investigate the molecular biology of PCSK9, including the PCSK9 secretory pathway and, upon secretion PCSK9's interaction with LDLR, as well as the molecular mechanism of PCSK9/LDLR lysosomal degradation.

In chapter 3, I investigated the role of the C-terminal domain (CTD) of PCSK9 and SEC24, the cargo adaptor protein of the coated protein complex II (COPII), in PCSK9 maturation and secretion. I found that mutant PCSK9$^{1\text{-}528}$, in which amino acids from 528 to the end (amino acid 692) were deleted, was maturated and secreted from cells as efficiently as

the wild-type protein. Conversely, mutants PCSK9$^{1-446}$, PCSK9$^{1-445}$, and PCSK9$^{1-444}$ that missing amino acids 447-692, 446-692, and 445-692, respectively, all significantly impaired PCSK9 maturation and secretion to a similar extent. Mutant PCSK9$^{1-444}$ essentially eliminated PCSK9 secretion. We also found that natural variants in the CTD, including S462P, S465L, E482G, R495Q and A522T, impaired PCSK9 secretion. Furthermore, knockdown of SEC24A, SEC24B, and SEC24C (not SEC24D) reduced the full-length PCSK9 secretion but had no effect on the secretion of mutant PCSK9$^{1-446}$. Together, these findings demonstrate the critical role of the CTD of PCSK9 and SEC24A, SEC24B, and SEC24C in PCSK9 maturation and secretion.

In chapter 4, I identified the amino acid residues in the ligand-binding repeat domain (LRs) of LDLR important for PCSK9 binding at the cell surface. We have previously shown that, in addition to the epidermal growth factor precursor homology repeat-A (EGF-A) of LDLR, at least three ligand-binding repeats of LDLR are required for PCSK9-promoted LDLR degradation. However, how exactly the LRs contribute to PCSK9's action on the receptor is not completely understood. Here, I found that substitution of Asp at position 172 in the linker between the LR4 and the LR5 of LDLR with Asn (D172N) reduced PCSK9 binding at pH 7.4 (mimic cell surface) but not at pH 6.0 (mimic endosomal environment). On the other hand, mutation of Asp at position 203 in the LR5 of LDLR to Asn (D203N) significantly reduced PCSK9 binding at both pH 7.4 and pH 6.0. These findings indicate that amino acid residues in the LRs of LDLR play an important role in PCSK9 binding to the receptor.

In chapter 5, I used the yeast-two hybrid system to identify the association of the CTD of PCSK9 with prosaposin (PSAP), a secretory and lysosomal protein participating in glycosphingolipid degradation. In this study, I demonstrated that knockdown (KD) of PSAP in cultured hepatoma-derived cells led to significantly elevated cell surface LDLR abundance

and LDL uptake. Further, knockdown of hepatic PSAP by AAV-shRNA increased LDLR levels in the liver and decreased plasma LDL-C levels in the wild-type mice but not the $Ldlr^{-/-}$ mice. Mechanistic studies showed that the effect of PSAP on LDLR was independent of PCSK9. On the other hand, data obtained from confocal microscopy and co-immunoprecipitation revealed a direct interaction between PSAP and LDLR. Further studies are ongoing to address the relevance and cellular mechanism by which PSAP induces LDLR degradation.

In summary, the work performed during this Ph.D. thesis will shed light on the molecular mechanism of PCSK9-promoted LDLR degradation. Yet, continued research promises to provide further progress in the development of PCSK9 inhibitors.

Preface

This thesis is an original work by Shijun Deng. All procedures regarding animal handling, feeding and surgeries were approved by the University of Alberta's Institutional Animal Care Committee in accordance with guidelines of the Canadian Council on Animal Care. The contributions made by the candidate Shijun Deng and co-authors of these studies are described below.

Parts of this thesis have been published and accepted in peer-reviewed journals, listed below in chronological order.

Chapter 4 is a copy of the publication: **Shi-jun Deng**, Adekunle Alabi, Hong-mei Gu, Ayinuer Adijiang, Shucun Qin, and Da-wei Zhang (2019). 'Identification of amino acid residues in the ligand-binding repeats of LDLR important for PCSK9 binding.' *Journal of Lipid Research.* 2019 March; 60(3): 516-527. doi: 10.1194/jlr.M0891193. I conceived and designed the study, performed 90% of experiments, drafted and assisted with editing the article, and generated all figures and tables. D.Z helped to conceive and design the study, interpret data, draft and revise the manuscript for important intellectual content. All authors provided critical feedback and helped shape the research, analysis and manuscript.

Chapter 3 is a manuscript submitted to the journal Biochimica et Biophysica Acta-Molecular and Cell Biology of Lipids as **Shi-jun Deng**, Yishi Shen, Hong-mei Gu, and Da-wei Zhang. 'The role of the C-terminal domain of PCSK9 and SEC24 isoforms in PCSK9 secretion.' I conceived and designed the study, performed 95% of experiments, drafted and assisted with editing the article, and generated all figures and tables. Yishi Shen performed the experiment of 'the effect of natural variants in PCSK9 CTD on its secretion.' D.Z helped to conceive and design the study, interpret data, draft and revise the manuscript for valuable

intellectual content. All authors provided critical feedback and helped shape the research, analysis and paper.

Chapter 5 is in preparation for publication as **Shi-jun Deng**, Hong-mei Gu, and Da-wei Zhang (2019). 'Investigating the role of prosaposin in the regulation of low-density lipoprotein receptor and cholesterol metabolism.' I conceived and designed the study, performed 99% of experiments, drafted and assisted with editing the article, and generated all figures and tables. D.Z helped to conceive and design the study, interpret data, write and revise the manuscript for important intellectual content. All authors provided critical feedback and helped shape the research, analysis and manuscript.

Acknowledgments

First and foremost, I would like to extend infinite thanks to my supervisor Dr. Da-wei Zhang for his constant support, patience, and valuable life and career guidance. I am extremely grateful to have been his student and have learned so much from him. I also would like to thank Mrs. Hong-mei Gu for her guidance, suggestions, and aid from the bench to the desk.

To my supervisory committee (Drs. Richard Lehner, Paul Melancon and Dr. Maria Febbraio), their ongoing assistance, insights and comments were invaluable to my achievement.

I offer my enduring gratitude to all members of the Zhang Laboratory. I always consider myself enormously fortunate to have the opportunity to work with such a knowledgeable and friendly team. They have helped and guided in so many ways that it is hard to put into words. Thank you: Dr. Faqi Wang (Kasa), Adekunle Alabi (Jamal), Yishi Shen, Xiaodan Xia.

I am also thankful to all the faculty, staff and students at the Group on Molecular and Cell Biology of Lipids, and the Department of Pediatrics. Many people assisted me at different moments of this work. I would like to individually thank Drs. Jean Vance, Denis Vance and Serena Wan for scientific and moral support and friendship.

Finally, this thesis is dedicated to my parents and partner for their unconditional support throughout my studies.

Table of Contents

Abstract ..... *ii*
Preface ..... *v*
Acknowledgements ..... *vii*
Lists of Figures ..... *xiii*
Lists of Tables ..... *xv*
List of Abbreviations ..... *xvi*
Chapter 1 ..... *1*
Introduction *1*
Abstract *2*
1.1 Atherosclerotic cardiovascular disease *2*
1.2 Low-density lipoprotein *4*
1.3 LDL Receptor *5*
1.3.1 LDLR synthesis and structure 7
1.3.2 *LDLR* gene expression 7
1.4 Statins *9*
1.5 The discovery of PCSK9 ..... *9*
1.6 PCSK9 gain-of-function and loss-of-function mutations *10*
1.7 Transcriptional regulation of PCSK9 ..... *13*
1.7.1 SREBP2 13
1.7.2 HNF1α and E2F1 14
1.8 Post-translational regulation of PCSK9 ..... *16*
1.9 PCSK9 synthesis, processing and secretion *17*
1.9.1 PCSK9 synthesis and maturation 17
1.9.2 Transport of PCSK9 to Golgi 17
1.9.3 PCSK9 secretion from Golgi 19

1.10 The molecular mechanism of PCSK9-promoted LDLR degradation *20*

1.10.1 PCSK9 binds to LDLR 20

1.10.2 PCSK9/LDLR endocytosis 21

1.10.3 Lysosomal degradation 21

1.10.4 The intracellular degradation pathway 22

1.11 PCSK9 inhibition as a therapy for lowering LDL-C *23*

1.12 Study hypothesis and research objectives *24*

1.12.1 Rationale and hypothesis 24

1.12.2 Research objectives 25

Chapter 2 ..... *27*

Materials and Methods *27*

2.1 Materials 28

2.2 Antibodies *29*

2.3 Site-directed mutagenesis of LDLR and PCSK9 29

2.4 Cell culture and transfection 32

2.5 Immunoblotting 33

2.6 Immunofluorescence of LDLR and PSAP 33

2.7 Biotinylation of cell surface protein 34

2.8 Binding of PCSK9 to LDLR and PCSK9-promoted LDLR degradation. 35

2.9 RNA isolation from cultured cells or mouse liver 36

2.10 Quantitative Real-Time PCR (qRT-PCR) 37

2.11 Dil-LDL binding assay 38

2.12 Immunohistochemistry 39

2.13 Co-immunoprecipitation 39

2.14 Plasma cholesterol, alanine aminotransferase (ALT) analysis 40

2.15 Preparation of adeno-associated virus (AAV) 40

2.16 Deglycosylation of LDLR 41

2.17 Inhibition of N-glycosylation 41

2.18 Statistic analysis *42*

Chapter 3: Manuscript I *43*

The role of the C-terminal domain of PCSK9 and SEC24 isoforms in PCSK9 secretion *43*

(submitted to Biochimica et Biophysica Acta - Molecular and Cell Biology of Lipids) *43*

Abstract *44*

3.1 Introduction *46*

3.2 Results *48*

3.2.1 The impact of C-terminal truncated mutants on PCSK9 secretion 48

3.2.2 The role of proline at position 445 in PCSK9 secretion 53

3.2.3 The effects of natural mutations in CTD on PCSK9 secretion. 55

3.2.4 Role of SEC24 isotypes in PCSK9 secretion 57

3.3 Discussion *61*

Chapter 4: Manuscript II *66*

Identification of amino acid residues in the ligand binding repeat of LDLR important for PCSK9 binding *66*

(The Journal of Lipid Research. 2019 Mar; 60(3): 516–527) *66*

Abstract *68*

4.1 Introduction *69*

4.2 Results *71*

4.2.1 Effect of mutations in LDLR-ΔLR4-LR7 on PCSK9 binding 71

4.2.2 Effect of mutations in the full-length LDLR on PCSK9 binding 74

4.2.3 Effects of D172N and D203N on LDL binding and LDLR trafficking 81

4.2.4 Effect of mutations of Asp172 and Asp203 on PCSK9 binding 86

4.3 Discussion *89*

Supplementary figures *93*

Chapter 5: Manuscript III *95*

Investigating the role of PSAP in the regulation of LDLR and cholesterol metabolism *95*

(Manuscript in preparation) *95*

Abstract *96*

5.1 Introduction *97*

5.2 Results *101*

5.2.1 Knockdown of PSAP increased LDLR abundance *in vitro* 101

5.2.2 Knockdown of hepatic PSAP increased LDLR *in vivo* 105

5.2.3 Effect of knocking down *PSAP* in *Ldlr*$^{-/-}$ mice on plasma cholesterol 111

5.2.4 The effect of Knockdown PSAP on lysosomal function 114

5.2.5 PSAP-regulated LDLR was independent of PCSK9 118

5.2.6 PSAP directly interacted LDLR 120

5.3 Discussion *123*

Supplementary figures *126*

Chapter 6 ..... *130*

Discussion and Future Perspectives *130*

6.1 The role of PCSK9 CTD in its maturation and secretion *131*

6.1.1 The length of CTD is important for PCSK9 maturation and secretion 131

6.1.2 SEC24 isoforms play a role in PCSK9 ER exit 132

6.1.3 Conclusion 132

6.2 The binding motif between LDLR and PCSK9 ..... *133*

6.2.1 The role of Asp203 of LDLR in PCSK9 binding 133

6.2.2 The role of Asp172 of LDLR in PCSK9 binding 133

6.2.3 Conclusion 135

6.3 PSAP regulated LDLR degradation *135*

6.3.1 PSAP versus PCSK9 135

6.3.2 Intracellular PSAP-promoted LDLR degradation 136

6.4 Future directions *136*

6.4.1 To uncover the binding motif in PSAP for its interaction with LDLR 136

6.4.2 To investigate the role of sortilin in PSAP-induced LDLR degradation 137

6.4.3 To study the effect of PSAP knockdown in atherosclerosis 138

6.5 Concluding remarks *139*

References *141*

Lists of Figures

Figure 1.1 Initiation and progression of atherosclerosis.

Figure 1.2 Structure of LDL and cholesterol.

Figure 1.3 LDLR recycling and degradation pathways.

Figure 1.4 Structural domains of LDLR.

Figure 1.5 PCSK9 transports from ER to the Golgi.

Figure 1.6 Regulation of PCSK9.

Figure 1.7 Study hypothesis and research objectives.

Figure 3.1 Secretion of the wild-type and mutant PCSK9.

Figure 3.2 Secretion of the wild-type and mutant PCSK9.

Figure 3.3 Effect of mutations in position 445 on mutant $PCSK9^{1-445}$ and full-length PCSK9 secretion.

Figure 3.4 Effect of natural mutations in PCSK9 on its secretion.

Figure 3.5 Role of SEC24s in PCSK9 secretion.

Figure 3.6 Role of SEC24s in mutant PCSK9 secretion.

Figure 3.7 Crystal structure of PCSK9 in cartoon.

Figure 4.1 Binding of PCSK9 to the wild-type and mutated LDLR-ΔLR4-LR7.

Figure 4.2 Binding of PCSK9 to the wild-type and mutant full-length LDLR.

Figure 4.3 Binding of PCSK9 to the wild-type and mutant LDLR.

Figure 4.4 PCSK9-promoted LDLR degradation.

Figure 4.5 Binding of LDL to the wild-type and mutant LDLR.

Figure 4.6 Cellular localization of the wild-type and mutant LDLR.

Figure 4.7 Binding of PCSK9 to the wild-type and mutant LDLR.

Supplemental figure 4.1S Binding of PCSK9 to the wild-type and mutant LDLR-ΔLR4-LR7 at pH 7.4 and pH 6.0.

Supplemental figure 4.2S Effect of mutation D203N on LDLR expression.

Figure 5.1 Effect of KD PSAP in cultured hepatoma-derived cells.

Figure 5.2 Effect of KD PSAP in mouse liver on LDLR and plasma PCSK9.

Figure 5.3 Effect of KD PSAP in mouse liver on plasma cholesterol

Figure 5.4 Effect of KD PSAP in $Ldlr^{-/-}$ mice

Figure 5.5 Effect of KD PSAP on lysosome function.

Figure 5.6 Role of PCSK9 in PSAP-regulated LDLR.

Figure 5.7 Putative interaction between PSAP and LDLR.

Figure 5.8 Effect of extracellular PSAP on LDLR

Figure 5.1S PSAP structure, its intracellular trafficking and secretion.

Figure 5.2S Effects of KD PSAP on LDLR and PCSK9 in Huh7.

Figure 5.3S Effect of KD PSAP on mouse liver.

Figure 6.1 Final working model.

Lists of Tables

Table 2.1 Used antibodies and dilutions.

Table 2.2 Cycling parameters for the QuickChange Site-Directed Mutagenesis.

Table 2.3 Primers for mutagenesis.

Table 2.4 DsiRNAs for knocking down experiments.

Table 2.5 Primers for qRT-PCR.

List of Abbreviations

AAV	Adeno-associated virus
ApoB	Apolipoprotein B
ALT	Alanine aminotransferase
ARH	Autosomal recessive hypercholesterolemia
BCA	Bicinchoninic acid
BSA	Bovine serine albumin
cDNA	Complementary DNA
CE	Cholesterol ester
COPII	Coat protein complex II
CVD	Cardiovascular disease
CTD	C-terminal domain
DAPI	4’,6-diamidino-2-phenylindole
DMEM	Dulbecco Modified Eagle Medium
DsiRNA	Dicer-substrate siRNA
ER	Endoplasmic reticulum
EGF	Epidermal growth factor
FBS	Fetal bovine serum
FH	Familial hypercholesterolemia
FL	Full-length
GAPDH	Glyceraldehyde-3-phosphate dehydrogenase
GOF	Gain-of-function mutation
HDL	High-density lipoprotein
HEK293	Human embryonic kidney 293
H&E	Hematoxylin and eosin stain
IDOL	Inducible degrader of LDLR
HMGCR	3-hydroxy-3-methylglutaryl coenzyme A reductase
KD	Knock down
LDL-C	Low-density lipoprotein cholesterol
LDLR	Low-density lipoprotein receptor
LR	Ligand-binding repeat domain
LRP	LDLR-related protein
Lp (a)	Lipoprotein (a)
LOF	Loss-of-function mutation
NCLPPS	Newborn calf lipoprotein poor serum
PBS	Phosphate buffered saline

PCSK9	Proprotein convertase subtilisin/kexin type 9
PCR	Polymerase chain reaction
PEI	Polyethylenimine
PSAP	Prosaposin
SREBP2	Sterol regulatory element-binding protein 2
SDS-PAGE	Sodium dodecyl-sulfate-polyacrylamide electrophoresis
SP	Signal peptide
PRP	Prodomain
CAT	Catalytic domain
CTD	C-terminal domain
TG	Triacylglycerol
TFR	Transferrin receptor
VLDL	Very low-density lipoprotein
WT	Wild-type

Chapter 1

Introduction

Chapter 1. Introduction

Abstract

Atherosclerotic CVD is the leading cause of mortality and morbidity worldwide. Long-term elevated LDL-C levels in the blood is a major risk factor for the development of atherosclerotic lesions, which can eventually lead to myocardial infarction and many strokes, as well as disabling peripheral artery disease. Lowering LDL-C levels remains the cornerstone of the management of CVD. LDLR in the liver is mainly responsible for the removal of LDL-C from the blood. PCSK9 regulates cholesterol metabolism by promoting LDLR degradation. An array of pharmaceutical companies have created therapeutic agents to inhibit PCSK9 and block its interaction with LDLR, including PCSK9 monoclonal antibodies and small interfering RNAs. These PCSK9 inhibitors, in combination with the existing cholesterol-lowering drugs statins, have been shown to significantly reduce circulating LDL-C levels and the risk of CVD in a wide variety of subjects. PCSK9 is now common parlance among scientists and clinicians interested in the prevention and treatment of atherosclerotic CVD. What makes PCSK9 so special is not only the fact that it uncovers previously unknown biology but also that these important scientific insights have been translated into an effective medical therapy in record short time that was first discovered in 2003 and approved for clinical application in 2015. However, the PCSK9 saga is far from complete. This introduction will give an overview of the cellular and molecular biology of PCSK9, as well as its application in the treatment of CVD.

1.1 Atherosclerotic cardiovascular disease

Atherosclerosis is the formation of fibrofatty plaques in the artery wall. Progressive accumulation of atherosclerotic plaque leads to severe problems, including heart attack, stroke

or even death (1). The development of these complex, unstable fibrofatty lesions originates from long-term elevated levels of LDL-C in the blood. Numerous studies have well established a positive correlation between LDL-C and atherosclerosis. Thus, lowering LDL-C is the primary target of therapies for the prevention and treatment of CVD (2).

Atherosclerotic plaque formation starts with LDL transcytosis from the blood into the endothelial space of the vessel wall, where LDL is oxidized by reactive oxygen species (Fig 1.1). Upon exposed to pro-inflammatory conditions and endothelial damage, circulating monocytes bind to the endothelial surface and then migrate across the endothelium into the artery wall, where they differentiate into macrophages. The macrophages express scavenger receptors which take up oxidized LDL, leading to the formation of macrophage foam cells. Foam cells secrete pro-inflammatory cytokines, including tumor necrosis factor-α and interleukin-1, which further results in the recruitment of more monocytes into the artery wall (3). Apoptotic foam cells, cholesterol crystals and monocytes accumulate and form the necrotic core of the plaques. To stabilize the plaque surface, intimal smooth muscle cells proliferate and synthesize collagen. The plaque is eventually ruptured due to the continued presence of the necrotic core, secretion of collagen proteases from macrophages and mechanical shear stress from the bloodstream (4). Subsequently, a thrombus is produced by the interaction between lipids, platelets, coagulation factors and red blood cells that are released from the ruptured plaque, which narrows the artery lumen, resulting in a myocardial infarction or stroke (4,5). Therefore, the uptake and removal of circulating LDL are paramount to reducing atherosclerotic plaque formation and CVD events.

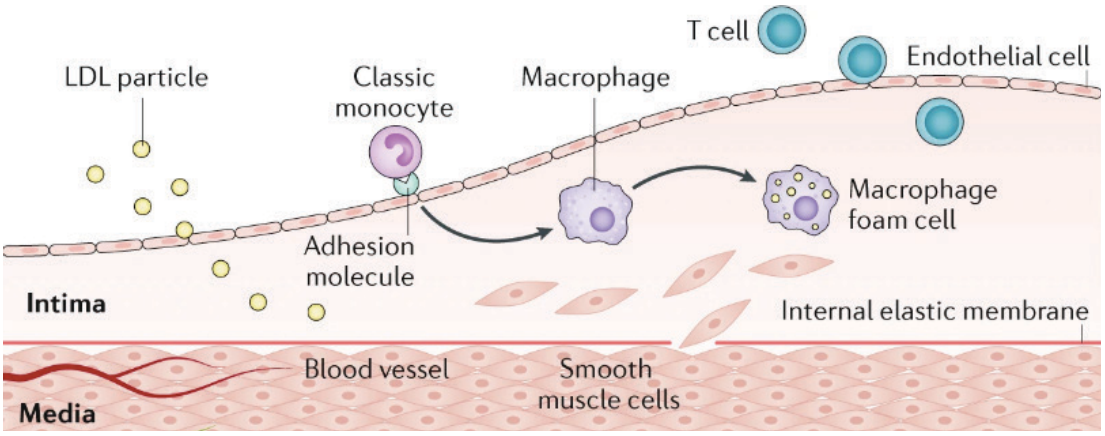

Figure 1.1 Initiation of atherosclerosis.

This figure is modified from Libby *et al.* (6).

1.2 Low-density lipoprotein

The development of atherosclerotic plaque requires long-term elevated plasma LDL-C. Cholesterol in the blood is transported as a component of large macromolecular lipoproteins. These are spherical particles consisting of a core of cholesterol esters (CE) and triacylglycerol (TG), which are surrounded by a monolayer of phospholipids, un-esterified cholesterol and apolipoproteins (7). There are five major classes of lipoproteins in human plasma: chylomicron/remnant (CM), very low-density lipoprotein (VLDL), intermediate-density lipoprotein (IDL), LDL and high-density lipoprotein (HDL). A subspecies of LDL is lipoprotein (a) (Lp(a)), which consists of an LDL particle linked by a disulfide bond to an apo(a) protein through apolipoprotein B100 (apoB100) (8). The density of lipoproteins is determined by the amount of lipid relative to protein, with LDL being the second-most dense lipoprotein class, and CM being the largest and least dense of all lipoproteins (9). ApoB100 is the major structural protein of LDL and VLDL and apoB48 is a unique protein in CM from the small intestine, whereas apoA-I is the most abundant apolipoprotein associated with HDL (10). ApoE is present at varying concentrations in CM, VLDL, IDL, and HDL (11).

LDL is a spherical particle with a diameter of about 22 nm and a molecular mass of 3000 kDa (12). Each particle contains approximately 1500 molecules of CE in an oily core that is shielded from the aqueous plasma by a hydrophilic coat composed of 800 molecules of phospholipid, 500 molecules of unesterified free cholesterol, and one apoB100 molecule of 500 kDa protein (13). LDL is derived from VLDL, which is assembled in the liver and secreted into plasma. VLDL acquires apoE from circulating HDL. Moreover, lipoprotein lipase hydrolyzes TG in the VLDL to produce IDL and LDL (14,15). LDL is removed from the blood predominantly by the LDLR in the liver.

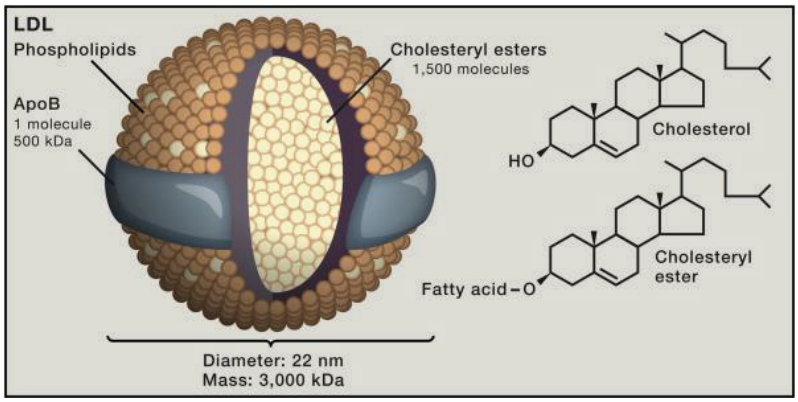

Figure 1.2 Structure of LDL and cholesterol. This figure is adapted from Goldstein and Brown (13).

1.3 LDL Receptor

LDLR in the liver plays a critical role in regulating the levels of LDL-C in the blood. The amount of LDLR on the surface of liver cells determines how efficiently LDL-C is removed from the bloodstream. The transmembrane protein LDLR captures LDL by binding to apoB100 through its ligand-binding repeat domain (LR), after which the LDL/LDLR complex is endocytosed in clathrin-coated pits with the assistance of an adaptor protein (LDLRAP/ARH) (16). After entering the cell, the LDL/LDLR complex is transported to the

endosomes. In the low pH environment of the endosomes, LDLR undergoes a conformational change so that LR4 and LR5 form a physical interaction with the YWTD repeats, promoting the release of bound LDL for delivery to the lysosome for degradation (Fig 1.3) (17). LDLR is routed back to the plasma membrane for binding and internalizing additional LDL particles. The LDLR can be recycled in this way up to 150 times before it is eventually degraded in the lysosome (18,19) (Fig 1.3). Defective function of the LDLR causes an inherited form of high cholesterol called familial hypercholesterolemia (FH). More than 1000 mutations in the *LDLR* gene have been identified in humans.

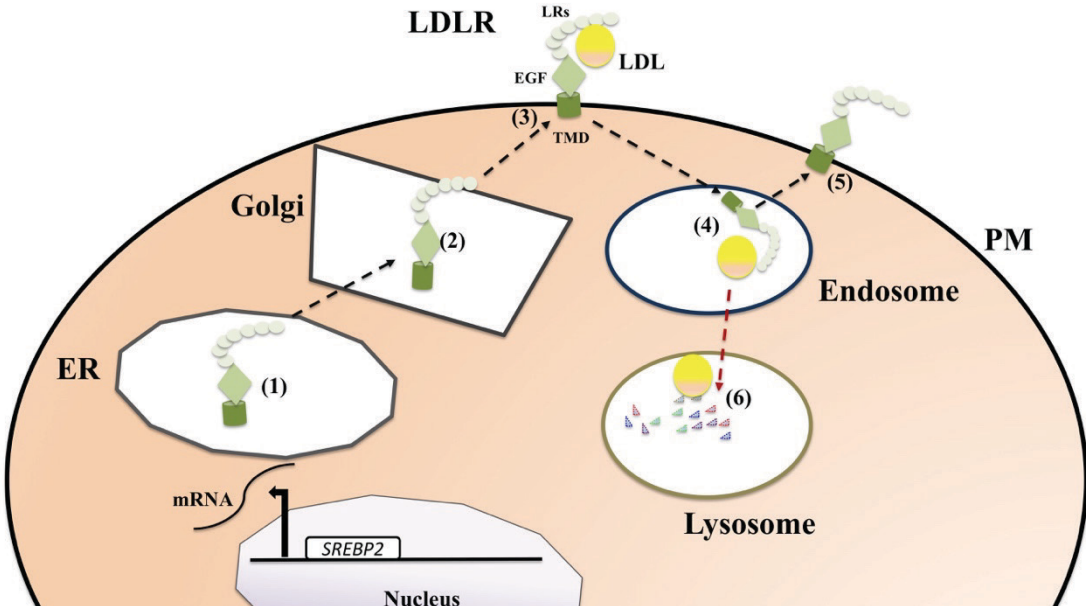

Figure 1.3 LDL uptake and LDLR recycling. (1) LDLR is synthesized in the ER. (2) LDLR is transported to the Golgi, where post-translational modifications, such as glycosylation, occur. (3) Mature LDLR is retained in the plasma membrane via its transmembrane domain (TMD). (4) LDLR-mediated endocytosis takes place. (5) LDLR recycles to the cell surface. (6) LDL is degraded in the lysosome.

1.3.1 LDLR synthesis and structure

LDLR is synthesized as a 120 kDa precursor in the endoplasmic reticulum (ER), where it binds to a chaperone receptor-associated protein (RAP), facilitating its transport to the Golgi. In the Golgi, LDLR dissociates from RAP and acquires carbohydrate residues that increase its molecular mass to 160 kDa. The mature LDLR is then transported along the secretory pathway from the Golgi to the cell surface (20).

Structurally, LDLR consists of seven LRs at its N-terminal domain, followed by the epidermal growth factor (EGF) precursor homology domain and the YWTD repeat (six-stranded-propeller structure) (Fig 1.4). The EGF homology domain consists of three epidermal growth factor repeats: EGF-A, EGF-B, EGF-C. The EGF-C repeat is separated from the EGF-B by a beta-propeller domain (21). Next in the LDLR amino acid sequence is the clustered O-linked sugar region, followed by the transmembrane domain and a cytoplasmic tail (22).

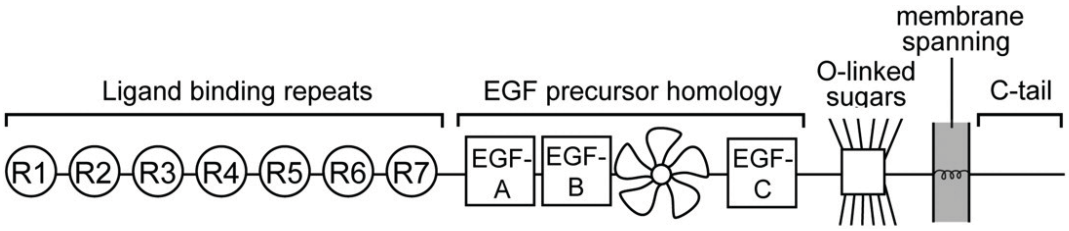

Figure 1.4 Structural domains of LDLR. This figure is adapted from Zhang et al. (23).

1.3.2 *LDLR* gene expression

The transcription of the *LDLR* gene is mainly regulated by intracellular cholesterol levels via the sterol regulatory element-binding protein 2 (SREBP2), the master transcriptional factor for cholesterol homeostasis. Intracellular cholesterol levels are delicately balanced between cholesterol uptake and cholesterol synthesis through a complex feedback mechanism that is governed by SREBP2. SREBP2 regulates the expression of genes controlling

cholesterol biosynthesis through *HMG-CoA reductase* (*HMGCR*) as well as cholesterol uptake through the *LDLR* (24).To date, there are three SREBPs identified in mammals, including SREBP1a, SREBP1c and SREBP2. SREBP1a regulates the expression of genes involved in both lipogenesis and cholesterol metabolism, while SREBP1c is linked primarily with fatty acid metabolism (25). SREBP2 regulates the expression of genes governing cholesterol biosynthesis and cholesterol uptake (24).

The structure of all the SREBPs is similar: An N-terminal domain that is exposed on the cytosolic space of the ER membrane bilayer and two hydrophobic transmembrane domains that pass through the ER membrane. Their transmembrane domains associate with the SREBP cleavage activating protein (SCAP), which, in turn, is bound to another transmembrane protein, insulin-induced gene 1 (INSIG-1) (26). SREBP2 processing is tightly regulated by cholesterol levels in the ER. When cholesterol levels in the ER become higher than 5% of total lipids, SCAP remains tightly bound to SREBP2 and INSIG-1 (27). However, when ER cholesterol decreases below the 5% threshold, INSIG-1 dissociates from SREBP2 and SCAP. The SREBP2/SCAP complex is translocated to the Golgi, where SREBP2 is cleaved into the individual components by the subtilisin kexin isoenzyme 1/site 1 protease (SKI-1/S1P) (28). A site 2 protease (S2P) then cleaves the first transmembrane domain of SREBP2, liberating its N-terminal domain (nSREBP2). The nSREBP2 is translocated to the nucleus, where it binds to the promoter region of target genes that contain a sterol regulatory element (SRE) sequence (29,30). This series of events increases the transcription and expression of 35 genes involved in cholesterol metabolism, including *HMGCR, LDLR and PCSK9* (31).

1.4 Statins

Statins, which were introduced in 1987, are the most prescribed drugs for the treatment of hypercholesterolemia worldwide (13). Statins inhibit HMGCR, the rate-limiting enzyme in the cholesterol biosynthesis pathway in the ER. Subsequently, this reduction of cholesterol levels inside the cell activates the processing of SREBP2, thereby increasing the transcription of LDLR, and thus decreasing plasma LDL-C. The efficacy and safety of statin therapy have been revealed by meta-analyses of 26 randomized clinical trials, indicating that each 1 mmol/l reduction in plasma LDL-C results in a 20% reduction of CVD risk and decreases mortality by 10% (32). Despite their intensive cholesterol-lowering effect, it has been noted that more than 10% of patients are 'statin-intolerant.' The most common side-effects include myalgia and other musculoskeletal complaints (33). Furthermore, growing evidence suggests that inhibition of HMGCR by statins might increase the risk of new-onset type 2 diabetes in patients with established risk factors (34,35). These unexpected outcomes have prompted researchers to develop alternative therapy for lowering LDL-C.

1.5 The discovery of PCSK9

PCSK9 was first discovered in 2003, later resulting in a major change in cholesterol-lowering therapy and the treatment of CVD (36). PCSK9 is the ninth member of the proprotein convertase family that cleaves and activates mammalian secretory proteins. The nine members include PC1/3, furin, PC4, PC5/6, PACE4, PC7 and SKI-1/S1P, which are involved in the catalysis and maturation of pro-hormones, proteolytic enzymes, growth factors and receptors (37). The *PCSK9* gene was first cloned by Seidah et al. in 2002 (38). In 2003, Abifadel et al. identified two mutations in the *PCSK9* gene in two French families with a history of FH. These mutations resulted in single amino acid substitutions, S127R and F216L,

in the protein sequence of PCSK9 (36). This study was followed by three independent reports from Norway, the United States and the United Kingdom of people with a D373Y mutation in PCSK9 causing FH (39-41). Mutations in the *PCSK9* gene that cause autosomal dominant hypercholesterolemia, makes it the third genetic cause of FH besides LDLR and apoB100 (42).

1.6 PCSK9 gain-of-function and loss-of-function mutations

PCSK9 is mainly expressed in the liver, kidney and small intestine. A recent study suggests that PCSK9 is also expressed in human visceral adipose tissue (43). Circulating PCSK9 interferes with, and blocks the recycling of, hepatic LDLR, resulting in the reduction of LDL-C clearance from the blood (44). Humans carrying loss-of-function (LOF) mutations in the *PCSK9* gene present with low LDL-C levels in the plasma and decreased CVD risk, whereas gain-of-function (GOF) mutations in the *PCSK9* genes are associated with high LDL-C levels and increased risk for CVD (45). Many GOF mutations in the *PCSK9* gene have been reported to occur in patients with FH. For example, the F216R, S217R, D374Y and R496W mutations increase the binding affinity between PCSK9 and LDLR, enhance LDLR degradation and increase circulating LDL-C levels (46-50). The most severe GOF mutation known to date, D374Y, results in a 10- to 25-fold higher binding affinity to the LDLR than the wild-type (WT) PCSK9 (46).

The first LOF mutation in the *PCSK9* gene was reported in a cohort of African-American subjects. In 2006, Cohen et al. reported that the nonsense *PCSK9* mutations, Y142X and C679X, lower LDL-C levels, and reduce 88% of the incidence of CVD over a period of 15 years. After this finding, a number of mutations in PCSK9 have been reported to cause its loss-of-function, leading to reducing PCSK9 synthesis, secretion or function. For example, the

Y142X mutation results in no detectable PCSK9 protein due to introduction of a premature stop codon (51). In the C679X mutation, PCSK9 is misfolded, which impairs its exit from the ER. The Q152H mutation prevents the autocatalytic processing of the PCSK9 precursor, resulting in a dominant negative form of the protein that reduces the circulating levels of PCSK9 and LDL-C by 80% (52). In addition, the R46L, L253F, G106R and Q554E mutations also either reduce PCSK9 secretion or decrease its affinity for LDLR (53).

Homozygous LOF mutations have been described in two females with complete PCSK9 deficiency. One of them is a 53-year-old participant in the Dallas Heart Study and is a compound heterozygote for the Y142X and C679X mutations in the *PCSK9* gene. The other subject, from Zimbabwe, is homozygous for the C679X mutation (54). Neither of these individuals have immunodetectable circulating PCSK9, and both also have very low circulating LDL-C levels (<0.8 mmol/L). Long-term studies have revealed that both subjects are otherwise healthy and fertile. The low circulating LDL-C levels in people with PCSK9 LOF mutations appear to reduce the incidence of CVD without apparent negative impacts on health (55).

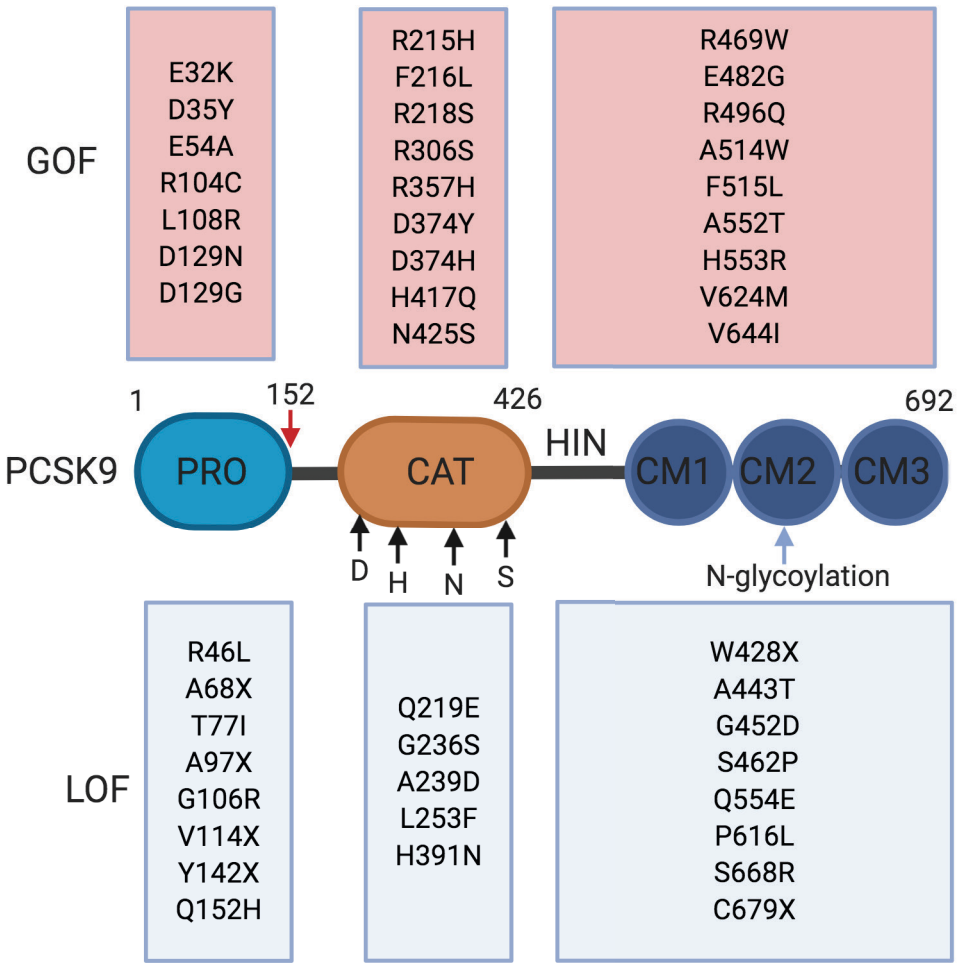

Figure 1.5 PCSK9 structure and mutations. The PCSK9 precursor is autocatalytically processed at VFAQ152-SIP (red arrow) to produce mature PCSK9. Note the active site residues Asp (D), His (H), and Ser (S) and the oxyanion hole Asn (N) as well as the single N-glycosylation site (blue).

PCSK9 knockout (PCSK9-KO) in animals also appears to be safe and protect against atherosclerosis. Compared to the WT mice, PCSK9-KO mice have 2.8-fold higher hepatic LDLR expression and 42-48% lower plasma levels of total cholesterol and apoB (56,57). In atherosclerosis-prone apoE-deficient mice, there is a 39% reduction in atherosclerotic plaque formation in PCSK9-KO mice compared with control mice (58). In the same study, LDLR

knockout (LDLR-KO) mice expressing high, normal or low levels of PCSK9 are not significantly difference in plasma cholesterol levels, suggesting that PCSK9 regulates LDL-C exclusively via the LDLR (58). Taken together, these findings, in conjunction with the human LOF studies, suggest that a pharmacological compound inhibiting PCSK9 might be a safe and effective therapeutic option to lower LDL-C levels and protect against CVD in hypercholesterolemia patients.

1.7 Transcriptional regulation of PCSK9

1.7.1 SREBP2

The human *PCSK9* gene is located on chromosome 1. The transcription of *PCSK9* mRNA is mainly regulated by SREBP2 (59). The proximal promoter of the *PCSK9* gene contains a functional SRE, which is required for SREBP2 to initiate *PCSK9* transcription. Statins stimulate the expression of *PCSK9* mRNA by increasing SREBP2 processing, which attenuates their effect on lowering LDL-C (60). Plasma PCSK9 levels can increase by 14-47%, depending on the types and doses of statins (61). For example, rosuvastatin treatment of patients in the JUPITER trial has shown a significant relationship between increased circulating PCSK9 levels and the magnitude of LDL-C reduction (62). These data explain why only some hypercholesterolemic subjects can achieve optimal LDL-C levels with a maximum amount of the statin being accompanied by only a 6% decrease in LDL-C levels in some cases (63,64). Moreover, the upregulation of PCSK9 expression by statins attenuates some of their effects on increased LDLR expression. Consequently, this effect of statins on PCSK9 expression has turned attention to the development of novel strategies to inhibit PCSK9 for further decreasing circulating LDL-C levels in statin-treated subjects.

1.7.2 HNF1α and E2F1

Hepatocyte nuclear factor 1 alpha (HNF1α) also plays a critical role in the transcription of the *PCSK9* gene since the gene contains an HNF1α binding motif in the proximal region of its promoter (65). The plant-derived cholesterol-lowering compound berberine and activation of mechanistic target of rapamycin complex 1 (mTORC1), have been shown to downregulate HNF1α levels and PCSK9 expression (66). Furthermore, E2F1, a transcription factor controlling the cell cycle, binds to and transactivates the *PCSK9* promoter and mRNA transcription. Thus, E2F1 deficiency in cellular and mouse models leads to a marked decrease in PCSK9 expression and an increase in LDLR levels (67).

In addition to these transcription factors, a number of other regulators affect *PCSK9* mRNA content *in vitro*. For example, thyroid-stimulating hormone (TSH) recombinant protein increases *PCSK9* mRNA levels in human hepatoma-derived HepG2 cells. Moreover, circulating TSH levels in subclinical hypothyroid patients have been shown to correlate with plasma PCSK9 levels (68). Berberrubine, an analog of berberine, has also been proposed to exert a potent inhibitory effect on PCSK9 via the extracellular signal-regulated kinase (ERK) pathway, which results in higher LDLR levels in cellular models (69). Moreover, recent work has suggested that miR-191, miR-222 and miR-224 directly interact with the 3'-untranslated region (3'-UTR) of *PCSK9* mRNA and regulate PCSK9 translation; however, the significance of these findings remains to be investigated (70) (Fig 1.5).

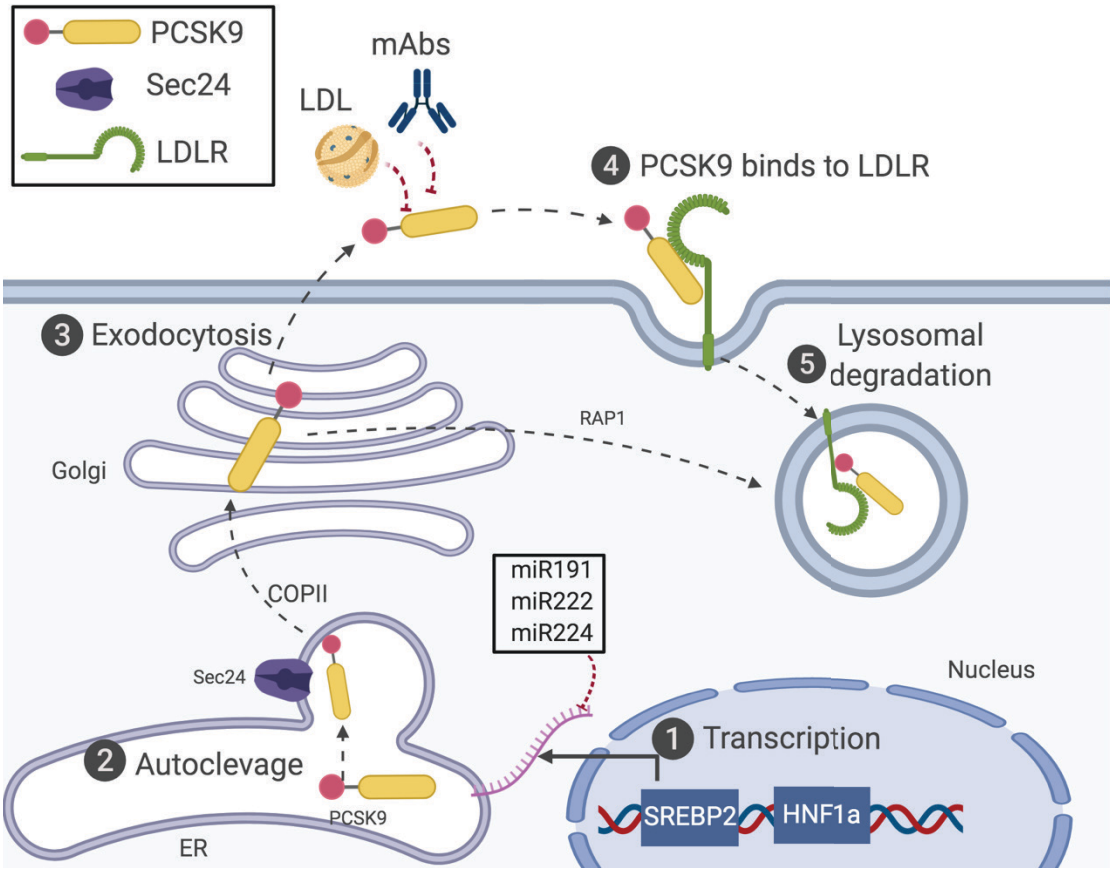

Figure 1.5 Regulation of PCSK9. (1) *PCSK9* mRNA is transcriptionally regulated by SREBP2 and HNF1α. (2) PCSK9 is synthesized as a zymogen in the ER and undergoes autocatalytic cleavage between the prodomain and the catalytic domain. The cleaved prodomain is tightly associated with the catalytic domain. (3) PCSK9 is transported to the Golgi, where post-translational modifications, such as glycosylation, occur. Mature PCSK9 is secreted to the extracellular space. (4) The catalytic domain and prodomain of PCSK9 bind to the EGF-A and YWTD repeats of the LDLR, respectively. The PCSK9/LDLR complex enter the cell via clathrin-coated pits and is delivered to the endosomes. (5) PCSK9 strongly binds to the LDLR and blocks the recycling of LDLR to the cell surface. The PCSK9/LDLR complex is transported to the lysosome for degradation.

1.8 Post-translational regulation of PCSK9

A number of recent studies have described post-transcriptional mechanisms of regulating PCSK9 activity. Previous work has shown that intracellular cell signaling stimulates the PCSK9 lysosomal degradation (71-73). For example, silencing of hepatic glucagon receptor or inhibition of the glucagon action results in increased plasma levels of PCSK9 and LDL-C, whereas glucagon treatment of the wild-type mice has the opposite effect. Mechanistically, they showed that Ras-related protein 1 (RAP1) enhances lysosomal degradation of PCSK9 without any effect on *PCSK9* mRNA levels. However, the underlying mechanism has not been fully uncovered. In addition, PCSK9 is cleaved by furin in the extracellular space. The furin-cleaved shorter fragment of PCSK9 has reduced LDLR-binding capacity and is unable to promote LDLR degradation in the lysosome (74) (75).

On the other hand, diet and nutritional status affect PCSK9 expression. It has been reported that fasting decreases PCSK9 expression while re-feeding restores PCSK9 levels. During fasting, mice, rats, hamsters and humans have 58%-70% lower circulating PCSK9 levels (76). Insulin also influences hepatic *PCSK9* gene expression. For instance, *in vitro* experiments in mouse and rat hepatocyte and *in vivo* studies in rats have shown that insulin upregulates *Pcsk9* expression via *Srebp1c* (66,77). Circulating PCSK9 levels are also significantly correlated with insulin levels in subjects without diabetes (78,79). However, following an insulin infusion, plasma PCSK9 levels do not increase in subjects without diabetes or in subjects with type 2 diabetes (80). The role of insulin in regulating PCSK9 expression remains to be investigated further.

1.9 PCSK9 synthesis, processing and secretion

1.9.1 PCSK9 synthesis and maturation

The *PCSK9* gene consists of 12 exons located on chromosome 1p32 and is approximately 22 kb long (60). In the ER, PCSK9 is synthesized as a 692-amino-acid (74 kDa) zymogen. Structurally, it is composed of a signal peptide (SP) (aa 1-30), a prodomain (PRO) (aa 31-152), a catalytic domain (CAT) (aa 153-454) and C-terminal cysteine-histidine-rich domain (CTD) (aa 455-692) (81). In the ER lumen, PCSK9 undergoes autocatalytic cleavage that leads to PCSK9 maturation and activation. The signal peptide is first removed from the N-terminus of the precursor of PCSK9. Autocatalytic processing of the 14 kDa prodomain occurs at the site SVFAQ^{152}SIP (82). Unlike other members of the proprotein convertase family, PCSK9 is unique in that the auto-cleaved prodomain remains associated with the 60 kDa mature form via hydrophobic and electrostatic interactions, which results in its trafficking to the Golgi as an inactive dimer complex (83). The self-cleavage of PCSK9 is critical for its function, and agents or conditions that disrupt the ER function have been reported to affect PCSK9 maturation and secretion. For example, Tunicamycin, an ER stress-causing agent, retains PCSK9 in the ER (84). Of note, recent work has shown that some LOF PCSK9 mutants accumulate in the ER without activating the ER stress response (85).

1.9.2 Transport of PCSK9 to the Golgi

Like many other secretory proteins, COPII is essential for PCSK9's exit from the ER and trafficking to the Golgi apparatus. The incorporation of PCSK9 into the membrane-bound vesicles is the critical step (86). The formation of COPII is driven by the SAR1 GTPase, heterodimers of SEC23/24, and heterodimers of SEC13/SEC31. Protein cargoes are incorporated into COPII vesicles by two mechanisms: receptor-mediated cargo capture or

'bulk flow.' In the bulk flow model, cargoes enter COPII through passive diffusion, while the cargo capture model is a receptor-mediated, active sorting of selected cargoes. It remains unclear to what extent PCSK9 recruitment into the COPII is driven by selective cargo versus passive bulk flow (87).

The sorting process of secreted PCSK9 into COPII-coated vesicles is reported to be driven primarily by SEC24 isoforms. A recent study has shown that SEC24A, a COPII adaptor protein, incorporates PCSK9 into transport vesicles for export from the ER to the Golgi (Fig 1.6). SEC24A-KO mice have lower plasma levels of cholesterol and PCSK9 than the WT mice (88). This finding reveals an active receptor-mediated mechanism for PCSK9 recruitment into COPII vesicles. However, SEC24A localizes in the cytoplasmic side of the ER membrane, and PCSK9 is on the luminal side; therefore, a direct physical interaction between SEC24A and PCSK9 is implausible since neither protein possesses a transmembrane domain. A recent study demonstrated that surfeit locus protein 4 (Surf4), an ER cargo receptor, interacts with PCSK9 in HEK293 cells and promotes the efficient ER exit of PCSK9 (89). The knockdown of Surf4 causes accumulation of PCSK9 in the ER and impairs PCSK9 secretion. However, we found that Surf4 regulates PCSK9 expression but is not required for endogenous PCSKK9 secretion from cultured human hepatocytes (90). The molecular mechanism of PCSK9 exit from ER remains unclear.

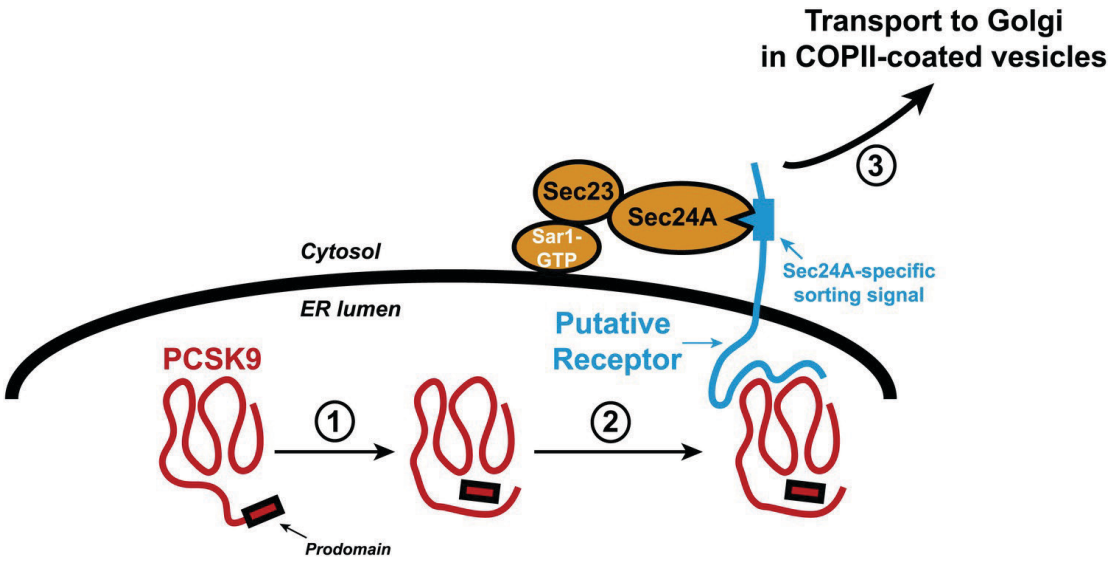

Figure 1.6 PCSK9 transport from the ER to the Golgi. (1) PCSK9 (shown in red) is synthesized in the lumen of ER, where it undergoes autocatalytic cleavage. The prodomain remains attached to PCSK9 when it is exported from the ER to the Golgi. (2) PCSK9 might be captured by a putative transmembrane receptor (shown in blue), which could present PCSK9 to a cytosolic SEC23/SEC24A complex. This selection is likely mediated by specific interactions between the sorting signal in the cytosolic domain of the receptor and binding sites in SEC24A. (3) PCSK9 is then incorporated into COPII-coated vesicles for transport to the Golgi and subsequent secretion. The Sar1 enzyme initiates the formation of the COPII by binding to the ER membrane (thick black line). This figure is modified from Debose-Boyd and Horton (91).

1.9.3 PCSK9 secretion from Golgi

In the trans-Golgi apparatus, sortilin, a sorting receptor, has been reported to be involved in the intracellular transport of PCSK9 (92). Gustafsen et al. have demonstrated by immunofluorescence confocal microscopy that sortilin and PCSK9 co-localize in the trans-Golgi network in HepG2 cells. Knockdown of sortilin reduces PCSK9 secretion and increases

its subcellular localization in the ER, while overexpression of sortilin in mice increases circulating PCSK9 levels. The levels of metalloproteinase-cleaved ectodomain of sortilin have been shown to correlate with circulating PCSK9 levels in human plasma (92,93). Conversely, studies from Butkinaree et al. showed that knockdown of sortilin in cultured cells, or knockout of sortilin in mice, had no detectable effect on PCSK9 secretion (94). Together, these findings reveal the complexity and heterogeneity of PCSK9 secretion in different types of cells.

1.10 The molecular mechanism of PCSK9-promoted LDLR degradation

1.10.1 PCSK9 binds to LDLR

Plasma PCSK9 binds to, and promotes, LDLR degradation in hepatocytes. PCSK9-promoted LDLR degradation is initiated when the catalytic domain (CAT) of PCSK9 binds to the EGF-A domain of the LDLR, followed by the pro-domain (PRO) of PCSK9 binding to YWTD repeat of the LDLR at the cell surface (95-97). This binding occurs in a calcium-dependent manner (98). Recently, we demonstrated that Asp residues in the LR domain of the LDLR also contribute to the binding of PCSK9 to the receptor (99). It is noteworthy that PCSK9 binding to the LDLR has tissue specificity, with liver being the most responsive tissue to this regulation, suggesting the requirement of a coreceptor specific for liver. Gustafsen et al. revealed that heparin sulfate proteoglycans, highly present on the surface of the hepatocytes, capture PCSK9, and that this binding is required for PCSK9/LDLR complex formation and LDLR degradation (100). Moreover, heparan-sulfate mimetics, such as dextran sulfate and pentosane sulfate, bind to PCSK9 and inhibit PCSK9-mediated LDLR degradation. Heparin-like molecules can also interact with LDL and play an important role in LDL-induced inhibition of PCSK9 uptake into the cells (101).

1.10.2 PCSK9/LDLR endocytosis

After the initial cell surface binding stage, the PCSK9/LDLR complex enters the cells via clathrin-dependent endocytosis and is delivered to the endosomes. Evidence for these events comes from the siRNA knockdown of the clathrin heavy chain, which reduces the internalization and functional activity of PCSK9 (71,102). A very recent study proposed a novel notion that LDLR degradation is mediated by caveolin instead of clathrin. Jang et al. reported that cyclase-associated protein 1 (CAP1), a component of the saccharomyces cerevisiae adenylyl cyclase complex, binds to the CTD of PCSK9 and acts as a liaison between the PCSK9/LDLR complex and caveolin, which directs the complex to caveolae-mediated endocytosis and lysosomal degradation (103). In the low pH environment of the endosomes, the PCSK9/LDLR complex undergoes a conformational change that increases the affinity of PCSK9 for LDLR (96,104). This event prevents dissociation of the LDLR/PCSK9 complex, inhibits LDLR from adopting a closed conformation, as it normally does at pH 5.5, and precludes LDLR from being recycled to the cell surface. Consequently, the PCSK9/LDLR complex is transported to the lysosome for degradation (105-107).

1.10.3 Lysosomal degradation

The cell surface endocytosis of the PCSK9/LDLR complex initiates a dominant degradation pathway that prevents the typical recycling of LDLR. Previous studies have demonstrated that the CAT domain of PCSK9 interacts with the EGF-A domain of the LDLR on the cell surface (96,97). However, the CTD domain of PCSK9 does not directly interact with LDLR, but it is required for LDLR degradation (97,104,108). The specific role of CTD in PCSK9-promoted LDLR degradation remains obscure. Piper et al. reported that the CTD of PCSK9 has a novel protein fold and may contain protein-protein interaction motifs (83,109).

Furthermore, natural mutations that occur within the CTD result in either gain-of-function (H553R) or loss-of-function mutations (Q554E), affecting its potency in mediating LDLR degradation (110). Incubation of purified mutant PCSK9 lacking the CTD (PCSK9ΔCTD) in cultured hepatocytes shows no detectable reduction of cell surface LDLR levels, even at a high concentration of 5 ug/ml, which is 10 times higher than the physiological concentration (97,108). Interestingly, PCSK9ΔCTD can bind to LDLR at the cell surface and participate in endocytosis of the complex to the endosomes (104,108,111,112). Therefore, the inability of PCSK9ΔCTD to enhance LDLR degradation is not due to its lack of LDLR binding or its internalization with LDLR, suggesting that the CTD carry structural requirements to achieve the critical later steps of LDLR sorting and degradation within endosomes/lysosomes. Most recently, Poirier et al. demonstrated that reconstitution of PCSK9ΔCTD with a foreign lysosomal targeting motif rescues its intracellular lysosomal targeting and induces LDLR degradation, emphasizing a role for the CTD in sorting of the PCSK9-LDLR complex towards the late endocytic compartments (111). Since both LDLR and PCSK9 lack a lysosomal targeting motif, it is possible that the CTD of PCSK9 recruits other partner(s) to the PCSK9/LDLR complex that can direct LDLR to the lysosome or block binding of the cofactor(s) required for LDLR recycling from endosomes to the cell surface.

1.10.4 The intracellular degradation pathway

While PCSK9 is mainly a secreted factor that binds extracellularly to the LDLR, it has also been suggested that PCSK9 might target the LDLR to the lysosome within the cell. Within the secretory pathway, PCSK9 can interact with LDLR and be transported to the lysosome for degradation, which is prevented by the binding of PCSK9 to glucose-regulated protein 94 (GRP94) in the ER (113). In the trans-Golgi network, blocking the trafficking of

PCSK9/LDLR complex by knockdown of clathrin heavy chains results in the LDLR being directed toward the lysosomal degradation (102,114).

1.11 PCSK9 inhibition as a therapy for lowering LDL-C

Due to the efficient and rapid translation from basic science to clinical practice, PCSK9 has become one of the most interesting drug targets in the last 15 years. Alirocumab and evolocumab are two fully human monoclonal antibodies raised against PCSK9 that have been approved by the US Food and Drug Administration for use in patients with FH and clinical atherosclerotic CVD (115). Two independent trials have demonstrated positive cardiovascular outcomes. Patients treated with alirocumab, combined with statins, have a 60% lowering of LDL-C and are protected against cardiac ischemic events (116). Moreover, inhibition of PCSK9 with evolocumab achieves additional lowering of LDL-C levels in patients with homozygous and heterozygous FH who respond poorly to high-dose statins (117). These data suggest that PCSK9 inhibition improves cardiovascular health and life expectancy of these patients. Current data also indicate that both alirocumab and evolocumab are well tolerated and do not result in increased risk for adverse events, such as an increase in new-onset type 2 diabetes, liver toxicity or impairment in cognitive function. Moreover, extremely low LDL-C concentrations (less than 20 mg/dl) with PCSK9 inhibition has been shown to have no side effects (118).

Anti-PCSK9 antibody treatment needs monthly subcutaneous injections, which has limited its wide-spread use. Currently, alternative approaches are under development to target PCSK9. Small interfering RNAs directly against hepatic *PCSK9* mRNA have shown significant reductions in LDL-C (119). This inhibition strategy is more durable and improves adherence without severe adverse outcomes (120). However, long-term follow-up on the

effectiveness and safety of this approach is needed. On the other hand, several approaches such as development of PCSK9 vaccine or CRISPR-Cas9 gene editing are ongoing to reduce PCSK9 levels (121,122). Despite these beneficial effects of PCSK9 inhibition, more mechanistic data are needed, which could potentially provide the proof of concept that future treatments with small molecule inhibitors of PCSK9 are feasible.

1.12 Study hypothesis and research objectives

1.12.1 Rationale and hypothesis

The important role for PCSK9 in cholesterol metabolism has been described above. I also emphasized the significance of the recently approved PCSK9 inhibitors for reducing hypercholesterolemia and the risk of CVD. It is clear that PCSK9 inhibitors are very promising therapeutic targets and have many beneficial effects besides LDL-C management. Nevertheless, more mechanistic data are needed for further understanding the biology of PCSK9, which could potentially be harnessed for therapeutic intervention and guide the use of anti-PCSK9 therapies.

This thesis investigates the molecular biology of PCSK9 with a focus on the role of the PCSK9 C-terminus. Previous studies have demonstrated the essential role of the CTD in PCSK9 physiology. First, the CTD has been implicated in PCSK9 secretion since LOF mutations such as E498K and S462P located in the C-terminus of PCSK9 impair its secretion (52,123,124). Removal of part of the C-terminus impairs PCSK9 secretion (108,125). However, how exactly the CTD contributes to PCSK9 secretion is not completely understood.

Second, the CTD does not directly interact with the LDLR, but is required for LDLR degradation (97,104,108). The CTD of PCSK9 has a novel protein fold and might also mediate protein-protein interactions (83,109). Moreover, natural mutations that occur within

this domain (H553R, Q554E) affect PCSK9's potency in mediating LDLR degradation (110). Incubation of purified mutant PCSK9 lacking the CTD (PCSK9ΔCTD) shows no detectable reduction of cell surface LDLR levels (97,108), whereas reconstitution of PCSK9ΔCTD with a foreign lysosomal targeting motif rescues its intracellular lysosomal targeting and induces LDLR degradation, emphasizing a role for the CTD in sorting of the PCSK9/LDLR complex towards the late endocytic compartments (111). These data suggest that the CTD carries structural requirements to achieve the critical later steps of LDLR sorting and degradation within endosomes/lysosomes. Since both the LDLR and PCSK9 lack a lysosomal targeting motif, it is possible that the CTD of PCSK9 recruits other partner(s) to the PCSK9/LDLR complex that can direct LDLR to the lysosome or block binding of the cofactor(s) that is/are required for LDLR recycling from endosomes to the cell surface.

My overall hypothesis is that the CTD of PCSK9 plays a critical role in the secretion of PCSK9 and in the lysosomal degradation of LDLR induced by PCSK9 through recruiting cofactors.

1.12.2 Research objectives

To test my hypothesis, I developed the following research aims as shown in Figure 1.7:

1. To characterize the role of PCSK9 C-terminus and the COPII adaptor protein SEC24 isoforms in PCSK9 secretion;

2. To identify the amino acid residues in the ligand-binding repeat domain of the LDLR important for PCSK9 C-terminus binding at the cell surface;

3. To investigate the role of unknown PCSK9 C-terminus-binding partner(s) in the regulation of LDLR and cholesterol metabolism *in vitro* and *in vivo*.

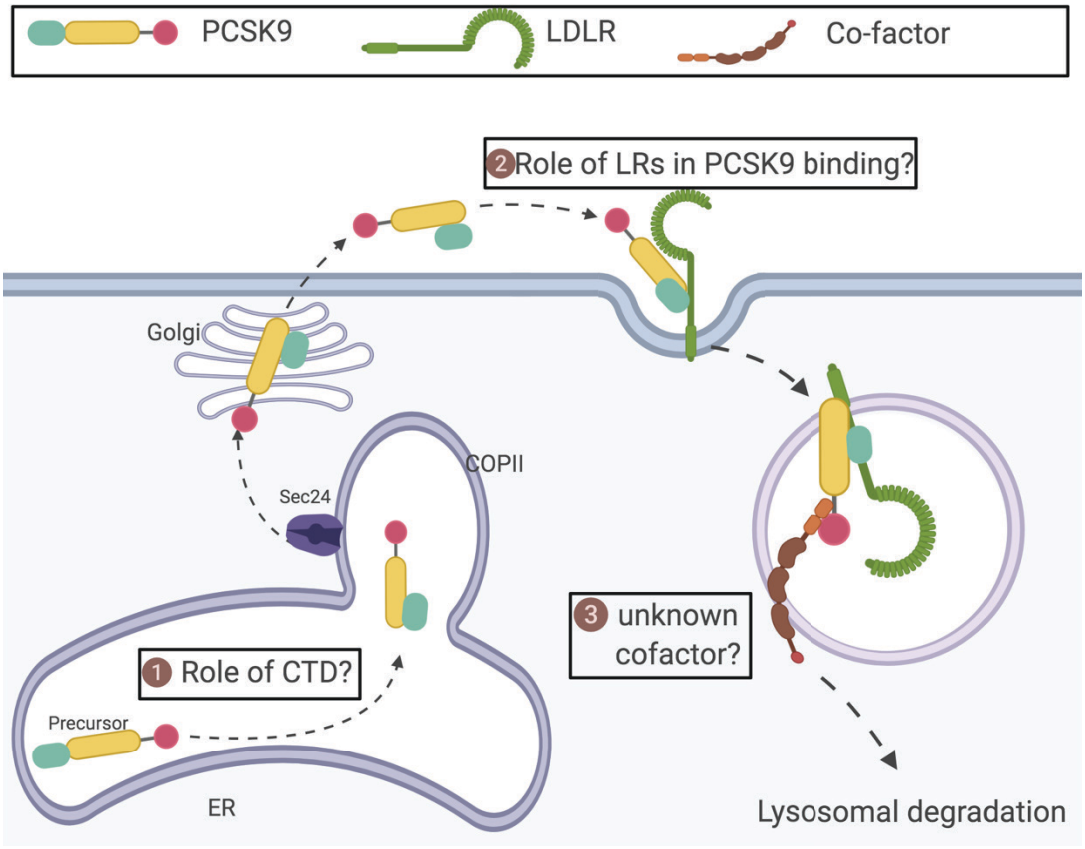

Figure 1.7 Study hypothesis and research objectives.

This dissertation aims to address the above three important questions about PCSK9 and LDLR. In Chapter 3, the structural requirements of CTD for PCSK9 secretion and adaptor proteins for its ER exit are investigated. The amino acid residues in the ligand-binding repeat domain of LDLR important for PCSK9 binding at the cell surface are characterized in Chapter 4. In Chapter 5, an unknown cofactor, prosaposin, is identified to play an important role in regulating LDLR and cholesterol *in vitro* and *in vivo*. In these chapters, mouse models as well as cultured cells, are used to investigate the potential relevance of such findings. The data provided not only shed important light on the role and regulation of PCSK9 in LDLR but also reveal novel mechanisms involved in the control of cholesterol metabolic homeostasis.

Chapter 2

Materials and Methods

2.1 Materials

DMEM, penicillin-streptomycin, trypsin-EDTA solution, Dil-labeled human LDL, and unlabeled human LDL were obtained from ThermoFisher Scientific. Complete EDTA-free protease inhibitors and X-tremeGENE HP DNA transfection reagent were purchased from Millipore Sigma. Peptide N-glycosidase F (PNGase F) was obtained from New England Biolabs (Beverly, MA). Lipofectamine RNAiMax, Lipofectamine^{TM} 3000 were obtained from Invitrogen. Culture medium and antibiotics were purchased from Thermo Scientific. Bovine serum albumin (BSA), complete EDTA-free protease inhibitors and fetal bovine serum (FBS) were purchased from Sigma. IRDye Secondary Antibodies (IRDye 800CW Goat anti-Rabbit IgG and IRDye 680 Goat anti-Mouse IgG) were purchased from Licor Biosciences. QuickChange Lightning Site-Directed Mutagenesis Kits were purchased from Agilent Technologies. PVDF (polyvinyl difluoride) membranes and nitrocellulose membranes were purchased from Thermo Scientific and GE Healthcare, respectively. The antifade reagent was purchased from Vector Laboratories (Burlingame, CA). All other reagents were obtained from Fisher Scientific unless otherwise indicated. Protein purity was monitored by sodium dodecyl sulfate polyacrylamide gel electrophoresis (SDS-PAGE) and protein staining using EZ-Run protein gel staining solution.

2.2 Antibodies

All antibodies used for immunoblotting and immunohistochemistry are listed in Table 2.1. Catalogue number, immunogen and dilution ratio were provided as followed.

Table 2.1 Used antibodies and dilutions

Antibody	Catalogue no.	immunogen	host	dilutions
PSAP	RC2174551A	AA 1-250	Rabbit	1:3,000
PCSK9	15A6	CTD	Mouse	1:1000
PCSK9	13D3	CAT	Mouse	1:3000
HA	OPA1-10980	YPYDVPDYA	Rabbit	1:1,000
MPSAP	GR7466-16	n/a	Rabbit	1:1,000
ATPASE	610993	AA 1-100	Rabbit	1:500
ACTIN	612657	n/a	Mouse	1:10,000
CALNEXIN	610524	AA 116-301	Mouse	1:2,000
APOA1	3350	n/a	Mouse	1:3,000
ANTI-MYC	C 3956	EQKLISEEDL	Rabbit	1:1000
TFR	612125	AA 517-623	Mouse	1:10,000
LDLR	HL-1	C-terminus	Mouse	1:5,000
SEC24A	HOOO 10802-MO1	AA 642-672	Rabbit	1:1000
SEC24B	F1611	n/a	Goat	1:500
SEC24C	8531s	n/a	Rabbit	1:500
SEC24D	A1411	n/a	Rabbit	1:300

2.3 Site-directed mutagenesis of LDLR and PCSK9

The cDNAs of human LDLR and PCSK9 cDNA were also cloned into the directional pcDNA3.1 vector. The mutations were generated using the QuickChange Lightning Site-Directed Mutagenesis Kits according to the manufacturer's instructions. Oligonucleotides bearing mismatched bases at the residue to be mutated were synthesized by IDT, Inc. (Coralville, IA). The sample reactions were set up at 25 µl volume, containing 2.5 µl of 10× reaction buffer, 50 ng of dsDNA template, 125 ng of oligonucleotide primer (forward), 125 ng

of oligonucleotide primer (reverse), 0.5 µl of dNTP mix, 0.75 µl of QuikSolution reagent and 0.5 µl of QuikChange Lightning Enzyme. The reaction conditions are listed in Table 2.2.

Table 2.2 Cycling Parameters for the QuickChange Site-Directed Mutagenesis

segment	cycles	temperature	time
1	1	95 ℃	30 seconds
2	12-18	95℃	30 seconds
		55℃	1 minute
		68℃	1 minute/kb

The amplification reaction samples were then incubated with 1 µl of Dpn I restriction enzyme at 37°C for 1 h. 1 µl of Dpn I treated DNA from each reaction sample was transformed into 50 µl DH5-α competent cells. DNA and competent cells were gently mixed and incubated on ice for 30 min, and then cells were heat-shocked at 42°C for 30 seconds, following with incubation on ice for 2 min. With the addition of 500 ul pre-warmed NZY^+ broth, the transformants were incubated at 37°C for 1 hour with shaking at 225-250 rpm, and then selected on the agar plates containing antibiotic ampicillin (at 100µg/ml). The presence of the desired mutation and the integrity of each construct were verified by DNA sequencing (TAGC, Edmonton, Canada).

All primers used for site-directed mutagenesis are listed in Table 2.3.

Table 2.3 Primers for mutagenesis

Target	Forward primer	Reverse primer
	PCSK9	
PCSK9$^{1-527}$	5'-AGG TGC TGC CTG CTA TGA CAG GCC AAC TGC-3'	5'-GCA GTT GGC CTG TCA TAG CAG GCA GCA CCT-3'
PCSK9$^{1-452}$	5'-CAT GGG GCA GGT TGG TAG CTG TTT TGC AGG -3'	5'-CCT GCA AAA CAG CTA CCA ACC TGC CCC ATG-3'
PCSK9$^{1-446}$	5'-GCC CTG CCC CCC TGA ACC CAT GGG GCA-3'	5'-TGC CCC ATG GGT TCA GGG GGG CAG GGC-3'
PCSK9$^{1-445}$	5'-GCC GCC CTG CCC TGA AGC ACC CAT GGG-3'	5'-CCC ATG GGT GCT TCA GGG CAG GGC GGC-3'
PCSK9$^{1-444}$	5'-GTG GCG GCC CTG TGA CCC AGC ACC CAT G-3'	5'-CAT GGG TGC TGG GTC ACA GGG CGG CCA C-3'
PCSK9$^{1-442}$	5'-CTG GTG GCC GCC TAG CCT CCC AGC ACC CA-3'	5'-TGG GTG CTG GGA GGC TAG GCG GCC ACC AG-3'
PCSK9$^{1-425}$	5'-AAA GAT GTC ATC AAT TAG GCC TGG TTC CC-3'	5'-GGG AAC CAG GCC TAA TTG ATG ACA TCT TT-3'
P445A	5'- GCC GCC CTG CCC GCC AGC ACC CAT GGG-3'	5'- CCC ATG GGT GCT GGC GGG CAG GGC GGC -3'
P445F	5'- GGT GGC CGC CCT GTT CTG AAG CAC CCA TGG -3'	5'- CCA TGG GTG CTT CAG AAC AGG GCG GCC ACC -3'
P445D	5'- GGT GGC CGC CCT GGA CTG AAG CAC CCA TGG -3'	5'- CCA TGG GTG CTT CAG TCC AGG GCG GCC ACC -3'
P445T	5'- GGT GGC CGC CCT GAC CTG AAG CAC CCA TG -3'	5'- CAT GGG TGC TTC AGG TCA GGG CGG CCA CC -3'
P445A-FL	5'-GGT GGC CGC CCT GGC CCC CAG CAC CCA TG-3'	5'-CAT GGG TGC TGG GGG CCA GGG CGG CCA CC-3'
P445F-FL	5'-GGT GGC CGC CCT GTT CCC CAG CAC CCA TGG-3'	5'-CCA TGG GTG CTG GGG AAC AGG GCG GCC ACC-3'
S462P	5'-TGCAGGACTGTGTGGCCAGCACACTCGGGG-3'	5'-CCCCGAGTGTGCTGGCCACACAGTCCTGCA-3'
S565L	5'-GTGTGGTCAGCACACTTGGGGCCTACACGG-3'	5'-CCGTGTAGGCCCCAAGTGTGCTGACCACAC-3'
R469W	5'-CACTCGGGG CCTACATGGATGGCCACAGCCAT-3'	5'-ATGGCTGTGGCCATCCATGTAGGCCCCGAGTG-3'
D480N	5'-GCC CGC TGC GCC CCA AAT GAG GAG CTGCTG-3'	5'-TCA GCA GCT CCT CAT TTG GGG CGC AGC GGG C-3'
E482G	5'-GCG CCC CAG ATG AGG GGC TGC TGA GCT GCT C-3'	5'-GAG CAG CTC AGC AGC CCC TCA TCT GGG GCG C-3'
R495Q	5'-TCCAGGAGTGGG AAG CAG CGG GGC GAGCGC AT-	5'-ATG CGC TCG CCCCGCTGC TTC CCACTCCTGGA-3'
R496W	5'-AGGAGTGGGAAGCGGTGGGGCGAGCGCATG-3'	5'-CATGCGCTCGCCCCACCGCTTCCCACTCCT-3'
R499H	5'-AAGCGG CGGGGCGAGCAC ATG GAG GCCCAAGGG-	5'-CCCTTGGGCCTCCATGTG GTC GCC CCG CCG CTT-3'
A522T	5'-GGT GAG GGT GTC TAC ACC ATT GCC AGG TGC-3'	5'-GCA CCT GGC AAT GGT GTA GAC ACC CTC ACC-3'
	LDLR	
D196N	5'-CCA GCT GGC GCT GTA ATG GTG GCC CCG CCG AC-	5'-GTC GGG GCC ACC ATT ACA GCG CCA GCT GG-3'
D203N	5'-GCC CCG ACT GCA AGA ACA AAT CTG ACG AG-3'	5'-CTC GTC AGA TTT GTT CTT GCA GTC GGG GC-3'
E208Q	5'-CAA ATC TGA CGA GCA AAA CTG CGC TGT GGC-3'	5'-GCC ACA GCG CAG TTT TGC TCG TCA GAT TTG-3'
E180Q	5'-CCT GCT CGG CCT TCC AGT TCC ACT GCC TA-3'	5'-TAG GCA GTG GAA CTG GAA GGC CGA GCA GG-3'
D203Q	5'-CCT CGT CAG ATT TCT GCT TGC AGT CGG G-3'	5'-CCC GAC TGC AAG GCC AAA TCT GAC GAG-3'
D203A	5'-CCC GAC TGC AAG GCC AAA TCT GAC GAG-3'	5'-CTC GTC AGA TTT GGC CTT GCA GTC GGG-3'
D203V	5'-CCC GAC TGC AAG GTC AAA TCT GAC GAG-3'	5'-CTC GTC AGA TTT GAC CTT GCA GTC GGG-3'
D203G	5'-CCC GAC TGC AAG GGC AAA TCT GAC GAG-3'	5'-CTC GTC AGA TTT GCC CTT GCA GTC GGG-3'

2.4 Cell culture and transfection

All cells were cultured at 37 ℃ in a 5% CO_2 humidified incubator. HEK293, HepG2, Huh7 cells were maintained in DMEM (high glucose) containing 10% (v/v) FBS. Hepa1c1c7 cells were maintained in MEM α containing 10% FBS. Dicer-Substrate siRNA (DsiRNA) and plasmid DNA were introduced into cells using Lipofectamine™ RNAiMAX and X-tremeGENE™ HP (HEK293, Huh7, and Hepa1c1c7 cells) or Lipofectamine™ 3000 (HepG2 cells), respectively, according to the manufacturer's instructions. Scrambled and predesigned DsiRNAs against PSAP, PCSK9, SEC24s were purchased from IDT® and listed in Table 2.4.

For siRNA transfection, Huh7 and HepG2 cells were seed at a 12-well plate with a density of 1.0 x 10^5 cell/well without antibiotics. The next day, cells were transfected with Lipofectamine® RNAiMAX transfection reagent. 1 ul of 10 uM siRNA was added to 50 ul Opti-MEM and mixed with 3 ul of RNAiMAX in 50 ul Opti-MEM for 5 min (final concentration 10 nM). Mixtures were added to each well dropwise. After 48 hours, whole cell lysate was subjected to immunoblotting. Scrambled siRNA was served as controls.

In the case of lysosomal staining, cells were pre-incubated with LysoTracker Red (100 nM) for 30 minutes, washed twice with ice-cold PBS and placed in cell imaging medium (10 μM HEPES-HBSS, pH 7.4) for live-cell imaging.

Table 2.4 DsiRNAs for knocking down experiments

Target	forward	reverse
scramble	5'-AUUAGUGUGCGAUGUACCCAGGAAC-3'	5'-GUUCCUGGGUACAUCGCACACUAAUAU-3'
SEC24A	5'-UGCUAAUCAUUUAACCACAAGCATG-3'	5'-CAUGCUUGUGGUUAAAUGAUUAGCACC-3'
SEC24B	5'-ACUUACUGAAUGCAUUACCAAACAT-3'	5'-AUGUUUGGUAAUGCAUUCAGUAAGUCU-3'
SEC24C	5'-GCAUGAAGCUACUCCCAGUUUACCT-3'	5'-AGGUAAACUGGGAGUAGCUUCAUGCAC-3'
SEC24D	5'-GGUCACUACAGAUUGCAUGAUACAA-3'	5'-UUGUAUCAUGCAAUCUGUAUUGACCAG-3'

2.5 Immunoblotting

The cells were lysed in the lysis buffer B (1% Triton, 150 mM NaCl, 50 mM HEPES, pH 7.4) containing 1xComplete EDTA-free protease inhibitors for 30 min on ice. After centrifugation for 10 min at 20,000 × g at 4 °C, the supernatant was collected, and protein concentrations were determined by the BCA protein assay. Same amount of cell lysate proteins or culture medium was subjected to SDS polyacrylamide gel electrophoresis (SDS-PAGE, 4%-20%) and then transferred to nitrocellulose membranes (GE Healthcare) by electroblotting. Membranes were blocked for 30 min in 1XPBS containing 0.01% Tween-20 and 5% non-fat milk. Immunoblotting was performed using specific antibodies as indicated. 15A6, a monoclonal anti-LDLR antibody HL-1 (1:5000), a monoclonal anti-PCSK9 antibody 15A6 (1:2000) (126); 13D3, a monoclonal anti-catalytic domain of PCSK9 antibody (1:3000) (97); a monoclonal anti-actin antibody (1:5000, BD Bioscience); a monoclonal anti-transferrin receptor antibody (1:5000, BD Bioscience), a monoclonal anti-SEC24A antibody (1:1000, Abnova), a goat anti-SEC24B antibody (1:300, Santa Cruz), a rabbit polyclonal anti-SEC24C antibody (1:500, Cell Signaling Tech.), a rabbit anti-SEC24D antibody (1:1000, Cell Signaling Tech.). After incubation at 4 °C overnight, antibody binding was detected using IRDye680 or IRDye800-labeled goat anti-mouse or anti-rabbit IgG (Li-Cor). The signals were detected on a Licor Odyssey Infrared Imaging System (Li-Cor).

2.6 Immunofluorescence of LDLR and PSAP

Confocal microscopy was carried out as described previously (127-129). Approximately 1.5×10^5 HEK 293 cells were seeded in each well of a 12-well tissue culture dish on coverslips. After 24 h, the cells were transfected with plasmids expressing WT or mutant LDLR using X-tremeGENE HP (1.0 μg DNA and 2.5 μl HP/well) according to the

manufacturer's protocol. 48 h later, the cells were washed and fixed with 3% paraformaldehyde in phosphate buffered saline (PBS). Cells were permeabilized using cold methanol (-20°C) for 20 min and washed with a blocking solution of 1% BSA in PBS. Then cells were incubated overnight in a blocking solution containing an anti-LDLR monoclonal antibody, HL-1 (used at 1:300 dilution). After washing with blocking solution for 10 min, cells were incubated with Alexa Fluor 488 goat anti-mouse IgG for 1 h, following with another 3 times washing with the blocking solution, 10 min for each. Coverslips were mounted on the slides with one drop of Antifade reagent containing 4',6-diamidino-2-phenylindole (DAPI) (Vector Laboratories, Burlingame, CA). Localization of LDLR in the transfected cells was determined using a Leica SP5 laser scanning confocal microscope (filters: 461 nm for DAPI, 488 nm for Fluor 488).

2.7 Biotinylation of cell surface protein

Biotin labelling of cell surface proteins was carried out exactly as previously described (32). For transient transfection, HEK 293 cells were set up in a 6-well plate and transfected with plasmids expressing WT or mutant LDLR as described previously. After 48 h, HEK 293 cells overexpressing WT or mutant LDLR were washed twice with ice-cold PBS buffer, and then biotinylated using EZ-Link Sulfo-NHS-LC-Biotin following the manufacturer's protocol (Thermo Scientific). Specifically, cells were incubated with 0.5 mg/ml EZ-Link Sulfo-NHS-LC-Biotin in amine-free PBS buffer, gently rocking at 4°C for 30 min. Cells were then washed with cold PBS buffer twice, and the reaction was terminated by blocking with cold PBS containing 100 mM glycine for 20 min at room temperature (RT). After 3 times washing with PBS, cells were lysed in 200 μl of lysis buffer B (1% triton, 150 mM NaCl, 50 mM Tris-HCl, pH 7.4). A total of 45 μl of the cell lysate was saved, and 150 μl of the lysate was added to 60

μl of 50% slurry of Streptavidin-agarose (Thermo Scientific) and another 200 μl of lysis buffer B. The mixture was rotated overnight at 4°C. After centrifugation at 7000 rpm for 5 min, the pellets were washed three times with lysis buffer B by centrifugation at 7000 rpm for 5 min and the cell surface proteins were eluted from the beads by adding 60 μl 2× SDS loading buffer (62 mM Tris-HCl, pH 6.8, 2% SDS, 50% glycerol, 0.005% bromophenol). A 15 μl 4× SDS loading buffer was added to the saved 45 μl cell lysate, and both cell lysate and cell surface proteins were incubated for 5 min at 95°C. Proteins were then subjected to SDS/PAGE (8%) and analyzed by immunoblotting with a mouse anti-LDLR monoclonal antibody (HL-1) and a mouse anti-transferrin receptor monoclonal antibody.

2.8 Binding of PCSK9 to LDLR and PCSK9-promoted LDLR degradation.

The experiments were performed as described in our previous studies (23,97,127). Basically, the recombinant full-length human PCSK9 contained a FLAG tag at the C-terminus was purified from HEK 293S cells as described (23,97,127). Cells were seeded in 12-well dishes in 1 ml of culture medium containing 1.5×10^5 cells/well. 24 h later, the cells were transfected with empty plasmid or a plasmid carrying the wild-type or mutant LDLR cDNA using X-tremeGENE HP (1.0 μg DNA and 2.5 μl HP/well) according to the manufacturer's protocol. For PCSK9 binding, 48 h after transfection, binding of PCSK9 to LDLR at different pH values was carried out as described (127). Briefly, cells were washed twice with ice-cold pH 7.4 buffer (50 mM Tris-HCl, 150 mM NaCl, 2 mM $CaCl_2$, and 2.5% non-fat milk) or pH 6.0 buffer (25 mM Tris-Maleate buffer, 150 mM NaCl, 2 mM $CaCl_2$, and 2.5% non-fat milk), chilled on ice for 30 min in the pH buffer to inhibit LDLR endocytosis. PCSK9 (2 μg/well) was then added to the chilled cells in the ice-cold relevant pH buffer and incubated for 2-hour on ice that could inhibit PCSK9-promoted LDLR degradation. After, the cells were washed

twice in the ice-cold relevant pH buffer and then collected for the preparation of whole cell lysate. For PCSK9-promoted LDLR degradation, 48 h after transfection, the cells were washed twice in DMEM and then incubated with DMEM containing different amounts of PCSK9 as indicated for 12 h at 37 °C in a 5% CO_2 humidified incubator. The cells were then washed twice in PBS and collected for the preparation of whole cell lysate. Protein concentrations were determined by the BCA protein assay. Same amount of whole cell lysate was subjected to SDS-PAGE (8%) and immunoblotting using the following antibodies: 15A6, a monoclonal anti-PCSK9 antibody; 13D3, a monoclonal anti-the catalytic domain of PCSK9 antibody (97); 9E10, a monoclonal anti-Myc tag antibody; HL-1, a monoclonal anti-LDLR antibody (23,97); a monoclonal anti-actin antibody, and a polyclonal anti-calnexin antibody (Invitrogen).

2.9 RNA isolation from cultured cells or mouse liver

Total RNAs were extracted from transfected Huh7 cells or from 50 mg of mouse liver using RNeasy Plus Mini Kit (Qiagen) or Trizol (Life Technologies), respectively. Liver was weighted 50 mg per sample, and briefly washed with PBS before 1 mL of Trizol reagent was applied to the homogenizer. The mixture was then transferred to an RNase-free tube and incubated at room temperature for 5 min before 200 μl of chloroform were added. The aqueous phase containing RNA was collected after centrifugation at 13,000 x g at 4 °C for 15 min. RNA was precipitated with an equal volume of isopropanol and centrifugation at 13,000 x g at 4 °C for 15 min. The purified RNA was further washed with 1 mL of 75% RNase-free ethanol to remove salts. The RNA was pelleted by centrifugation as above, dried at room temperature for several minutes, and dissolved in an appropriate amount of RNase-free water.

RNA concentration was determined by a NanoDrop 2000 spectrophotometer (Thermo Scientific).

2.10 Quantitative Real-Time PCR (qRT-PCR)

The cDNA for RT-PCR was prepared using 2000 ng RNA per sample, and a reverse transcription reaction was performed using the Superscript III system (Life Technologies). Relative qRT-PCR was carried out on StepOnePlus™ using SYBR®Select Master Mix according to the manufacturer's instruction. The human genes detected included *PSAP, GAPDH, LDLR, PCSK9 and SREBP2* and the mouse genes included *Psap, Gapdh, Pcsk9, Ldlr and Srebpf2*. Relative gene expression was normalized to the glyceraldehyde-3-phosphate dehydrogenase gene (*GAPDH*) that had a similar amplification efficiency as that of the target genes. Primers for human and mouse genes were designed by PrimerQuest Real-Time PCR Design Tool, synthesized by IDT, Inc., and listed in Table 2.5.

Table 2.5 Primers for qRT-PCR

Target	Forward primer	Reverse primer
GAPDH	5'-ACA TCG CTC AGA CAC CAT G-3'	5'-TGT AGT TGA GGT CAA TGA AGG G-3'
LDLR	5'-TTC ACT CCA TCT CAA GCA TCG-3'	5'-ACT GAA AAT GGC TTC GTT GAT G-3'
PCSK9	5'-CAC AGA GTG GGA CAT CAC AG-3'	5'-TTT GGC AGA GAA GTG GAT CAG-3'
PSAP	5'-TGC CAG AAT GTG AAG ACG G-3'	5'-TCC TTC AGC ATA TCA CCA GC-3'
IDOL	5'-TGC TGT GTT ATG TGA CGA GG-3'	5'-CTT TGC TAC CCG TAA ACT GC-3'
SREBP2	5'-TTC CTG TGC CTC TCC TTT AAC-3'	5'-TCA TCC AGT CAA ACC AGC C-3'
HMGCR	5'-ACA GAT ACT TGG GAA TGC AGA-3'	5'-CTG TCG GCG AAT AGA TACACC-3'
MPCSK9	5'-TTT TAT GAC CTC TTC CCT GGC-3'	5'-ATT CGC TCC AGG TTC CAT G-3'
MPSAP	5'-TGG ACA TGA TTA AGG GCG AG-3'	5'-CTG TTT CTG GTT TTG CTC GG-3'
MLDLR	5'-AAC CGC CAA GAT CAA GAA AG-3'	5'-GCT GGA GAT AGA GTG TTT G-3'
MSREBF2	5'-CCC TAT TCC ATT GAC TCT GAG C-3'	5'-CAC ATA GGA TTC GAG AGC G-3'
MGAPDH	5'-CTT TGT CAA GCT CAT TTC CTG G-3'	5'-TCT TGC TCA GTG TCC TTG C-3'
MHMGCR	5'-GCC CTC AGT TCA AAT TCA CAG-3'	5'-TTC CAC AAG AGC GTC AAG AG-3'
SEC24A	5'-TTC CTT CTCAGT GGA CAG TAT TC-3'	5'-GCT GAT GAT GGT AAG AGG GAT AG-3'
SEC24B	5'-CTC AGT TAC ACA GCC ATC AGA G-3'	5'-TCA ACA CCT GCT TCC TCA TC-3'
SEC24C	5'-TGA TGG TTG TGT CTG ATG TGG-3'	5'-TGT CTC TGT TTC CCT TGT GTC-3'
SEC24D	5'-GAA CGA GCA TAC CAG AGA CAG-3'	5'-GAA AGA CGG GAC TCA GAG C-3'

2.11 Dil-LDL binding assay

For LDL uptake by mutant LDLR, hepa1c1c7 cells were seed at a density of 30,000 cells/well in a 96-well plate in 100 μl of MEM-α containing 10% FBS. 24 h later, the cells were transfected with a plasmid carrying the wild-type or mutant LDLR cDNA using X-tremeGENE HP (0.1 μg DNA and 0.25 μl HP/well) or siRNA against mouse PSAP using Lipofectamine RNAiMAX according to the manufacturer's protocol. 48 h after transfection, the LDL binding assay was performed as previously described (130,131). Briefly, cells were

washed with Opti-MEM. Dil-labelled LDL (10 μg/ml) was then added to cells in 100 μl of MEM-α containing 5% newborn calf lipoprotein-poor serum (NCLPPS) in the presence or absence of unlabeled human LDL (600 μg/ml). The plates were incubated at 37 °C for 6 h. After, the cells were washed four times in the washing buffer (50 mM Tris-HCl, pH7.4, 150 mM NaCl, 2 mg/ml BSA) and then lysed in 100 μl of RIPA buffer (50 mM Tris-HCl, ph7.4, 150 mM NaCl, 1% Triton X-100, 0.5% sodium deoxycholate, 0.1% SDS) contacting protease inhibitors. The lysate was then transferred to a 96-well black plate for the measurement of fluorescence using a SYNERGY plate reader at an excitation wavelength of 520 nm and an emission wavelength of 580 nm. The concentrations of total proteins in each well were measured using the BCA protein assay. LDL uptake was calculated by normalization of the fluorescence units to the amount of total proteins in the same well. The results obtained in the presence of excess unlabeled LDL revealed the nonspecific binding. Specific binding was calculated by subtraction of nonspecific binding from the total counts measured in the absence of unlabeled LDL.

2.12 Immunohistochemistry

All liver sectioning and staining were performed by the HistoCore facility in Alberta Diabetes Institute at the University of Alberta. The slides were stained with hematoxylin and eosin (H&E), trichrome, or Oil Red O, and then imaged on ZEISS Axio Observer A1.

2.13 Co-immunoprecipitation

Huh7 cells were plated in 100 mm^2-plates and transiently transfected with 10 ug of DNA coding for LDLR and PSAP using polyethyleneimine (PEI). 48 h after transfection, whole cell lysate was prepared in 300 ul lysis buffer B and immunoprecipitated with 2 μl anti-myc antibody 9E10 or anti-LDLR antibody HL-1 for 2 h. Then 20 μl protein G-beads were

then added to each tube and rotated at 4 °C overnight. The samples were washed 3 times with lysis buffer B in the following day. The immunoprecipitated proteins were then eluted with 20 µl 1x SDS loading buffer and subjected to SDS-PAGE and immunoblotting.

2.14 Plasma cholesterol, alanine aminotransferase (ALT) analysis

Heparin-plasma was isolated from blood collected from tail or saphenous veins of mice on the Western-Type diet. Plasma ALT, total cholesterol, HDL, and non-HDL cholesterol were measured using their specific commercial kits. Briefly, plasma total cholesterol levels were measured using colorimetric kits (Wako). Plasma lipoproteins were analyzed by running pooled plasma onto a fast protein liquid chromatography system by the Lipidomic Core Facility at the University of Alberta.

2.15 Preparation of adeno-associated virus (AAV)

Two PSAP shRNAs and a scrambled control shRNA were designed by the BLOCK-iT™ RNAi Designer and siRNA Wizard, respectively. Both were synthesized by Integrated DNA Technologies and then cloned into the pAAV-U6-GFP vector. pAAV-U6-shRNA-GFP, pAAV-helper, and pAAV-DJ/8 (Cell Biolabs) were co-transfected into HEK293 cells. After 72 h, cells were collected and lysed via freeze-thaw cycles and centrifuged for 10 min at 10,000 X g. AAVs in the supernatant were applied to a Optiprep density gradient ultracentrifugation. AAVs (density = 1.33 g/mL) were collected, diluted in 1XPBS and concentrated using a 100-kDa cut-off centrifugal filter to remove Optiprep. The titer of AAV was quantified using qRT-PCR and expressed as a genomic copy as described (132,133).

2.16 Deglycosylation of LDLR

HEK293 cells transiently expressing the wild-type or mutant LDLR were washed twice with PBS and collected in 1 mL of ice-cold PBS containing 2 mM EDTA. After centrifugation at 20,000 × g for 2 min at 4 °C, the cell pellets were resuspended in 20 µl of 1 × glycoprotein denaturing buffer, gently mixed, heated at 100 °C for 10 min, and then chilled on ice for 10 seconds. After, 4 µl of 10 × G7 reaction buffer (New England Biolabs), 4 µl of 10% Nonidet P-40 (vol/vol), and 12 µl of H_2O were added to the sample. Each sample was then supplied with 2 µl of PNGase F or H_2O, followed by incubation at 37 °C for 1 h. Protein glycosylation was monitored by immunoblotting.

2.17 Inhibition of N-glycosylation

HEK293 cells seeded in a 12-well plate were transfected with empty plasmid or a plasmid carrying the wild-type or mutant LDLR cDNA using X-tremeGENE HP (1 µg DNA, and 2.5 µl HP/well). 24 h later, the cells were incubated with tunicamycin dissolved in DMSO (Sigma, 0.5 µg/mL) or DMSO at 37 °C for 24 h. The cells were then washed twice in PBS and collected for the preparation of whole cell lysate and immunoblotting.

2.18 Animal handling and diets

All procedures were approved by the University of Alberta's Institutional Animal Care Committee in accordance with guidelines of the Canadian Council on Animal Care. Male C57BL/6 (backcrossed >7 generations) were exposed to a 12 h light-dark cycle and housed with free access to water and standard chow diet (LabDiet, #5001) with 58% calories from carbohydrate and 13% from fat. Tissues were collected and stored at -80 °C until analysis or preserved in 10% phosphate-buffered formalin for histology.

2.19 Statistic analysis

All statistical analyses were carried out by GraphPad Prism version 4.0 (GraphPad Software). Student's t-test or one-way ANOVA with Tukey post-hoc test was carried out to determine the significant differences between groups. All data met normal distribution criteria and variance between groups that was analyzed by F-test showed no significant difference ($P>0.05$). Values of all data unless otherwise indicated were mean ± S.D. The significance was defined as $*p<0.05$, $**$ $p<0.01$, $***$ $p<0.001$. All experiments except for where indicated were repeated at least three times.

Chapter 3: Manuscript I

The role of the C-terminal domain of PCSK9 and SEC24 isoforms in PCSK9 secretion

(submitted to Biochimica et Biophysica Acta - Molecular and Cell Biology of Lipids)

The role of the C-terminal domain of PCSK9 and SEC24 isoforms in PCSK9 secretion

Shi-jun Deng [a], Yishi Shen [a], Hong-mei Gu [a], and Da-wei Zhang [a, b] *

[a] Department of Pediatrics, Group on the Molecular and Cell Biology of Lipids, Faculty of Medicine and Dentistry, University of Alberta, Edmonton, Alberta, Canada.

Abstract

Proprotein convertase subtilisin/kexin type 9 (PCSK9) is a secretory protein that promotes LDL receptor (LDLR) degradation and thereby regulates plasma levels of LDL cholesterol. Previous studies have shown that the C-terminal domain (CTD) of PCSK9 is required for PCSK9 secretion. However, how exactly the CTD contributes to PCSK9 secretion is not completely understood. Here, we investigated the role of its CTD and SEC24, the cargo adaptor protein of the coated protein complex II, in PCSK9 secretion. We found that mutant $PCSK9^{1-528}$, in which amino acids from 529 to the end (amino acid 692) were deleted, was maturated and secreted from cells as efficiently as the wild type protein. Lacking amino acids from 454 to 692 in mutant $PCSK9^{1-453}$ significantly reduced its maturation and secretion, but to a lesser extent as compared to mutants $PCSK9^{1-446}$, $PCSK9^{1-445}$, and $PCSK9^{1-444}$ that missing amino acids 447-692, 446-692, and 445-692 respectively. These three mutants all significantly impaired PCSK9 maturation to a similar extent. However, mutant $PCSK9^{1-444}$ essentially eliminated PCSK9 secretion while $PCSK9^{1-446}$ and $PCSK9^{1-445}$ could be fairly secreted to culture medium. We also found that natural variants in the CTD including S462P, S465L, E482G, R495Q and A522T, impaired PCSK9 secretion. Furthermore, knockdown of SEC24A, SEC24B, SEC24C but not SEC24D reduced secretion of the full length PCSK9 but not mutant $PCSK9^{1-446}$. Together, these findings demonstrate the important role of the CTD of PCSK9 and SEC24A, SEC24B, and SEC24C in PCSK9 secretion.

Research highlights: ♦ Amino acids from 529 to 692 in C-terminus of PCSK9 is not required for its maturation and secretion. ♦ Removal of amino acids 445-692 essentially eliminates PCSK9 secretion. ♦ Natural variants S462P, S465L, E482G, R495Q and A522T impair PCSK9 secretion. ♦ SEC24A, B, C facilitate endogenous human PCSK9 secretion.

Keywords: Atherosclerosis, PCSK9, protein secretion, lipoprotein metabolism, LDL receptor

Abbreviations: COPII, the coat protein complex II; CTD, C-terminal domain (CTD); HEK293, human embryonic kidney; EGF-A, the epidermal growth factor precursor homology repeat-A; ER, endoplasmic reticulum; FH, familial hypercholesterolemia; LDL-C, low density lipoprotein cholesterol; LDLR, LDL receptor; NCLPPS, newborn calf lipoprotein-poor serum; PCSK9, proprotein convertase subtilisin/kexin type 9; SDS-PAGE, SDS polyacrylamide gel electrophoresis

3.1 Introduction

Proprotein convertase subtilisin/kexin type 9 (PCSK9) is a 692-amino acid secretory glycoprotein. It consists of a 30 amino acid signal sequence followed by a prodomain (PRO), a catalytic domain (CAT), and a C-terminal domain (CTD). The CTD domain contains an exposed hinge region (residues 426-439) and three repeat modules, module 1 (CM1: amino acids 457-528), module 2 (CM2: amino acids 534-601), and module 3 (CM3: amino acids 608-692) (105,108,125). GOF mutations in PCSK9 lead to elevated plasma LDL-C levels and accelerated atherosclerosis and premature coronary heart disease (41,42). Conversely, LOF PCSK9 mutations lead to reduced plasma LDL-C levels and protection from coronary heart disease (51,134). Inhibition or silence of PCSK9 is a novel powerful therapeutic approach to lower LDL-C (135-137).

Mechanistically, PCSK9 targets LDLR for degradation mainly through the extracellular pathway that requires clathrin-mediated endocytosis of the cell surface LDLR (23,97,126,127,138). PCSK9 shunts the typical LDLR recycling route, resulting in decreased levels of hepatocyte cell surface LDLR and increased plasma levels of LDL-C (56,126). PCSK9 interacts with the epidermal growth factor precursor homology repeat-A (EGF-A) of LDLR at the cell surface and binds to the receptor with a much higher affinity at the acidic environment of the endosome. Consequently, the receptor is redirected from the endosome to the lysosome for degradation (23,97,104,112,126,127,139-141). The X-ray crystallographic structure of PCSK9 with the partial extracellular domain of LDLR at a neutral pH value shows that the prodomain of PCSK9 also binds to the YWTD repeats of LDLR (142). Recently, we demonstrated that in addition to the EGF-A and the YWTD repeats, negatively charged residues in the ligand-binding repeats of LDLR play an important role in PCSK9 binding to the receptor (127).

PCSK9 is synthesized as a zymogen and undergoes autocatalytic cleavage in the ER at the FAQ152/SIPK site, which is required for protein secretion (82). Some LOF PCSK9 mutations reduce PCSK9 secretion, while GOF mutation E32K enhances PSCK9 secretion (143,144). Further, circulating PCSK9 is rapidly cleared from plasma with a half-life of about 5 min in mouse blood (145). Thus, targeting PCSK9 secretion is a promising strategy to reduce LDL-C levels. Circulating PCSK9 is mainly secreted from the liver (57). However, the molecular mechanism of PCSK9 secretion is unclear.

The C-terminal PCSK9 has been implicated in its secretion. LOF mutations such as S462P and C679X located in the C-terminus of PCSK9 impair its secretion (52,123,124). Removal of part of C-terminus leads to deficient PCSK9 secretion (108,125). Here, we further characterized the role of the C-terminus of PCSK9 in its secretion. In addition, COPII transports secretory proteins from the ER to the Golgi for secretion. It has been shown that SEC24A and SEC24B facilitate PCSK9 secretion in mouse and in 293T cells (88). Mammalian cells express four SEC24 isoforms, SEC24A, SEC24B, SEC24C and SEC24D, each preferentially mediating the recruitment of specific cargo proteins into COPII vesicles for subsequent export from the ER (86,146,147). Considering plasma PCSK9 is mainly secreted from hepatocytes (57), we investigated the role of SEC24 isoforms in the secretion of endogenous human PCSK9 from human hepatoma-derived cells, Huh7. We found that the lack of amino acids 445 to 692 in mutant $PCSK9^{1-444}$ almost completely eliminated PCSK9 secretion and that SEC24A, SEC24B and SEC24C but not SEC24D were involved in endogenous human PCSK9 secretion.

3.2 Results

3.2.1 The impact of C-terminal truncated mutants on PCSK9 secretion

Given the role of the CTD in PCSK9 secretion and function (97,104,112,141), we assessed the minimum length requirement of CTD for PCSK9 secretion. C-terminal PCSK9 (amino acids 426-692) contains three modules and a hinge region that connects the C-terminus to the catalytic domain (Fig 3.1A). We introduced a stop codon at different positions to make five truncated PCSK9 mutants, $PCSK9^{1-528}$, $PCSK9^{1-453}$, $PCSK9^{1-446}$, $PCSK9^{1-445}$, and $PCSK9^{1-444}$, in which amino acids 529 to 692 including both CM2 (amino acids 534-601) and CM3 (amino acids 608-692), amino acids 454 to 692 including all three C-terminal modules, amino acids 447 to 692, amino acids 446 to 692, and amino acids 445 to 692 were removed, respectively (Fig 3.1A). We then transiently overexpressed these mutants in HEK293 cells and monitored their expression in whole cell lysate and their secretory form in culture medium. As shown in Figure 3.1B, all mutants could undergo self-cleavage to produce the mature form. To assess the effect of the deletions on PCSK9 maturation, we quantified the amount of the mature form of PCSK9 in whole cell lysate and culture medium and total PCSK9 (mature form + precursor). As shown in Figure 3.1C, mutant $PCSK9^{1-528}$ that retained CM1 had no significant effect on PCSK9 maturation (Fig 3.1C). On the other hand, when compared to the wild-type protein or mutant $PCSK9^{1-528}$, mutants $PCSK9^{1-444}$, $PCSK9^{1-445}$, and $PCSK9^{1-446}$ that lacked the entire CM1-CM3 domains and a partial hinge region all markedly reduced the amount of the mature form of PCSK9 to the same degree, mutant $PCSK9^{1-453}$ also significantly reduced PCSK9 maturation but to a lesser extent. The difference in PCSK9 maturation between mutants $PCSK9^{1-453}$ and $PCSK9^{1-446}$, or among the three mutants $PCSK9^{1-444}$, $PCSK9^{1-445}$, and $PCSK9^{1-446}$ was not statistically significant, but it was statistically

significant between mutants PCSK9$^{1-453}$ and PCSK9$^{1-444}$ or PCSK9$^{1-445}$.

We then defined the impact of these mutations on PCSK9 secretion. PCSK9 secretion efficiency was expressed as the ratio of the amount of mature PCSK9 in medium to that of total mature PCSK9 detected in cells plus medium. As shown in Figure 1D, the amount of secreted PCSK9 in culture medium was comparable between the wild-type PCSK9 and PCSK9$^{1-528}$, PCSK9$^{1-453}$ but significantly decreased in all other mutants tested. The difference among mutants PCSK9$^{1-453}$, PCSK9$^{1-446}$ and PCSK9$^{1-445}$ was either nonsignificant or only mild (Fig 3.1E). Conversely, PCSK9$^{1-444}$ dramatically suppressed PCSK9 secretion.

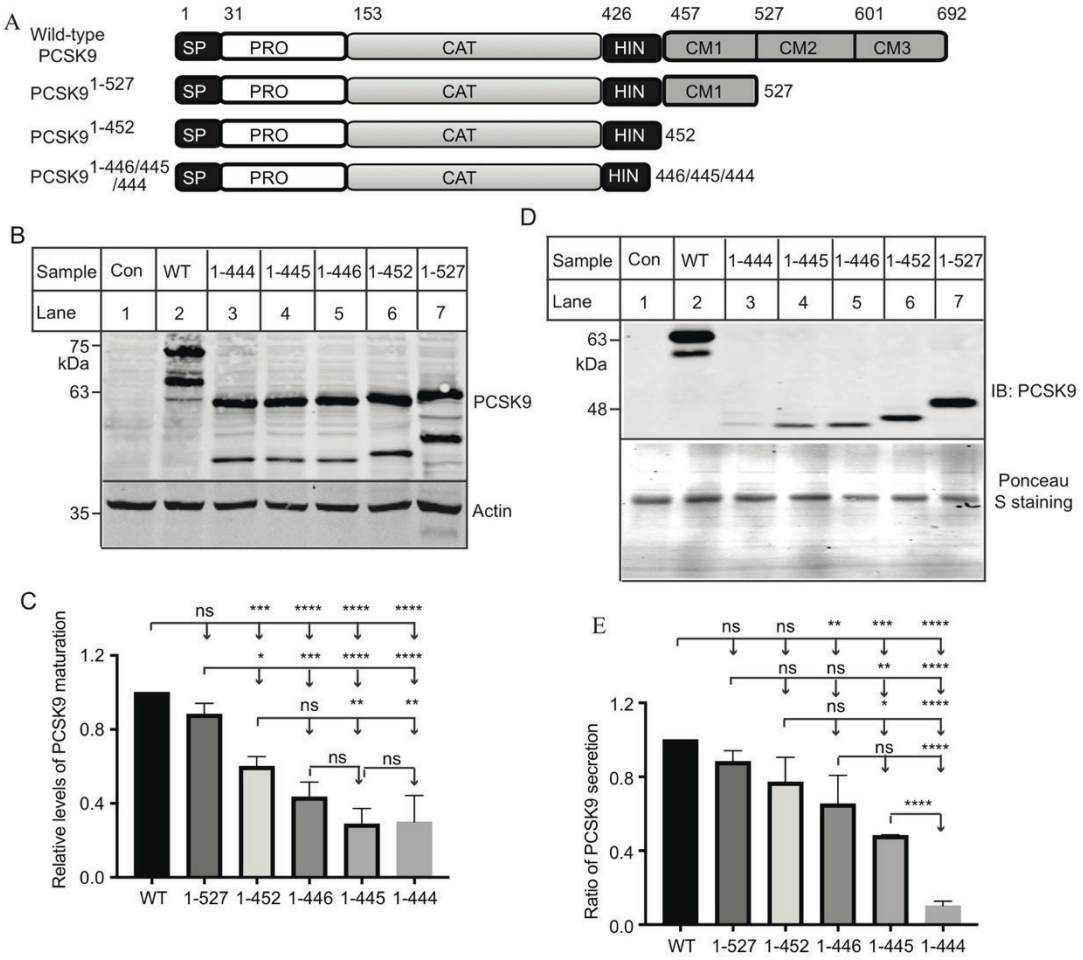

Figure 3.1 Secretion of the wild-type and mutant PCSK9. ***A. Schematic of the full-length and different C-terminal deletion mutant PCSK9.*** SP, signal peptide; PRO, prodomain; CAT, catalytic domain; HIN, hinge region; CM1, CM2 and CM3: three modules of C-terminal domain. Numbers on the top of the wild-type PCSK9 indicates the amino acid sequence of each domain. ***B to D. Maturation (B and C) and secretion (D and E) of the wild-type and mutant PCSK9 in HEK293 cells.*** HEK293 cells were transfected with the wild-type (WT) or mutant PCSK9 as indicated. Cells and medium were collected separately. Same amount of whole cell lysate or culture medium was subjected to SDS-PAGE, followed by immunoblotting using a monoclonal anti-PCSK9 antibody 13D3 and a monoclonal anti-actin antibody. Culture medium was applied to SDS-PAGE in duplicate, one for immunoblotting and one for ponceau S staining as the loading control. In the whole cell lysate, bottom band of PCSK9 was the cleaved mature form of PCSK9. Top band was the precursor form. **Control (Con)**: cells were transfected with the empty vector, pCDNA3.1. The relative levels of PCSK9 maturation were the ratio of the densitometry of PCSK9 mature form in whole cell lysate plus secreted PCSK9 in medium to that of total PCSK9 (precursor + mature form + secreted form). The ratio of PCSK9 maturation was the ratio of the relative levels of mutant PCSK9 to that of the wild-type PCSK9 that was defined as 1 **(C)**. The relative levels of PCSK9 secretion were the ratio of the densitometry of secreted PCSK9 in culture medium to that of total mature PCSK9 (mature form PCSK9 in whole cell lysate + secreted PCSK9 in culture medium). The ratio of PCSK9 secretion was the ratio of the relative levels of mutant PCSK9 secretion to that of the wild-type PCSK9 that was defined as 1. Values of all data were mean ± S.D. The significance was defined as *$p<0.05$, ** $p<0.01$, *** $p<0.001$. All experiments were repeated at least three times.

To further determine if PCSK9 secretion could be completed inhibited, we made two more mutants, PCSK9$^{1-443}$ that lacked a partial hinge region and the three C-terminal modules and PCSK9$^{1-425}$ that missed the whole hinge region and the three C-terminal modules (Fig 3.2A). The two mutations impaired PCSK9 maturation and secretion to a similar extent as mutant PCSK9$^{1-444}$, essentially eliminating PCSK9 secretion. Together, it appears that CM2 and CM3 (amino acids 529-692) in the C-terminus of PCSK9 is not required for PCSK9 maturation and secretion, whereas the length of and/or specific amino acid residues in CM1 (amino acids 454-528) and the hinge region (amino acids 426-453) play a role in PCSK9 maturation and secretion and amino acid residue at position 445 seems to be critical for PCSK9 secretion.

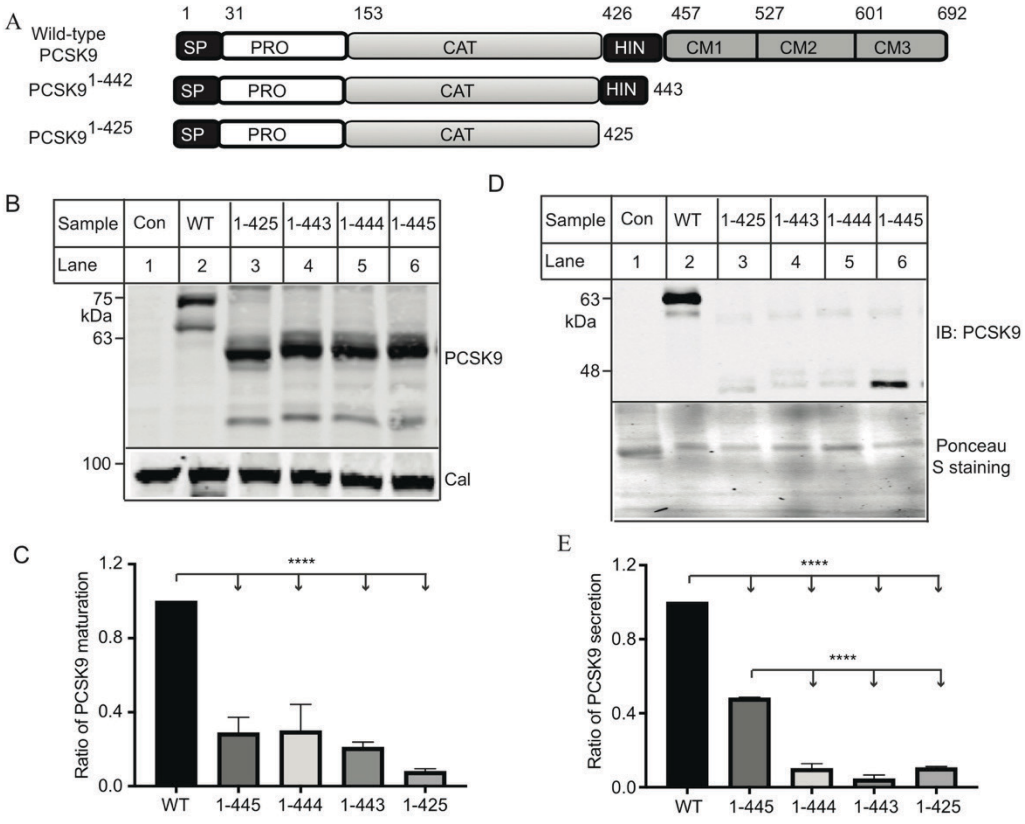

Figure 3.2 Secretion of the wild-type and mutant PCSK9. The experiments were

performed exactly as described in the legend to Figure 3.1 except that different mutant PCSK9 was used. Values of all data were mean ± S.D. The significance was defined as *$p<0.05$, ** $p<0.01$, *** $p<0.001$. All experiments except for where indicated were repeated at least three times.

3.2.2 The role of proline at position 445 in PCSK9 secretion

Next, we assessed the role of proline at position 445 (Pro^{445}) in PCSK9 secretion. Pro^{445} in mutant $PCSK9^{1-445}$ was replaced with a neutral amino acid residue Ala (P445A), a negatively charged residue Asp (P445D), a positively charged residues Lys (P445K), a hydrophobic aromatic amino acid Phe (P445F), and a polar amino acid Thr (P445T). The wild-type and mutant $PCSK9^{1-445}$ were transiently expressed in HEK293 cells. Whole cell lysate and culture medium were collected separately for immunoblotting. The amount of the precursor and mature form of PCSK9 in whole cell lysate was comparable between the wild-type and mutant $PCSK9^{1-445}$ except for mutation P445F that almost completely suppressed self-cleavage of $PCSK9^{1-445}$ (Fig 3.3A and 3.3B). On the other hand, all of the mutant PCSK9 significantly reduced the amount of secreted PCSK9 in culture medium (Fig 3.3C and 3.3D), indicating that these mutations impaired secretion of $PCSK9^{1-445}$. Thus, Pro at position 445 appears to be required for the efficient auto-cleavage and secretion of $PCSK9^{1-445}$.

We then replaced Pro^{445} with Ala (P445A) and Phe (P445F) in the full-length PCSK9 to investigate its effect on PCSK9. As shown in Figures 3.3E to 3.3H, the precursor and mature form of PCSK9 in cells and the mature form of PCSK9 in culture medium were comparable between mutation P445A and the wild type full-length PCSK9, indicating a negligible effect of this mutation on the full-length PCSK9 processing and secretion. Conversely, mutation P445F significantly reduced the amount of the mature form of PCSK9 in whole cell lysate but to a much lesser extent compared to the same mutation in $PCSK9^{1-445}$. P445F also reduced the amount of mature PCSK9 detected in culture medium, but when normalized to the amount of total mature PCSK9, this mutation had no significant effect on PCSK9 secretion. Thus, unlike mutant $PCSK9^{1-445}$, the full-length PCSK9 seems not to specifically require proline at position 445 for its efficient secretion.

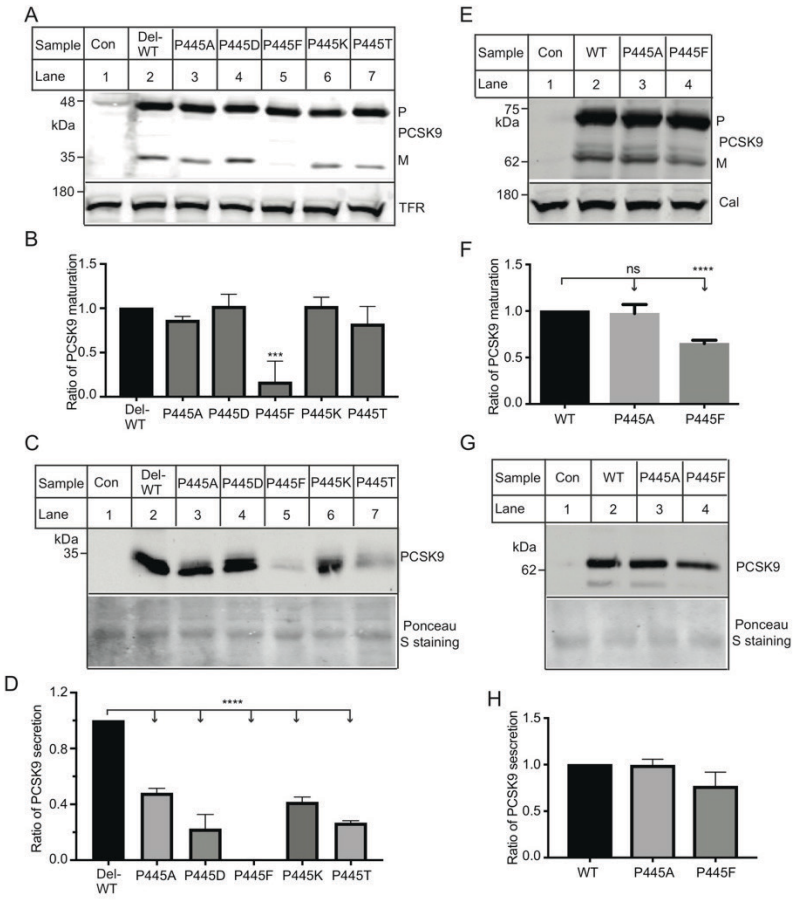

Figure 3.3 Effect of proline at position 445 on mutant PCSK9$^{1-445}$ and the full length PCSK9. The experiments were performed exactly as described in the legend to Figure 1 except that different mutant PCSK9 was used. HEK 293 cells were transfected with the wild type (Del-WT) or mutant PCSK9$^{1-445}$ (A to D) or the wild type (WT) or mutant full-length PCSK9 (E to H). **m**, the mature form of PCSK9. **p**, the precursor form of PCSK9. **Control (Con)**: cells were transfected with the empty vector, pCDNA3.1. Values of all data indicated were mean ± S.D. The significance was defined as *p<0.05, ** p<0.01, *** p<0.001. All experiments were repeated at least three times.

3.2.3 The effects of natural mutations in CTD on PCSK9 secretion.

Both gain-of-function and loss-of-function mutations have been identified in the C-terminal PCSK9. However, if and how these mutations affect PCSK9 secretion are not completely understood. Thus, we introduced these natural variations into PCSK9 including S462P, S465L, R469W, D480N, E482G, R495Q, R496W, K499H, and A522T and then transiently expressed them in HEK293 cells. The amount of the precursor and mature form of PCSK9 in cell lysate were determined with immunoblotting using an anti-PCSK9 antibody. Two bands of PCSK9 were observed in the whole cell lysate that corresponded to its precursor and mature form (Fig 3.4A). All mutant PCSK9 produced similar amount of the mature form of PCSK9 as the wild-type protein in the whole cell lysate, indicating a negligible effect on PCSK9 auto-cleavage (Fig 3.4A). When we examined secreted PCSK9 in cell culture medium, we also observed two bands. The lower band was the furin-cleaved PCSK9 as reported previously (148). We found that mutations R469W, D480N, R496W, E498K, and R499H had no detectable effect on PCSK9 secretion (Fig 3.4B). On the other hand, mutations S462P, S465L, E482G, R495Q, and A522T all reduced the amount of PCSK9 detected in medium. When normalized to the total amount of the mature form of PCSK9, these mutations significantly impaired PCSK9 secretion.

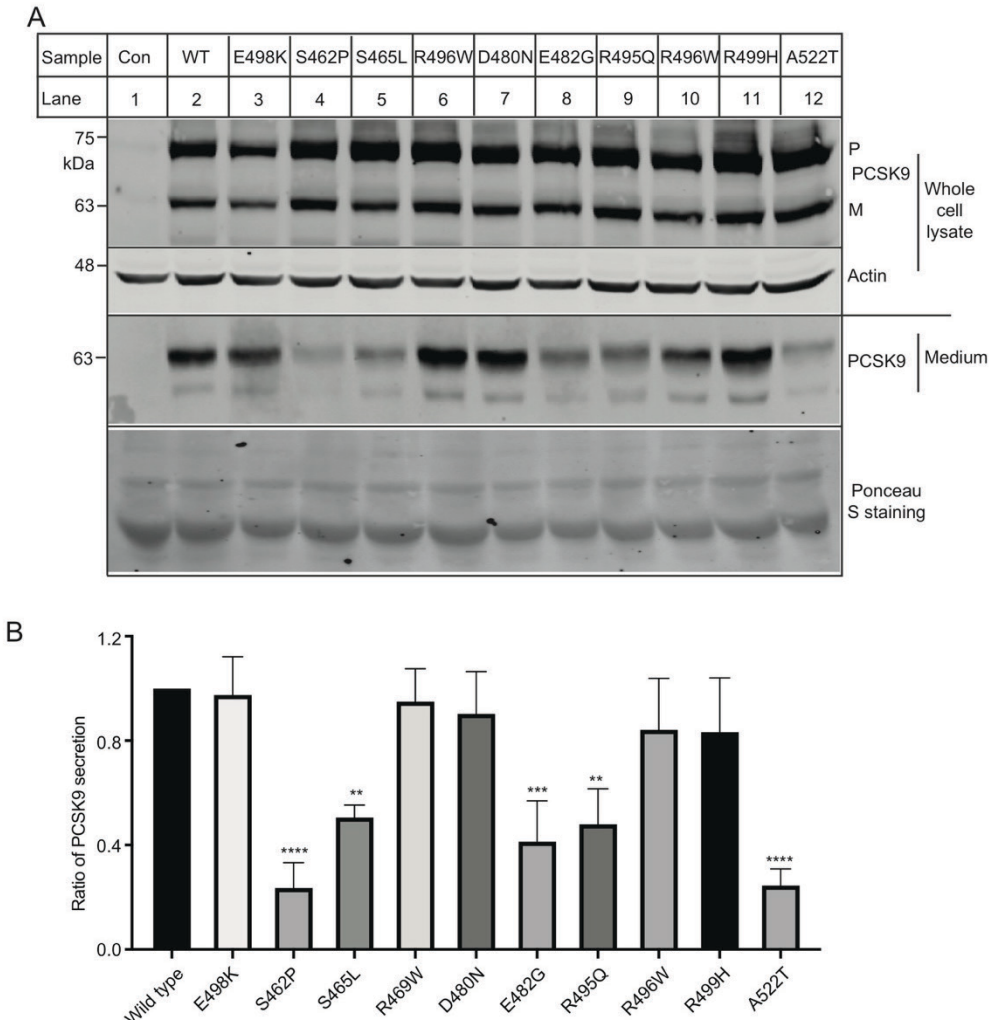

Figure 3.4 Effect of natural mutations in PCSK9 on its secretion. The experiments were performed exactly as described in the legend to Figure 3.1. HEK 293 cells were transfected with the wild-type or mutant PCSK9. Whole cell lysate and culture medium were subjected to immunoblotting and quantification. Values of all data indicated were mean ± S.D. The significance was defined as *$p<0.05$, ** $p<0.01$, *** $p<0.001$. All experiments were repeated at least three times.

3.2.4 Role of SEC24 isotypes in PCSK9 secretion

It has been reported that SEC24A and SEC24B facilitated endogenous PCSK9 secretion in mouse. Overexpression of human SEC24A and SEC24B also increased secretion of human PCSK9 stably overexpressed in 293T cells (88). Mammalian cells express four isoforms of SEC24, A, B, C, and D, and each provides specificity in cargo selection to the COPII vesicles. To test if SEC24s affect secretion of endogenous human PCSK9, we knocked down their expression in human hepatoma-derived cell line, Huh7 cells. siRNAs targeting specific SEC24 isoforms only dramatically reduced the levels of their own mRNA without any effect on other isoforms (Fig 3.5A). Data obtained from Western blot also showed that protein levels of SEC24A, SEC24B, SEC24C and SEC24D were markedly reduced by their specific siRNA (Fig 3.5B). We then examined the effects of SEC24 knockdown on PCSK9 secretion. As shown in Figures 3.5C and 3.5D, knockdown of SEC24A, SEC24B, and SEC24C but not SEC24D significantly reduced PCSK9 levels in culture medium. We then investigated if knockdown of SEC24 affected secretion of one of the CTD deletion mutant $PCSK9^{1-446}$ that significantly reduced PCSK9 secretion but still could be fairly secreted into culture medium (Fig 3.1D). As shown in Figures 3.6A-3.6C, reducing expression of SEC24 A, B, and C that impaired the full-length PCSK9 secretion had no marked effect on secretion of mutant $PCSK9^{1-446}$. These findings indicate that SEC24A, B and C facilitate efficient secretion of the full-length PCSK9 in cultured human hepatocytes.

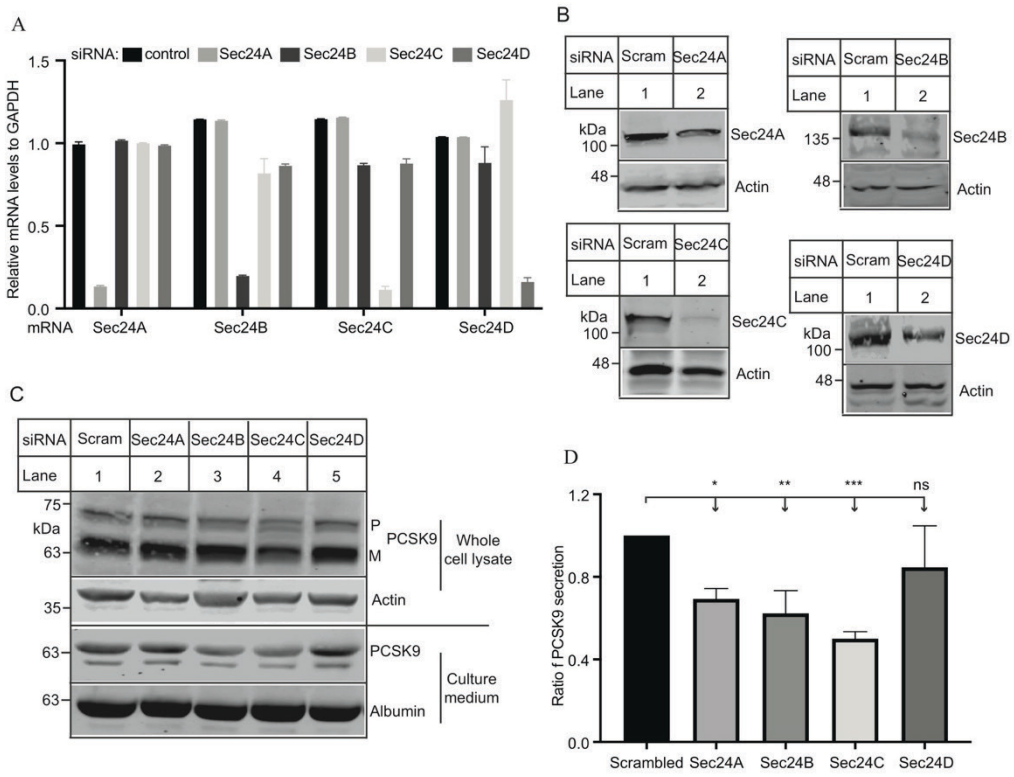

Figure 3.5 Role of SEC24s in PCSK9 secretion. ***A and B***. ***Knockdown efficiency.*** Huh7 cells were transfected with scrambled (Scram) or SEC24s siRNA as indicated. 48 h later, cells were collected to make total RNA for qRT-PCR (A) or whole cell lysate for immunoblotting (B). ***C and D. Effect of knockdown of SEC24 on PCSK9 secretion.*** Huh7 cells were transfected with scrambled (Scram) or SEC24s siRNA as indicated. 48 h after, the cells were washed once with DMEM and then cultured in DMEM without FBS for 24 h. Culture medium and whole cell lysate were subjected to immunoblotting with a monoclonal anti-PCSK9 antibody, 15A6, a monoclonal anti-actin antibody, and a goat anti-albumin antibody. The data were quantified as described to the figure legend to Figure 3.1. Values were mean ± S.D. The significance was defined as *$p<0.05$, ** $p<0.01$, *** $p<0.001$. All experiments were repeated at least three times.

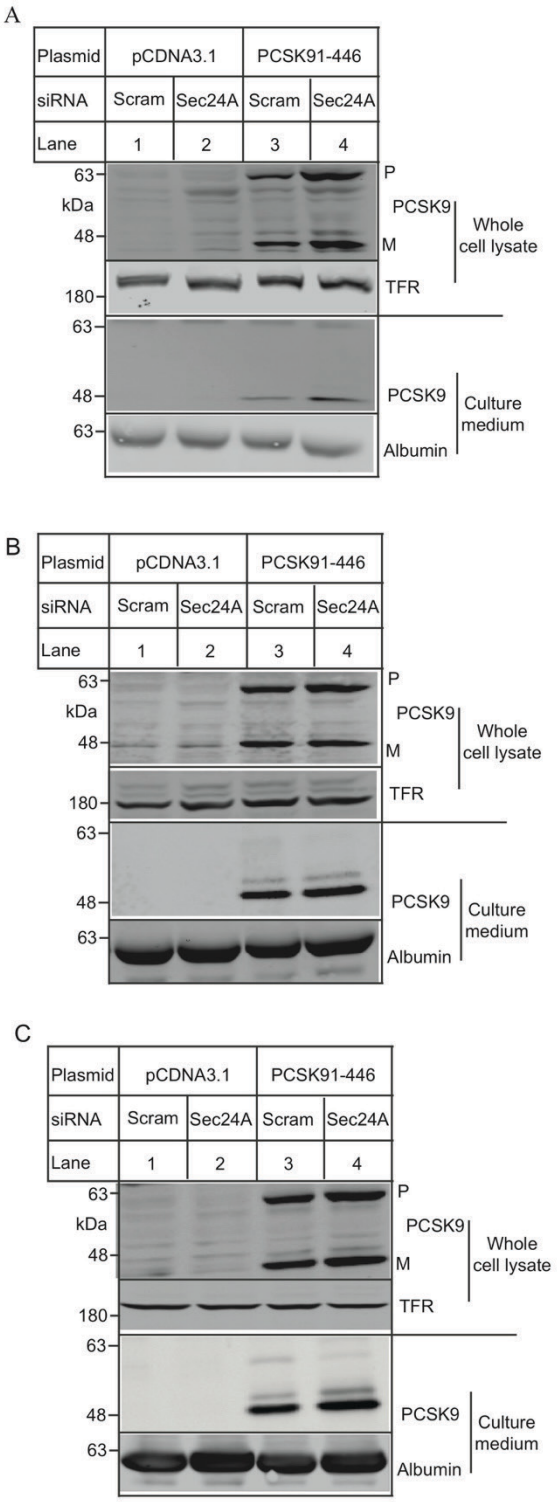

Figure 3.6 Role of SEC24s in mutant PCSK9$^{1-446}$ secretion. Huh7 cells were transfected with scrambled (Scram) or SEC24s siRNA as indicated. 24 hours later, cells were

transfected with empty plasmid pcDNA3.1 or pcDNA3.1 containing cDNA of $PCSK9^{1-446}$. 48 h after, the cells were washed once with DMEM and then cultured in DMEM without FBS for 24 h. Culture medium and whole cell lysate were subjected to immunoblotting with a monoclonal anti-PCSK9 antibody, 13D3, a monoclonal anti-transferrin antibody, and a goat anti-albumin antibody.

3.3 Discussion

Plasma PCSK9 is mainly secreted from hepatocytes and its levels are positively associated with LDL-C concentrations (149-151). However, the machinery system that assists PCSK9 secretion is unclear. The C-terminal domain is essential for PCSK9-promoted LDLR degradation but is not required for its binding to LDLR (97,104,112,141). It has been reported that deletion of all the three CMs or only CM2 and CM3 does not affect PCSK9 secretion (108,125). Consistently, we observed that mutant $PCSK9^{1-528}$ that lacked CM2 and CM3 displayed no significant difference in PCSK9 secretion compared to the full-length PCSK9 (Fig 3.1E). However, we did find that mutant $PCSK9^{1-453}$ mildly but significantly impaired PCSK9 maturation and secretion (Fig 3.1C). Neither Du et al. (125) nor Saavedra et al. (108) quantified the effect of the deletion of CM1 to CM3 on PCSK9 maturation even though the amount of cellular mature form of PCSK9 (ΔCD in Du's study and L455X in Saavedra's study) appeared to be less than that of the full-length PCSK9. Nonetheless, our findings indicate the potential role of CM1 in PCSK9 self-cleavage. Furthermore, we defined the role of the hinge region in PCSK9 secretion, which was not investigated in the two previous studies (108,125). We found that deletion of partial or full hinge region all markedly impaired PCSK9 maturation to a similar extent (Fig 3.2C). Conversely, mutant $PCSK9^{1-445}$ significantly reduced PCSK9 secretion but still could be fairly secreted to culture medium, whereas mutants $PCSK9^{1-444}$, $PCSK9^{1-443}$, and $PCSK9^{1-425}$ all essentially eliminated PCSK9 secretion (Fig 3.2E). The region between amino acids 449 to 453 is undefined in the crystal structure of PCSK9, but the rest of the hinge region is exposed on the surface and close to amino acids Ile161 to Arg167 in the N-terminal CAT (Fig 3.7A) (83,105,109,139). Thus, removal of the hinge region might interfere with the structure integrity of the CAT, thereby affecting PCSK9

auto-cleavage and maturation. Deletion of Pro^{445} in mutant $PCSK9^{1-444}$ was processed as efficiently as mutants $PCSK9^{1-445}$ and $PCSK9^{1-446}$ that included Pro^{445}, but $PCSK9^{1-444}$ markedly reduced PCSK9 secretion compared to the other two mutations (Fig 3.2E). Replacement of Pro^{445} with other amino acid residues in the deletion mutant $PCSK9^{1-445}$ dramatically reduced its secretion (Fig 3.3D), indicating the requirement of this specific amino acid residue. However, mutation of Pro^{445} in the full-length PCSK9 to either alanine or phenylalanine had no significant effect on PCSK9 secretion (Fig 3.3H). It is possible that loss of the contribution of proline at position 445 might be compensated by other residues in the C-terminus such as Pro^{446}. Interestingly, Pro^{445} resides inside a pocket that is surrounded by Leu^{444}, Pro^{163}, Ala^{402}, Met^{398}, Ala^{402}, *etc.* (Fig 3.7B) (83,105,109). This residue might play an important role in maintaining the integrity of the structure. It would be of interest to see if this pocket is involved binding of cofactors that contribute to PCSK9 secretion and/or PCSK9-promoted LDLR degradation.

Various naturally occurred mutations have been identified in the C-terminal PCSK9, many of them have not been fully characterized. We selected 10 mutants that were located in either the hinge region or CM1 from two databases, the Exome Aggregation Consortium (ExAC) and ClinVar. We found that mutations S462P S465L, E482G, R495Q, and A522T significantly reduced PCSK9 secretion , whereas mutations E498K, R496W, D480N, R496W, R499H had no significant effect (Fig 3.4). Consistently, S462P and S465L have been reported to impair PCSK9 secretion (124,152). The clinical significance of the variant R495Q is uncertain. S462P and A522T are associated with hypocholesterolemia (152,153), whereas S465L and E482G have been reported to be associated with hypercholesterolemia (110,154). It has been reported that mutations D129G and A168E impair PCSK9 secretion but enhance the ability of PCSK9 to induce LDLR degradation intracellularly, thereby causing

hypercholesterolemia (155). It will be of interest to determine if mutations S465L and E482G enhance PCSK9-promoted LDLR degradation via the intracellular pathway. Nonetheless, these findings reveal the complex mechanism by which PCSK9 regulates plasma LDL-C and may provide one possible explanation for the weak correlation between plasma levels of PCSK9 and LDL-C levels. For instance, Lakoski et al. reported that circulating PCSK9 concentrations only predicted less than 8% of the variation in plasma LDL-C levels (156).

Secretion of soluble proteins can be regulated by a default bulk flow pathway (157) and/or the cargo receptor-facilitated ER-to-Golgi transport in mammalian cells (158-161). It has been reported that a cargo receptor, surfeit 4 (Surf4), facilitated the secretion of PCSK9 overexpressed in 293T cells (89). Conversely, we observed that Surf4 played a negligible role in secretion of endogenous PCSK9 from cultured human hepatocytes (90). Similarly, conflicting data have been reported about the role of sortilin in PCSK9 secretion. Gustafsen et al. reported that sortilin interacted with PCSK9 in the trans-Golgi network and then facilitated its secretion (92). Conversely, studies from Butkinaree et al. showed that knockdown of sortilin in cultured cells or knockout of sortilin in mice had no detectable effect on PCSK9 secretion (94). Together, these findings reveal the complexity and heterogeneity of PCSK9 secretion in different types of cells.

Most recently, it has been reported that knockout of SEC24A and reduction of SEC24B expression but not SEC24D in mice decreased PCSK9 secretion (88). Consistently, we found that knockdown of SEC24A and SEC24B but not SEC24D impaired PCSK9 secretion in cultured human hepatocytes. Chen et al. also found that, unlike SEC24A and SEC24B, overexpression of SEC24C together with SEC23A did not enhance secretion of PCSK9 expressed in 293T cells (88). However, we observed that knockdown of SEC24C in Huh7 cells significantly reduced PCSK9 secretion. This discrepancy could be caused by that 1)

different cell lines were used. We investigated endogenous PCSK9 secretion from a human hepatoma-derived cell line, while Chen et al. overexpressed PCSK9 in 293T cells, in which endogenous PCSK9 is undetectable; and 2) we knocked down SEC24C expression, whereas Chen et al. overexpressed SEC24C paired with SEC23A in 293T cells (88). Further, considering the substrate specificity of SEC24 isoforms, it is possible that different SEC24 isoforms contribute to PCSK9 secretion in different cell types. Nevertheless, these findings demonstrate that SEC24 plays an important role in facilitating the ER-to-Golgi transport of PCSK9. The detailed molecular mechanism by which PCSK9 exits from the ER, however, has yet to be determined. Interestingly, we found that knockdown of SEC24A, SEC24B, or SEC24C did not affect the secretion of mutant PCSK9$^{1-446}$. PCSK9$^{1-446}$ dramatically reduced PCSK9 secretion but a decent amount of secreted protein could be detected in cell culture medium (Fig 3.1D). This raises some possibilities, 1) PCSK9$^{1-446}$ utilizes a completely different machinery system for its secretion, or 2) SEC24s are required for efficient secretion of PCSK9, but the basal level secretion of PCSK9 is regulated differently. Mutant PCSK9$^{1-446}$ lost SEC24s-facitlited secretion but still remained the basal level secretion. Experiments are undergoing in the lab to define these possibilities.

In summary, we demonstrated the important role of the hinge region of PCSK9 in its secretion and processing. We also found that both loss-of-function mutations (S462P and A522T) and gain-of-function mutations (S465L and E482G) could impair PCSK9 secretion. Further, we identified that SEC24A, B, and C but not SEC24D facilitated PCSK9 secretion in cultured human hepatocytes. Together, these findings would shed light on our understanding of PCSK9.

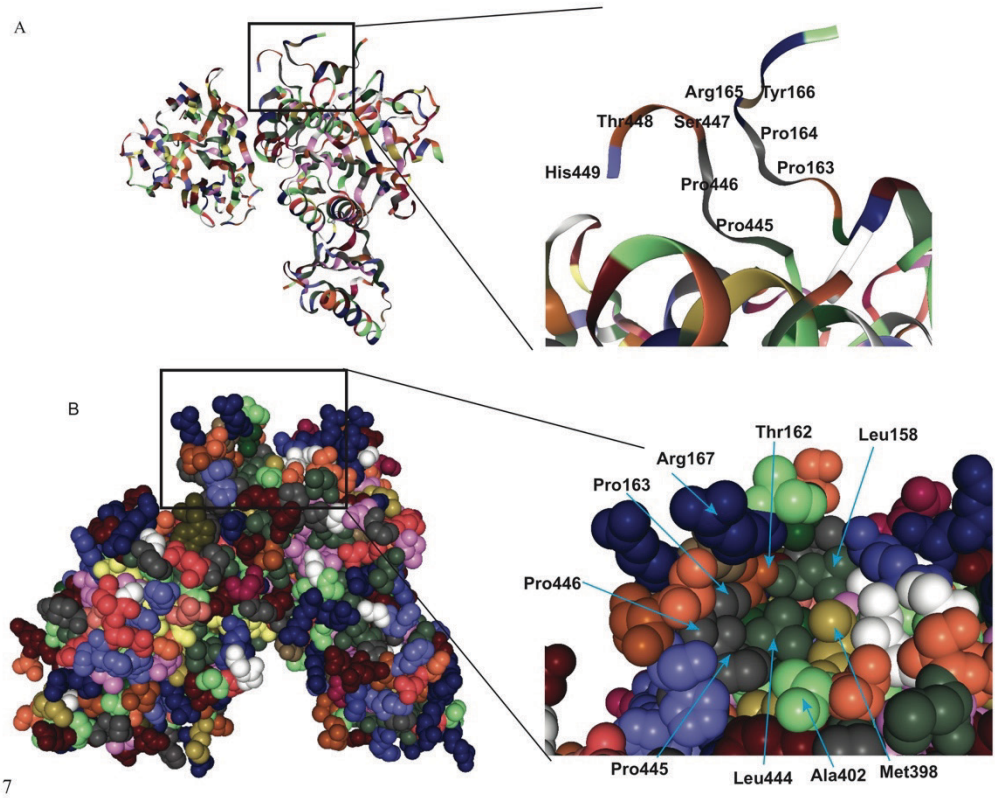

Figure 3.7 Crystal structure of PCSK9 (PDB code: 2P4E) in cartoon (A) and space fill (B) (105).

Chapter 4: Manuscript II

Identification of amino acid residues in the ligand binding repeat of LDLR important for PCSK9 binding

(The Journal of Lipid Research. 2019 Mar; 60(3): 516–527)

Identification of amino acid residues in the ligand binding repeats of LDLR important for PCSK9 binding

Shi-jun Deng [a], Adekunle Alabi [a, b], Hong-mei Gu [a], Ayinuer Adijiang [a], Shucun Qin [c], and Da-wei Zhang [a, b] *

[a]Department of Pediatrics, Group on the Molecular and Cell Biology of Lipids, [b] Department of Biochemistry, Faculty of Medicine and Dentistry, University of Alberta, Edmonton, Alberta, Canada. [c] Institute of Atherosclerosis in Taishan Medical University, Taian, China

Abbreviations: CHO, Chinese hamster ovary; DAPI, 4',6-diamidino-2-phenylindole (DAPI); EGF-A, the epidermal growth factor precursor homology repeat-A; FH, familial hypercholesterolemia; HEK, human embryonic kidney; LDL-C, LDL cholesterol; LDLR, LDL receptor; LR, ligand binding repeat; NCLPPS, newborn calf lipoprotein-poor serum; PCSK9, proprotein convertase subtilisin/kexin type 9; PNGase, Peptide-N-glycosidase; SDS-PAGE, SDS polyacrylamide gel electrophoresis

Abstract

Proprotein convertase subtilisin/kexin type 9 (PCSK9) promotes LDL receptor (LDLR) degradation, increasing plasma levels of LDL cholesterol (LDL-C) and the risk of cardiovascular disease. We have previously shown that, in addition to the epidermal growth factor precursor homology repeat-A of LDLR, at least three ligand-binding repeats (LRs) of LDLR are required for PCSK9-promoted LDLR degradation. However, how exactly the LRs contribute to PCSK9's action on the receptor is not completely understood. Here, we found that substitution of Asp at position 172 in the linker between the LR4 and the LR5 of full-length LDLR with Asn (D172N) reduced PCSK9 binding at pH 7.4 (mimic cell surface) but not at pH 6.0 (mimic endosomal environment). On the other hand, mutation of Asp at position 203 in the LR5 of full-length LDLR to Asn (D203N) significantly reduced PCSK9 binding at both pH 7.4 and pH 6.0. D203N also significantly reduced the ability of LDLR to mediate cellular LDL uptake while D172N had no detectable effect. These findings indicate that amino acid residues in the LRs of LDLR play an important role in PCSK9 binding to the receptor.

Keywords: LDLR, ligand binding repeats, PCSK9, LDL binding, site-directed mutagenesis.

4.1 Introduction

Plasma levels of cholesterol, especially LDL-C, are positively correlated with the risk of atherosclerosis (162,163). The LDLR-mediated LDL uptake plays an essential role in the clearance of plasma LDL-C (164). Upon LDL binding to the N-terminal ligand-binding repeats (LRs) of LDLR, the receptor and LDL complex is internalized via clathrin-coated pits and delivered to endosomes, where LDL is released from the receptor and delivered to lysosomes for degradation, LDLR is then recycled to the cell surface (17,163,165). Mutations in LDLR cause familial hypercholesterolemia (FH) and increase the risk for atherosclerotic coronary heart disease (163,164). *Ldlr*$^{-/-}$ mice display higher plasma levels of cholesterol, especially LDL-C, than wild-type (WT) littermates and develop atherosclerosis when fed a high cholesterol diet (166).

PCSK9 is a 692-amino acid secreted glycoprotein that consists of a 30 amino acid signal sequence followed by a prodomain (PRO), a catalytic domain (CAT), and a C-terminal domain (CTD). Expression of PCSK9 is high in the liver, intestine, kidney, and brain (143,144). PCSK9 binds to LDLR and redirects the receptor for lysosomal degradation (23,45,56,97,113,127,144), playing a central role in regulating plasma LDL-C. GOF mutations in PCSK9 lead to elevated plasma LDL-C levels and accelerated atherosclerosis and premature coronary heart disease (42). Conversely, LOF PCSK9 mutations lead to reduced plasma LDL-C levels and protection from coronary heart disease (51). Increased plasma levels of PCSK9 in mice preferentially promote LDLR degradation in the liver but not in other tissues (145). We and others have shown that PCSK9 interacts with the epidermal growth factor precursor homology repeat-A (EGF-A) of LDLR at the cell surface and binds to the receptor with a much higher affinity at the acidic environment of the endosome (23,139,140). Consequently, the receptor is redirected from the endosome to the lysosome for degradation,

rather than being recycled (23). The X-ray crystallographic structure of PCSK9 with the partial extracellular domain of LDLR at a neutral pH value shows that the EGF-A and YWTD repeats of LDLR interact with the catalytic domain and the prodomain of PCSK9, respectively (142). However, LR1 to LR6 of LDLR are absence in the structure. We have demonstrated that in addition to the EGF-A and YWTD repeats, a minimum of three ligand-binding repeats in LDLR are essential for efficient LDLR degradation induced by PCSK9 (97,127). Several biochemical studies indicate that the negatively charged ligand binding repeats of LDLR may interact with the positively charged CTD of PCSK9 at the cell surface and/or in the acidic endosomal environment to enhance PCSK9 binding (104,112,141). To further investigate the role of the LRs of LDLR in PCSK9-promoted LDLR degradation, we replaced negatively charged residues in the LRs of LDLR and assessed the effects of these mutations on PCSK9 binding. The numbers that indicated the positions of amino acid residues in LDLR in this study were counted from the N-terminus of the receptor without the 21 amino acid signal sequence. We found that Asp172 in the linker and Asp203 in the LR5 of LDLR played a role in PCSK9 binding.

4.2 Results

4.2.1 Effect of mutations in LDLR-ΔLR4-LR7 on PCSK9 binding

The C-terminal domain of PCSK9 is positively charged and the LRs of LDLR are negatively charged. Given the role of the LRs in PCSK9-promoted LDLR degradation (97,104,112,141), we assessed if negatively charged residues in the LRs of LDLR affected PCSK9 binding. To simplify the initial screening, we used a mutant LDLR (LDLR-ΔLR4-LR7), in which LRs 4 to 7 were deleted, since we have previously demonstrated that at least three LRs were required for PCSK9-promoted LDLR degradation (97). We first replaced all negatively charged residues Asp and Glu in the LR1 of LDLR-ΔLR4-LR7 with uncharged Asn and Gln individually or in combination (Fig 4.1A). The WT and mutant receptors were transiently expressed in HEK293 cells. The cells were then prechilled on ice for 30 min to inhibit LDLR endocytosis and then incubated with or without PCSK9 on ice in a pH 7.4 buffer to mimic PCSK9 binding to LDLR at the cell surface. As shown in Figure 4.1B and Supplementary Figure 4.1A, the expression levels of the WT and mutant LDLR-ΔLR4-LR7 were comparable in the presence and absence of PCSK9, indicating that PCSK9 did not promote LDLR degradation at this condition. After normalization to the levels of the mature form of LDLR, mutation of Asp at position 4 to Asn (D4N) significantly reduced PCSK9 binding to LDLR-ΔLR4-LR7 at pH 7.4 (Fig 4.1B, lane 6 *vs* 4), while substitution of Asp at other positions with Asn and replacement of Glu residues in the LR1 with Gln had no detectable effect on PCSK9 binding to the receptor (Fig 4.1B and Fig S4.1A).

Next, we performed the PCSK9 binding assay on ice in a pH 6.0 buffer to mimic PCSK9 binding at the acidic endosome as described in previous studies (104). We observed that only mutation D4N significantly reduced PCSK9 binding to the receptor in the acidic

environment, while other mutations had no effect (Fig 4.1C, lane 3 *vs* 2 and Fig. S4.1B). We also mutated Asp4 to a similarly charged Glu (D4E) and examined PCSK9 binding to the receptor at pH 7.4. As shown in Figure 4.1D, D4E mutation, unlike D4N, had no detectable effect on PCSK9 binding to LDLR-ΔLR4-LR7 (lane 8 *vs* 4). Together, these findings indicate that a negative charge at position 4 of the LR1 in LDLR-ΔLR4-LR7 plays an important role in PCSK9 binding. We then replaced Asp at position 4 in the LR1 of the full-length LDLR with Asn to assess its role in PCSK9 binding. We observed that binding of PCSK9 to the WT and D4N mutant full-length LDLR at pH 7.4 was comparable (Fig 4.1D, lane 12 *vs* 10), indicating a negligible role of Asp at position 4 of the full-length LDLR in PCSK9 binding.

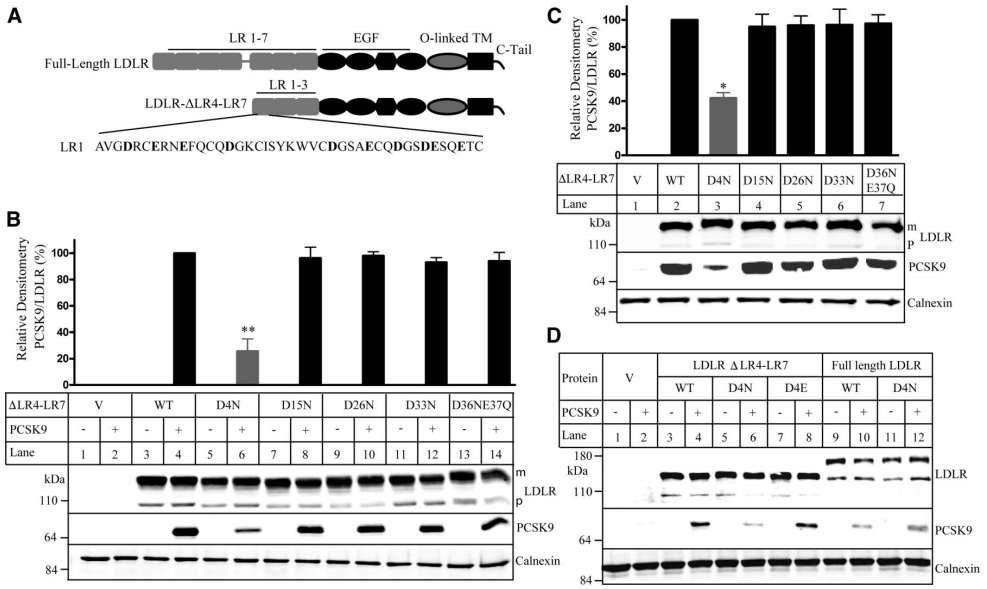

Figure 4.1 Binding of PCSK9 to the WT and mutated LDLR-ΔLR4-LR7. ***A.*** A schematic of the full-length LDLR and LDLR-ΔLR4-LR7 with an enlarged view of the LR1. Negatively charged amino acid residues in the LR1 were shown in Bold. TM, transmembrane domain. C-tail, C-terminal cytoplasmic tail. ***B, C, and D.*** Binding of PCSK9 to the WT and mutant LDLR-ΔLR4-LR7 at pH 7.4 (***B***) and pH 6.0 (***C***), or to the WT and mutant LDLR-ΔLR4-LR7 and full-length LDLR at pH 7.4 (***D***). HEK293 cells transiently expressing the WT

or mutant LDLR-ΔLR4-LR7 or full-length LDLR were incubated with PCSK9 (2 μg/well) at pH 7.4 (***B and D***) or pH 6.0 (***C***). Same amount of whole cell lysate was subjected to immunoblotting. The membrane was cut into halves. The top part was blotted with a monoclonal anti-LDLR antibody and a polyclonal anti-calnexin antibody. The bottom part was bloted with a monoclonal anti-PCSK9 antibody 15A6. The top bar charts in panels B and C were a percentage of the relative densitometry PCSK9 binding signal. It was the percentage of relative densitometry of PCSK9 binding to mutant LDLR to that of PCSK9 binding to the WT LDLR that was defined as 100%. The relative densitometry of PCSK9 binding to LDLR was the ratio of the densitometry of PCSK9 to that of the mature form of LDLR. Values were mean ± S.D. of three or more experiments. The bottom figures were representative ones of protein levels. Top bands of LDLR were the mature and fully glycosylated forms (m). Bottom bands of LDLR were the precursor forms (p). V: cells were transfected with the empty vector, pCDNA3.1. Similar results were obtained from at least three experiments. *, $p<0.05$. **, $p<0.01$.

4.2.2 Effect of mutations in the full-length LDLR on PCSK9 binding

Given that PCSK9 mainly binds to EGF-A of LDLR (23,139,142), it was possible that the relative distance of negatively charged residues in the LRs to the EGF-A affected their contributions to PCSK9 binding. The LR1 in LDLR-ΔLR4-LR7 corresponds to the LR5 in the full-length receptor (Fig 4.2A). Considering the high flexibility of the linker region between the LR4 and the LR5 (167), we replaced all negatively charged residues in the LR4, the 12-residue linker, and the LR5 of the full-length LDLR with non-charged Asn and Gln individually or in combination to examine their involvement in PCSK9 binding (Fig 4.2A). We observed that, when compared to the WT LDLR, replacement of Asp at position 203 in the LR5 to Asn (D203N) reduced PCSK9 binding at pH 7.4 by approximately 50% (Fig 4.2B, lane 8), and mutation of Asp at position 172 in the linker to Asn (D172N) also significantly reduced PCSK9 binding at pH 7.4 (Fig 4.2C, lane 3). Substitution of other negatively charged residues Asp and Glu in the LR4 and the LR5 with Asn and Gln, however, had no significant effect (Fig 4.2B and 4.2C). Mutation D196N had a tend to reduce PCSK9 binding but the reduction did not reach to statistical significance (Fig 4.2B). We did not study individual amino acid residues in the combination mutations shown in Figures 4.2B and 4.2C due to the lack of effect of these multiple mutations on PCSK9 binding. Next, we examined if mutations D172N and D203N affected PCSK9 binding in the acidic endosomal environment. As shown in Figure 4.2D, D203N markedly reduced PCSK9 binding at pH 6.0 (lane 3 *vs* 2), while D172N had no effect (lane 6 *vs* 5). Taken together, these findings indicate that Asp172 and Asp203 play a role in PCSK9 binding to the full-length LDLR.

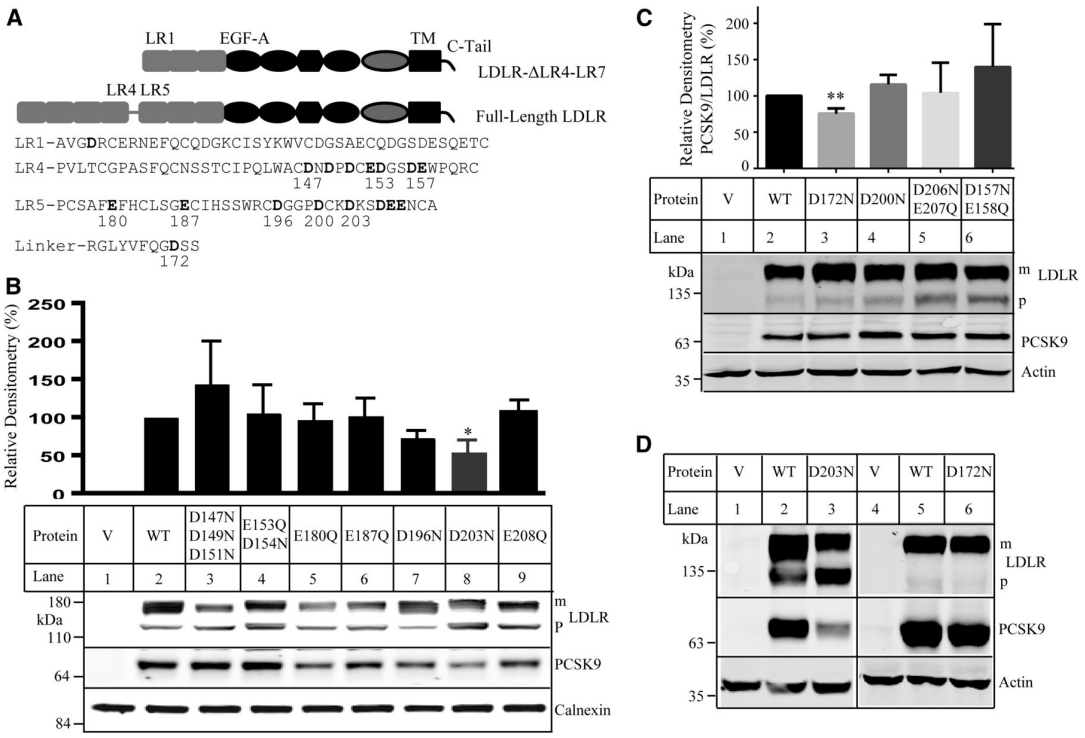

Figure 4.2 Binding of PCSK9 to the WT and mutant full-length LDLR. ***A***. A schematic of the full-length LDLR and ΔLR4-LR7 LDLR with an enlarged view of LR1, LR4, LR5, and the linker. Negatively charged amino acid residues in the LR4, LR5, and the linker were shown in Bold. TM, transmembrane domain. C-tail, C-terminal cytoplasmic tail. ***B to D.*** Binding of PCSK9 to the WT and mutant full-length LDLR. The experiments were performed as described in the legend to Figure 1. Briefly, HEK293 cells transiently expressing the WT or mutant LDLR were incubated with PCSK9 (2 μg/ml) on ice at a pH 7.4 (***B and C***) or pH 6.0 (***D***) buffer as indicated above. LDLR and PCSK9 were detected by HL-1, and 15A6, respectively. Top bands of LDLR were the mature forms (m). Bottom bands of LDLR were the precursor forms (p). Data shown in the top figure in panels ***B*** and ***C*** were quantified as described in the legend to Figure 1. V: cells were transfected with the empty vector, pCDNA3.1. Values were mean ± S.D. of ≥ 3 experiments. *, $p<0.05$. **, $p<0.01$.

We then investigated the potential role of the C-terminal PCSK9 in its binding to LDLR. We made mutant $PCSK9^{1-447}$ that lacked the whole C-terminus of PCSK9 and mutant $PCSK9^{1-454}$, in which the three C-terminal modules (amino acid residues 455 to 692) were deleted (Fig 4.3A). The mutant proteins were transiently expressed in HEK293 cells and could undergo self-cleavage to produce the mature form (Fig 4.3B, lanes 4 and 3). Culture medium was collected, concentrated, and applied to immunoblotting. Very limited amount of $PCSK9^{1-447}$ (data not shown) nor $PCSK9^{1-454}$ (Fig 4.3C, lane 1) could be detected in medium, indicating impaired secretion of the two mutant proteins. We then made another mutant $PCSK9^{1-529}$ that lacked the C-terminal modules 2 and 3 (amino acid residues 530 to 692) (Fig 4.3A). $PCSK9^{1-529}$ was processed in HEK293 cells (Fig 4.3B, lane 5) and its mature form could be detected in the concentrated culture medium (Fig 4.3C, lane 2). We then applied same amount of concentrated medium containing $PCSK9^{1-529}$ to HEK293 cells expressing the WT or mutant LDLR. As shown in Figures 4.3D and 4.3E, both D172N and D203N significantly reduced binding of $PCSK9^{1-529}$ to the receptor (lanes 3 and 4 *vs* 2). This finding suggests that amino acid residues 530 to 692 in the C-terminal PCSK9 are not required for the inhibitory effect of D172N and D203N on PCSK9 binding.

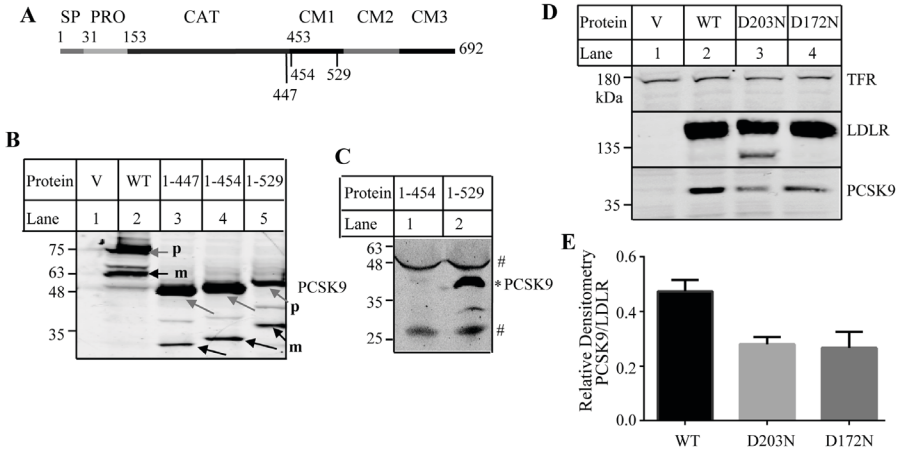

Figure 4.3 Binding of mutant PCSK9 to the WT and mutant LDLR. ***A.*** A schematic of PCSK9. Signal peptide (SP, amino acid residues 1-30); prodomain (PRO, amino acid residues 31-152); catalytical domain (CAT, amino acid residues 153-426); C-terminal domain (amino acid residues 453-692) with three modules, module 1 (CM1, amino acid residues 457-527), module 2 (CM2, amino acid residues 534-601), and module 3 (CM3, amino acid residues 608-692) (125). ***B and C.*** Expression of the WT and mutant PCSK9 in HEK293 cells (***B***) and culture medium (***C***). HEK293 cells transiently expressing the WT or mutant PCSK9 as indicated were collected for the preparation of whole cell lysate. Culture medium was collected from one 150-mm dish of HEK293 cells transiently transfected with mutant $PCSK9^{1-454}$ or $PCSK9^{1-529}$ and then concentrated using a 3-kDa cut-off centrifugal concentrator (Millipore). Same amount of total proteins of whole cell lysate (B) or same amount of concentrated medium (C) were subjected to immunoblotting using a monoclonal anti-PCSK9 antibody 13D3 that recognizes the catalytical domain of PCSK9. #, non-specific bands. *, mature form of $PCSK9^{1-529}$. ***D***. Binding of $PCSK9^{1-529}$ to the WT and mutant LDLR. The experiments were performed as described in the legend to Figure 1. Briefly, HEK293 cells transiently expressing the wild-type or mutant LDLR were incubated with same amount of

concentrated medium containing $PCSK9^{1-529}$ on ice at a pH7.4 value for 4 h. LDLR and PCSK9 were detected by HL-1, and 13D3, respectively. Transferrin receptor (TFR) was detected by its specific monoclonal antibody. **m**, cleaved mature form of PCSK9 (black arrows). **p**, the precursor form of PCSK9 (grey arrows). V: cells were transfected with the empty vector, pCDNA3.1. ***E***. Quantified PCSK9 binding data. The relative densitometry of PCSK9 was the ratio of the densitometry of PCSK9 to that of the mature form of LDLR. Values were mean ± S.D. of three experiments. **, $p<0.01$.

We also examined if mutations D172N and D203N affected PCSK9-promoted LDLR degradation. HEK293 cells expressing the WT or mutant LDLR were incubated with PCSK9 at 37 °C for 12 h. We observed that PCSK9 efficiently promoted degradation of the WT and two mutant LDLR at a concentration of 8 μg/ml (Fig. 4.4A, lane 4 *vs* 3, 6 *vs* 5, and 8 *vs* 7) even though D203N and D172N-expressing cells displayed less PCSK9 in whole cell lysate compared the WT LDLR expressing cells. On the other hand, PCSK9 at a concentration of 6 μg/ml could efficiently promote degradation of the WT (lane 4 *vs* 3) and mutant D172N LDLR (lane 8 *vs* 7) but failed to stimulate D203N degradation (lane 6 *vs* 5). However, neither the WT receptor nor the two mutant LDLR could be efficiently degraded by addition of PCSK9 at a concentration of 4 μg/ml (Fig 4.4C). These findings suggest that PCSK9-promoted degradation of D203N is less effective than its action on the WT LDLR.

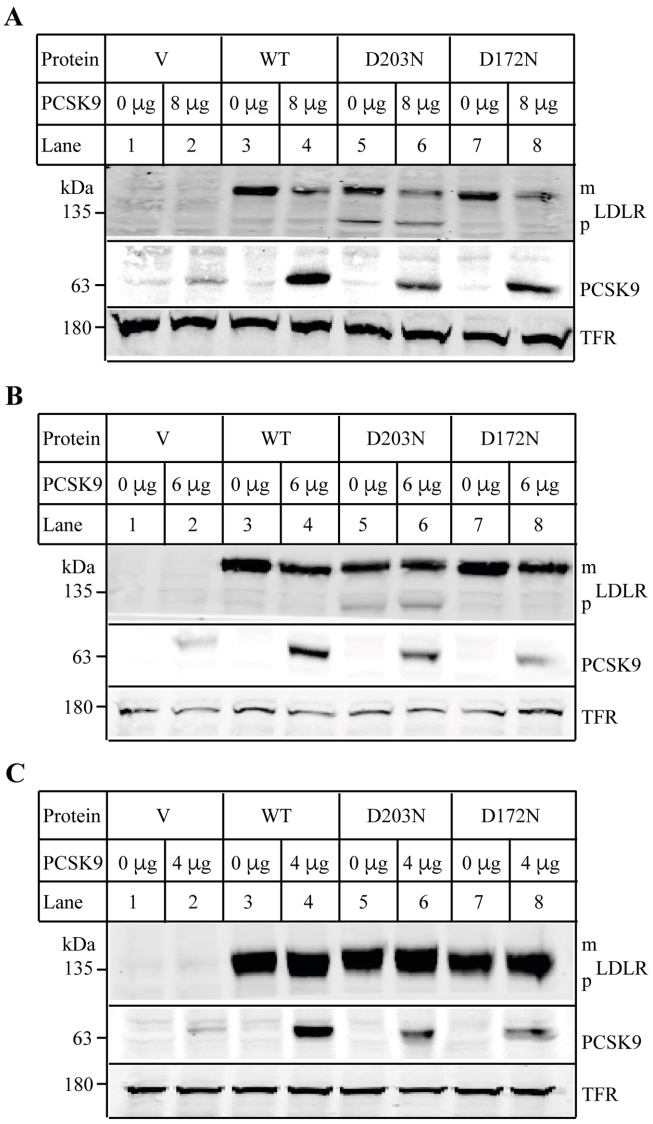

Figure 4.4 PCSK9-promoted LDLR degradation. HEK293 cells transiently expressing the WT or mutant LDLR were incubated with DMEM in the presence or absence of different amount of PCSK9 as indicated at 37 °C for 12 h. After washing, whole cell lysate was prepared, and same amount of total proteins was subjected to immunoblotting using 15A6 (PCSK9), HL-1 (LDLR), and a monoclonal anti-transferrin receptor (TFR). Similar results were obtained from at least one more experiment.

4.2.3 Effects of D172N and D203N on LDL binding and LDLR trafficking

LDLR directly binds to LDL and mediates cellular LDL uptake. Thus, we investigated if the two mutations that impaired PCSK9 bindings affected the ability of the receptor to bind LDL using Dil-LDL as described (130). We found that the levels of D203N and D172N in Hepa1c1c7 cells were comparable to that of the WT receptor (Fig 4.5A and 4.5B), but D203N significantly reduced LDL binding (Fig 4.5C), while D172N showed a similar LDL binding capacity as the WT LDLR (Fig 4.5D).

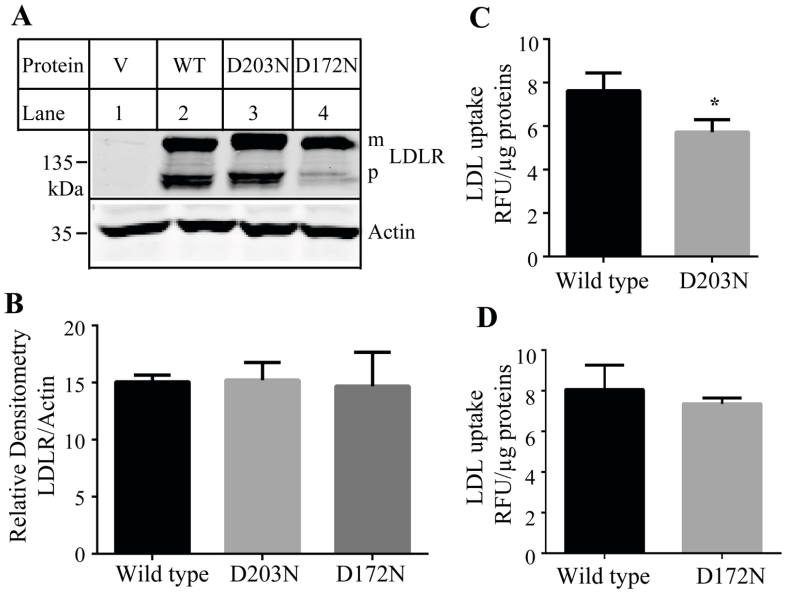

Figure 4.5 Binding of LDL to the wild-type and mutant LDLR. ***A and B***. Expression of the WT and mutant LDLR in Hepa1c1c7 cells. Briefly, same amount of total proteins isolated from Hepa1c1c7 cells transiently expressing the WT or mutant LDLR was subjected to immunoblotting using a monoclonal anti-LDLR antibody, HL-1, and a monoclonal anti-actin antibody. The relative densitometry of LDLR was the ratio of the densitometry of LDLR to that of actin. Values were mean ± S.D. of three experiments. ***C and D***. LDL uptake. Briefly, Hepa1c1c7 cells transiently expressing the WT or mutant LDLR were

incubated with Dil-LDL in the presence or absence of LDL. After washing, the fluorescence signal was measured. The relative fluorescence units (RFU) were normalized to total proteins (μg). The amount of specific LDL uptake was the difference between the total counts measured in the absence of unlabeled LDL and the counts measured in the presence of an excess of unlabeled LDL (non-specific background fluorescence).

Binding of PCSK9 and LDL to the receptor mainly occurs at the cell surface. To determine if the effect of D172N and D203N on PCSK9 binding might be attributable in part to changes in trafficking of LDLR, we labeled cells with biotin and precipitated biotinylated surface proteins from whole cell lysate using Neutravidin agarose. As shown in Figures 4.6A and 4.6B, the ratio of the cell surface levels of the two mutants, D172N and D203N, to their levels in whole cell lysate was comparable to that of the WT LDLR, indicating that the two mutants could be transported to plasma membrane. To further confirm these findings, we monitored the localization of the mutant as well as the WT LDLR in HEK293 cells by confocal microscopy. LDLR was shown as red. The plasma membrane marker, Na^+/K^+-ATPase, was shown as green. Endogenous levels of LDLR in HEK293 were very low. Thus, LDLR signal was undetectable in non-transfected cells (Fig 4.6C, arrow in up panel-merged). We found that a majority of the WT LDLR could be detected on the cell periphery (Top panel), which was co-localized with Na^+/K^+-ATPase that was shown as yellow in the merged panel (Top panel-right). D172N (Middle panel) and D203N (Bottom panel) were also colocalized with Na^+/K^+-ATPase, indicating that the two mutant LDLR could be transported to plasma membrane in HEK293 cells.

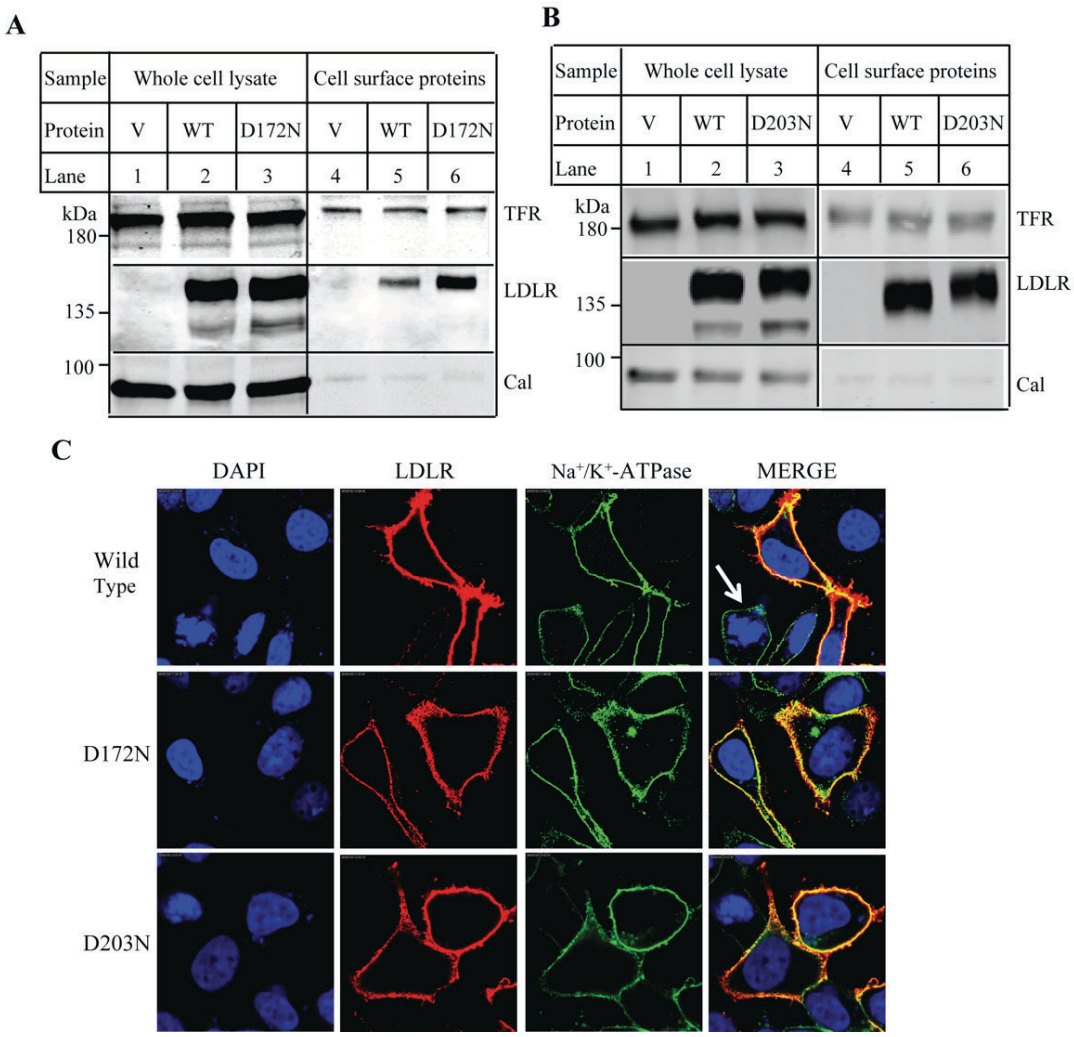

Figure 4.6 Cellular localization of the WT and mutant LDLR. ***A.*** Biotinylation of cell surface proteins. HEK293 cells transiently expressing the WT or mutant LDLR were incubated with Sulfo-(LC)-NHS-biotin. The whole cell lysate was then prepared and subjected to Neutravidin agarose to pull down biotinylated cell surface proteins. LDLR was detected by HL-1. Calnexin (Cal) and transferrin receptor (TFR) were detected by their specific antibodies. V: cells were transfected with the empty vector, pCDNA3.1. ***B.*** Confocal microscopy. HEK293 cells transiently expressing the WT or mutant LDLR were fixed, permeabilized, and then incubated with a monoclonal anti-LDLR antibody and a polyclonal anti-Na^+-K^+-ATPase antibody. Antibody binding was visualized with Alexa 568-conjugated

goat anti-mouse IgG (Red) and Alexa 488-conjugated goat anti-rabbit IgG (Green). Nuclei were visualized with DAPI and shown as blue. An x-y optical section of the cells illustrates the distribution of the wild-type and mutant proteins between plasma and intracellular membranes (magnification: 100X).

4.2.4 Effect of mutations of Asp172 and Asp203 on PCSK9 binding

Next, we investigated how specific the requirements were for Asp at positions 172 and 203 of LDLR for its ability to bind PCSK9 at pH 7.4. First, we replaced Asp172 and Asp203 with Glu (D172E and D203E) to determine whether another acidic residue could be substituted for Asp. Asp172 was also mutated to Ala, Lys, Thr, and Val. Asp203 was replaced with Gly, Ala, Val, and Gln. The WT and mutant LDLR were transiently expressed in HEK293 cells, and the PCSK9 binding assay was performed at pH 7.4. After normalization for differences in the levels of the mature form of LDLR, we found that mutation of Asp172 to another negatively charged residue Glu or other residues (Ala, Lys, Thr, or Val) all significantly reduced the ability of LDLR to bind PCSK9 (Fig 4.7A and 4.7B). All mutations at position 203 we tested including D203E also significantly decreased PCSK9 binding (Fig 4.7C). Thus, it appears that an Asp residue at positions 172 and 203 is specifically required for efficient PCSK9 binding.

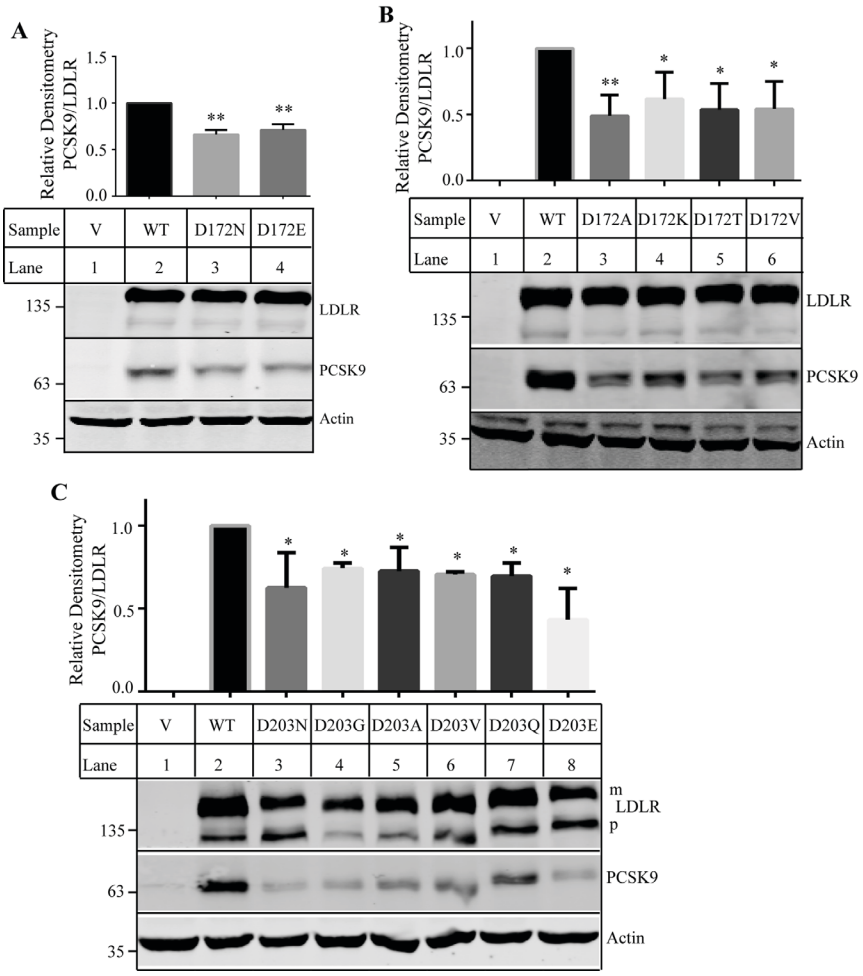

Figure 4.7 Binding of PCSK9 to the wild-type and mutant LDLR. The experiments were performed as described in the legend to Figure 4.1. Briefly, HEK293 cells transiently expressing the WT or mutant LDLR were incubated with PCSK9 (2 μg/well) at pH 7.4 for 2 h on ice. LDLR and PCSK9 were detected by HL-1 and 15A6, respectively. Actin was detected by a monoclonal antibody. The bottom figure was a representative one of protein levels. The top bar chart was a percentage of the relative densitometry of PCSK9 to that of the mature form of LDLR. It was calculated as described in the legend to Figure 4.3E. V: cells were transfected with the empty vector, pCDNA3.1. Values were mean ± S.D. of three or more experiments. *, $p<0.05$. **, $p<0.01$. ***, $p<0.005$.

We noticed that mutation D203N slightly increased the molecular mass of LDLR compared to that of the WT receptor (Fig 4.2B, lane 8; Fig 4.2D, lane 3; and Fig 4.6B, lanes 3 and 6). Considering that D203N introduces a novel canonical N-glycosylation motif (Asn-X-Ser) to the receptor (Fig. S4.2A), we investigated if the mutation conferred an extra N-glycan to LDLR. Whole cell lysate isolated from the WT and mutant LDLR-expressing cells was treated with PNGase F that cleaves oligosaccharides from the side chain amide of Asn. LDLR contains two N-linked oligosaccharides (168). Indeed, PNGase F treatment reduced the molecular mass of the WT LDLR, indicating that the enzyme efficiently removed N-linked glycans from the receptor (Fig. S4.2B, lane 5 *vs* 2). The size of mutant D203N was also reduced (lane 6 *vs* 3) and comparable to that of the WT LDLR when treated with PNGase F (lane 6 *vs* 5), indicating that PNGase F eliminated the increase in the molecular mass of mutation D203N. Next, we treated cells with tunicamycin that specifically inhibits N-linked glycosylation. LDLR contains only two N-glycosylation sites and is mainly O-glycosylated at the side chains of Ser and Thr residues (168). Consistent with previous reports (169), tunicamycin slightly reduced the molecular mass of the mature and precursor forms of the WT LDLR (Fig. S4.2C, lane 4 *vs* 3) since protein glycosylation starts in the ER and is matured in the Golgi. The molecular mass of the precursor of mutant D203N was also reduced by inhibition of N-linked glycosylation and displaced a similar size as that of the precursor of the WT LDLR (lane 6 *vs* 4). However, tunicamycin essentially eliminated the mature form of D203N without detectable effect on that of the WT receptor (Fig. S4.2B, lane 6 *vs* 4). The amount of the mature form of D203G and D203V was also reduced by tunicamycin but to a lesser extent than that of D203N. These findings indicate that mutation D203N might introduce an extra-N-glycan to LDLR.

4.3 Discussion

In the current study, we demonstrated the important role of negatively charged amino acids in the LRs of LDLR in PCSK9 binding. We showed that elimination of the negative charge on Asp at position 4 in the LR1 of mutant LDLR-ΔLR4-LR7 significantly reduced PCSK9 binding, while replacement of Asp4 in the full-length LDLR with Asn had no detectable effect. On the other hand, mutations D172N in the linker between the LR4 and the LR5 and D203N in the LR5 of the full-length LDLR significantly reduced PCSK9 binding to the receptor at pH 7.4. Further, D203N but not D172N reduced PCSK9 binding at pH 6.0 and LDLR-mediated LDL uptake. Together, these findings indicate that Asp residues at specific positions in the LRs regulate binding of PCSK9 to LDLR.

It has been reported that the side chain of Asp203 forms hydrogen bonds with the backbone amide of the LR5 (170), thereby playing an important in maintaining the structural stability. Indeed, mutations on Asp203 including D203N, D203G, D203A, and D203V have been identified in FH patients (171-173). However, we did observe the mature form and cell surface expression of D203N, indicating that the mutant LDLR could be delivered to plasma membrane. When normalized to the mature form of LDLR, D203N significantly reduced binding of PCSK9 and LDL to the receptor and PCSK9-promoted LDLR degradation. It is of note that patients carrying D203N display FH. Thus, the effect of D203N on LDL binding must be dominant over its effect on PCSK9 binding. In addition, mutations D203N, D154N and D172N all introduced a novel N-glycosylation site to the receptor (Fig. S4.2A). D203N and double mutation E153QD154N but not D172N seemed to cause a minor electrophoretic mobility shift on SDS-PAGE (Fig 4.2B and 4.2C). However, E153QD154N, unlike D172N and D203N, had no detectable effect on PCSK9 binding. In addition, we found that PNGase-F reduced the gel shift caused by D203N while tunicamycin treatment essentially eliminated the

mature form of D203N but had much less effect on trafficking of other D203 mutations. It would be of interest to investigate if and how these mutations affect N-glycosylation of LDLR and the related functional consequences.

Asp172 resides in the highly flexible C-terminal half of the linker between the LR4 and the LR5 (167). No FH mutation has been reported at this position except for a frameshift mutation that deletes three amino acid residues (172 to 174) and causes a premature stop (174). We found that mutation D172N showed a similar distribution pattern as the WT receptor in the Western blot and confocal microscopy. Further, mutation D172N had no detectable effect on LDL binding at pH 7.4 and PCSK9 binding at pH 6.0. These strongly suggest that D172N did not cause a major perturbation of the structure of the protein. However, we cannot exclude the possibility that D172N may result in a subtle structural change in LDLR.

PCSK9 mainly binds to the EGF-A domain of LDLR. How did mutations D172N and D203N in the ligand binding regions impair PCSK9 binding to the receptor? The crystallography structure of PCSK9 with the complete extracellular domain of LDLR at an acidic or neutral value is currently unavailable. Thus, how exactly D172N and D203N affect PCSK9 binding, especially at a neutral pH (cell surface), is unclear. We previously found that at least three ligand binding repeats were required for PCSK9-promoted LDLR degradation (97). Tyeten et al. also reported that binding of PCSK9 to mutant LDLR without the LRs was significantly lower at a neutral or acidic pH value than its binding to the full-length receptor (104). Yamamoto et al. further demonstrated that the LRs of LDLR bound to C-terminal PCSK9 at a pH-dependent manner with much stronger binding in the acidic endosomal environment (141). In addition, studies from Holla et al. indicated that the positively charged C-terminal PCSK9 might interact with the negatively charged LRs of LDLR (112). Similarly,

Cunningham et al. employed the Surface Plasmon Resonance (SPR) assay and revealed that C-terminal PCSK9 purified from Chinese Hamster Ovary (CHO) cells was important for PCSK9 binding to LDLR (105). These findings indicate that the negatively charged LRs of LDLR may interact with the positively charged C-terminal PCSK9. In this situation, D203N might affect the structural stability of the LR5 of LDLR and consequently impair PCSK9 binding. On the other hand, Asp172 that only affected PCSK9 binding at the neutral pH might involve the interaction with PCSK9. Further mutational analysis studies revealed that replacement of Asp at position 172 or 203 with other residues tested including the negatively charged Glu all significantly reduced PCSK9 binding, indicating a specific requirement of Asp at these two positions. It is possible that both the negative charge and the length of the side chain of amino acid residues at positions 172 and 203 are important for PCSK9 binding. In addition, we found that both D203N and D172N significantly reduced binding of $PCSK9^{1-529}$ to the receptor. This suggests that positively charged residues located between amino acid 529 and 692 in the C-terminal PCSK9 are not required for the effect of D203N and D172N on PCSK9 binding. Removal of the complete three C-terminal modules (amino acid residues 454-692), however, dramatically impaired PCSK9 secretion. Studies are ongoing in the lab to define the potential impact of amino acid residues 454-529 in PCSK9 on its binding to LDLR.

Findings discussed above were based on results obtained from cultured cell-based binding assays and PCSK9 purified from mammalian cells. On the other hand, two other groups, Bottomley et al. (140) and Surdo et al. (142) reported that the full-length and C-terminal deletion PCSK9 purified from *E. coli* bound to LDLR with a similar binding capacity. Surdo et al. proposed that the entire ligand binding repeats of LDLR did not directly associate with PCSK9 at a neutral pH value (142). Based on this model, the two Asp residues we identified would not directly interact with PCSK9 at pH 7.4. Given the flexibility of the

loops between the LRs (17,142,167), it is possible that the structural alteration in the LR5 caused by D203N may affect the structural stability of the LR7 via a possible intermodule crosstalk between different LRs as reported by Guttman et al. (167). This may eventually impair the integrity of the EGF-A due to the presence of the rigid structure between the LR7 and the EGF-A (175) and consequently interfere PCSK9 binding to the receptor. However, this cannot explain why mutation D172N impaired PCSK9 binding only at pH 7.4. In addition, mutations of other negatively charged residues in the LR4 and the LR5 including FH mutations D147N, D151N, D154N, and D157N that are believed to cause damaging effects on LDLR structure (176) and mutations of Asp at positions 196, 200, and 206, and Glu at position 207 that disrupt the calcium binding pocket of LR5 and its structure integrity (170,177) had no detectable effect on PCSK9 binding. Thus, how exactly D172N and D203N affect PCSK9 binding is unclear.

We noticed that, in the Bottomley study, the apparent IC_{50} value for mutant PCSK9 without the C-terminus to suppress the PCSK9-LDLR interaction was approximately 110 nM, while it was 80 nM for the full-length PCSK9 (140). Similarly, the binding affinity of the extracellular domain of LDLR without LR1-LR6 for PCSK9 was slightly lower than that of the complete extracellular domain of LDLR at pH7.4 (Kd=880 nM *vs* 750 nM) (142). We also observed that mutations D172N and D203N only mildly reduced PCSK9 binding. Together, these findings indicate a non-critical role of LR1-LR6 of LDLR in PCSK9 binding. However, it is also possible that the LRs, like the YWTD domain shown in the crystal structure (142), may have a minor interaction with PCSK9. Alternatively, several PCSK9 potential binding partners have been reported (113,178,179). It will be of interest to investigate if the LRs of LDLR, especially D172 and D203, are involved in the interaction with these potential partners.

Supplementary figures

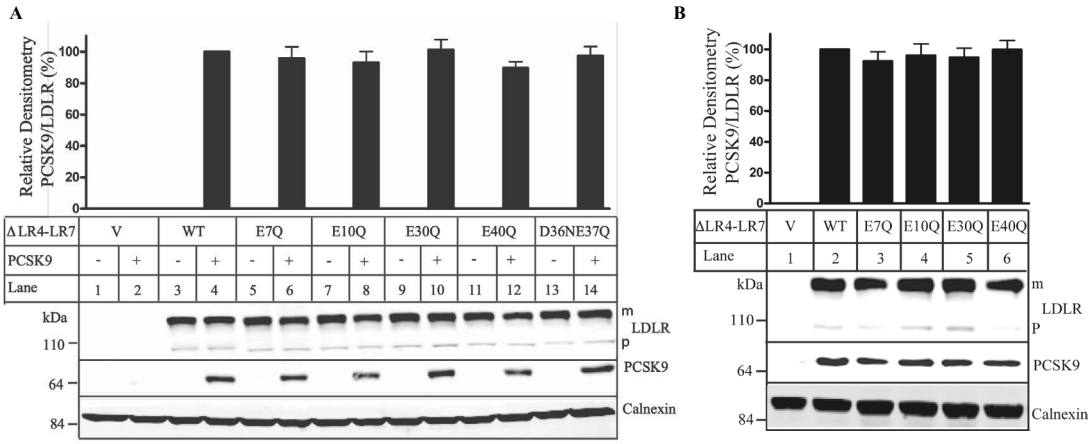

Supplemental Figure 4.1S. Binding of PCSK9 to the wild-type and mutant LDLR-ΔLR4-LR7 LDLR at pH 7.4 (A) or pH 6.0 (B). The experiments were performed as described in the legend to Figure 1. LDLR and PCSK9 were detected by HL-1, and 15A6, respectively. Calnexin was detected by a polyclonal antibody. Top bands of LDLR were the mature and fully glycosylated forms (m). Bottom bands of LDLR were the precursor forms (p). Bottom figures were representative ones of protein levels. V: cells were transfected with the empty vector, pCDNA3.1. Data shown in top figures were quantified as described in the legend to Figure 1B. The percentage of the relative densitometry of PCSK9 binding to the wild-type LDLR was defined as 100%. Values were mean ± S.D. of ≥ 3 experiments.

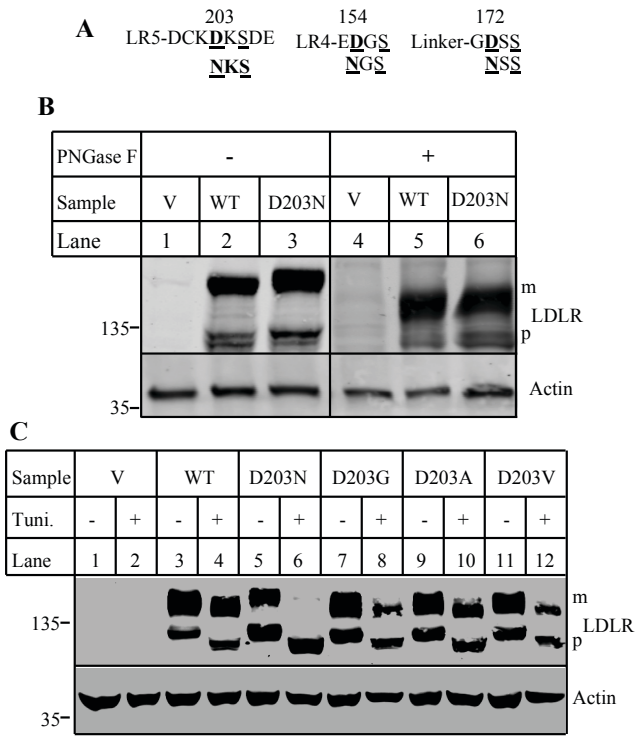

Supplemental Figure 4.2S. Effect of mutation D203N on LDLR expression. ***A.*** Amino acid sequences showing the canonical N-glycosylation motif introduced by mutations D203N, D154N, and D172N (underlined and bold). ***B.*** Deglycosylation of proteins in whole cell lysate using PNGase-F. HEK293 cells transiently expressing the WT or mutant LDLR (D203N) were collected for the preparation of whole cell lysate. Same amount of total proteins was incubated with or without PNGaseF and then subjected to SDS-PAGE (5%) and immunoblotting. ***C***, Inhibition of N-glycosylation of proteins using tunicamycin. HEK293 cells transiently expressing the WT or mutant LDLR were incubated with tunicamycin (0.5 μg/ml) for 24 h. After, whole cell lysate was prepared, and equal amount of total proteins was analyzed by immunoblotting. LDLR and actin were detected by HL-1 and a polyclonal anti-actin antibody, respectively. Top bands of LDLR were the mature forms (m). Bottom bands of LDLR were the precursor forms (p). V: cells were transfected with the empty vector, pCDNA3.1. Similar results were obtained from at least two experiments.

Chapter 5: Manuscript III

Investigating the role of PSAP in the regulation of LDLR and cholesterol metabolism

(Manuscript in preparation)

Investigating the role of prosaposin in the regulation of LDLR and LDL cholesterol metabolism

Abstract

Familial hypercholesterolemia (FH), characterized by elevated levels of plasma LDL cholesterol, is mainly caused by mutations in one of three genes, *LDLR*, its ligand *apoB*, and *PCSK9*. Thus, increasing hepatic LDLR level is a promising therapeutic for lowering plasma levels of LDL-C and the risk of cardiovascular disease (CVD). It has long been known that LDLR can be targeted to lysosome for degradation by an intracellular pathway. However, the underlying mechanism is unclear. Here we identified prosaposin (PSAP) as a novel regulator of LDLR. We demonstrated that knockdown (KD) of PSAP in cultured hepatoma-derived cells led to significantly elevated cell surface LDLR abundance and LDL uptake. Further, knockdown of hepatic PSAP by AAV-shRNA increased LDLR levels in the liver and decreased plasma LDL-C levels in the wild-type mice but not the $Ldlr^{-/-}$ mice. Mechanistic studies showed that the effect of KD PSAP on LDLR was independent of PCSK9. On the other hand, data obtained from confocal microscopy and co-immunoprecipitation revealed a direct interaction between PSAP and LDLR. Further studies are ongoing to address the relevance and cellular mechanism by which PSAP induces LDLR degradation.

Keywords: LDLR degradation, PSAP, PCSK9, AAV, plasma LDL-C, $Ldlr^{-/-}$ mice

5.1 Introduction

CVD is the leading cause of death worldwide. Reducing plasma levels of LDL-C lowers the risk of CVD. LDL-C levels in the blood are mainly controlled by LDLR in the liver. LDLR is transcriptionally regulated by sterol regulatory element-binding protein 2 (SREBP2) and post-translationally regulated by PCSK9 and inducible degrader of the LDLR (IDOL). PCSK9-promoted LDLR degradation requires the binding of PCSK9 to LDLR at the cell surface and internalization of the receptor (95). GOF in the *PCSK9* gene lead to higher plasma LDL-C levels and accelerate the development of CVDs (50,180,181). Conversely, *PCSK9* LOF mutations lead to lower plasma LDL-C levels and protect against CVD (51,182). Inhibition of PCSK9 shows an impressive LDL-lowering effect (up to 60%) and significantly reduces CVD events (183-185). Most recently, anti-PCSK9 monoclonal antibodies have been approved for the treatment of patients with FH. However, this therapy requires long-term injections and a high dose of antibodies to achieve clinical efficacy, leading to extremely high costs. Thus, there is an important and urgent need for novel therapeutic approaches to lower LDL-C effectively and cost-efficiently.

The cell surface endocytosis of the PCSK9/LDLR complex initiates a dominant degradation pathway that prevents the recycling of LDLR. Previous studies have demonstrated that the catalytic domain (CAT) of PCSK9 interacts with the EGF-A domain of the LDLR on the cell surface (96,97). The C-terminal domain (CTD) of PCSK9 does not directly interact with LDLR, but it is required for LDLR degradation (97,104,108). The specific role of the CTD in PCSK9-promoted LDLR degradation remains obscure. Piper et al. demonstrated that the CTD of PCSK9 has a novel protein fold and may mediate protein-protein interactions (83,109). Furthermore, natural mutations that occur within this domain result in either GOF (H553R) or LOF mutations (Q554E), affecting its potency in mediating LDLR degradation

(110). Incubation of purified mutant PCSK9 lacking the CTD (PCSK9ΔCTD) has showed no detectable reduction of cell surface LDLR levels, even at a high concentration of 5 μg/ml, which is 10 times higher than the physiological concentration (97,108). Interestingly, PCSK9ΔCTD can bind to LDLR at the cell surface and participate in endocytosis to the endosomes (104,108,111,112). Therefore, the inability of PCSK9ΔCTD to enhance LDLR degradation does not reside in its lack of LDLR binding or its internalization with LDLR, suggesting that the CTD may carry structural requirements to achieve the critical later steps of LDLR sorting and degradation within endosomes/lysosomes. Most recently, Poirier et al. demonstrated that reconstitution of PCSK9ΔCTD with a foreign lysosomal targeting motif is able to rescue its intracellular lysosomal targeting and induce LDLR degradation, emphasizing a role for the CTD in sorting of the PCSK9/LDLR complex towards the late endocytic compartments (111). Since both LDLR and PCSK9 lack the lysosomal targeting motif, we hypothesized that the CTD of PCSK9 might recruit other partner(s) to the PCSK9/LDLR complex that can direct LDLR to the lysosome or block the binding of the cofactor(s) that is required for LDLR recycling from endosomes to the cell surface.

To address these possibilities, we applied the Matchmaker Gold Yeast Two-Hybrid System (Clontech) to probe for potential PCSK9 binding proteins. Briefly, the CTD of PCSK9 (amino acid 440-692) was used as the bait protein to screen for the binding partners (the prey) from a human liver protein library. After two rounds of selections, we obtained several positive clones. DNA sequencing results revealed that prosaposin (PSAP) was one of the potential PCSK9 cofactors interacting with its CTD.

PSAP is the precursor of four glycosphingolipid activator proteins. It is composed of 527 amino acids, synthesized as a 53 kDa protein in the ER, and glycosylated into 65 kDa and 70 kDa forms in the Golgi (Figure S5.1). The 65 kDa PSAP is transported to the lysosomes by

mannose-6-phosphate receptor (M6PR) or a sorting receptor, sortilin (186). In the lysosome, PSAP is proteolytically cleaved to generate four mature saposins (saposin A, B, C, and D) by cathepsin D and other possible proteases (187). Saposins are highly homologous molecules, each with approximately 80 amino acids containing six cysteine residues and N-glycosylated carbohydrate chains that are highly conserved. The 70 kDa form of PSAP, instead, is secreted to the extracellular space and exists in various secretory body fluids such as plasma.

PSAP is a multifunctional protein that has various physiological roles (188,189). In the lysosome, saposins act as a cofactor and facilitate lysosomal enzymes to degrade glycosphingolipids (GSLs). Mice with global PSAP-deficiency have severe leukodystrophy with aberrant GSL storage in the brain and visceral organs. Fujita et al. has created a homozygous mouse model with a null allele PSAP (190). They found abnormally increased levels of lactosylceramide, glucosylceramide, galactosylceramide, globotriaosylceramide, ceramide and sulfatide in the brain, liver, and kidneys (191,192). Extracellular PSAP has been reported to possess biological activities beyond the enzymatic actions exhibited in the lysosome. For instance, some reports document a variety of neurotrophic activities of extracellular PSAP through a receptor-mediated mechanism (193). Meyer et al. observed that a 12-amino acid sequence within saposin C domain binds to G protein-coupled receptor GPR37, which participates in neuroprotection (194). Moreover, progranulin is a secretory glycoprotein that is recently implicated in several neurodegenerative diseases. Zhou et al. found that PSAP associates with progranulin extracellularly and facilitated its lysosomal trafficking via the low-density lipoprotein receptor-related protein 1 (LRP1) in fibroblasts (195).

Currently, there is limited literature on the role of PSAP in cholesterol homeostasis. Consistent with my findings, Ly et al. has identified PSAP as a potential PCSK9 interacting

protein from the HepG2 cell medium using an unbiased mass spectrometry approach (196). Moreover, Bartz et al. has demonstrated that knockdown of PSAP by RNAi altered cellular cholesterol content in Hela cells, indicating a potential regulatory role for PSAP in cholesterol homeostasis (197). However, the role of PSAP in the regulation of LDLR and cholesterol metabolism remains unknown. In this study, we found that KD of PSAP in cultured hepatoma-derived cells led to significantly elevated cell surface LDLR abundance and LDL uptake. Further, KD of hepatic PSAP by AAV-shRNA increased LDLR levels in the liver and decreased plasma LDL-C levels in the wild-type mice but not the $Ldlr^{-/-}$ mice.

5.2 Results

5.2.1 Knockdown of PSAP increased LDLR abundance *in vitro*

To determine whether reducing PSAP levels affected LDLR levels *in vitro*, we transfected human hepatoma-derived HepG2 cells with siRNAs targeting PSAP. After 2 days of transfection, the two PSAP siRNAs that targeted different regions in the *PSAP* mRNA efficiently reduced the protein levels of PSAP and caused a significant increase in LDLR in the lysate when compared with the control. More specifically, LDLR was increased over 2 folds in response to PSAP knockdown, whereas the levels of PCSK9 and β-actin were comparable in cells transfected with scrambled or PSAP siRNA (Fig 5.1A and B). To confirm this findings, we knocked down PSAP expression in another human hepatoma-derived cell line (Huh7) and found that LDLR levels were significantly increased in PSAP siRNA-transfected cells, whereas the levels of PCSK9 and β-actin were comparable in cells transfected with scrambled or PSAP siRNA (Fig S5.2).

LDLR resides on plasma membrane, where it binds to and mediates LDL internalization. Thus, cell surface proteins in Huh7 cells were labelled with biotin and then pulled down from whole cell lysate with Neutravidin beads. As shown in Figure 5.1C, the expression of PSAP in whole cell lysate was reduced by its siRNA. Conversely, LDLR levels were increased in both whole cell lysate and in the cell surface fraction in PSAP-knockdown cells. Transferrin receptor (TFR), a plasma membrane protein, but not PSAP, was not detected in the cell surface fraction. Consistently, knockdown of PSAP significantly increased cellular LDL uptake (Fig 5.1D). On the other hand, PSAP siRNA reduced mRNA levels of *PSAP* without any effect on the mRNA levels of *LDLR, SREBP2* and *PCSK9* (Fig 5.1E), suggesting that the effect of PSAP knockdown on LDLR was not likely through the transcriptional

regulation. Together, these findings demonstrated that KD of PSAP increased LDLR expression and function in cultured hepatocytes.

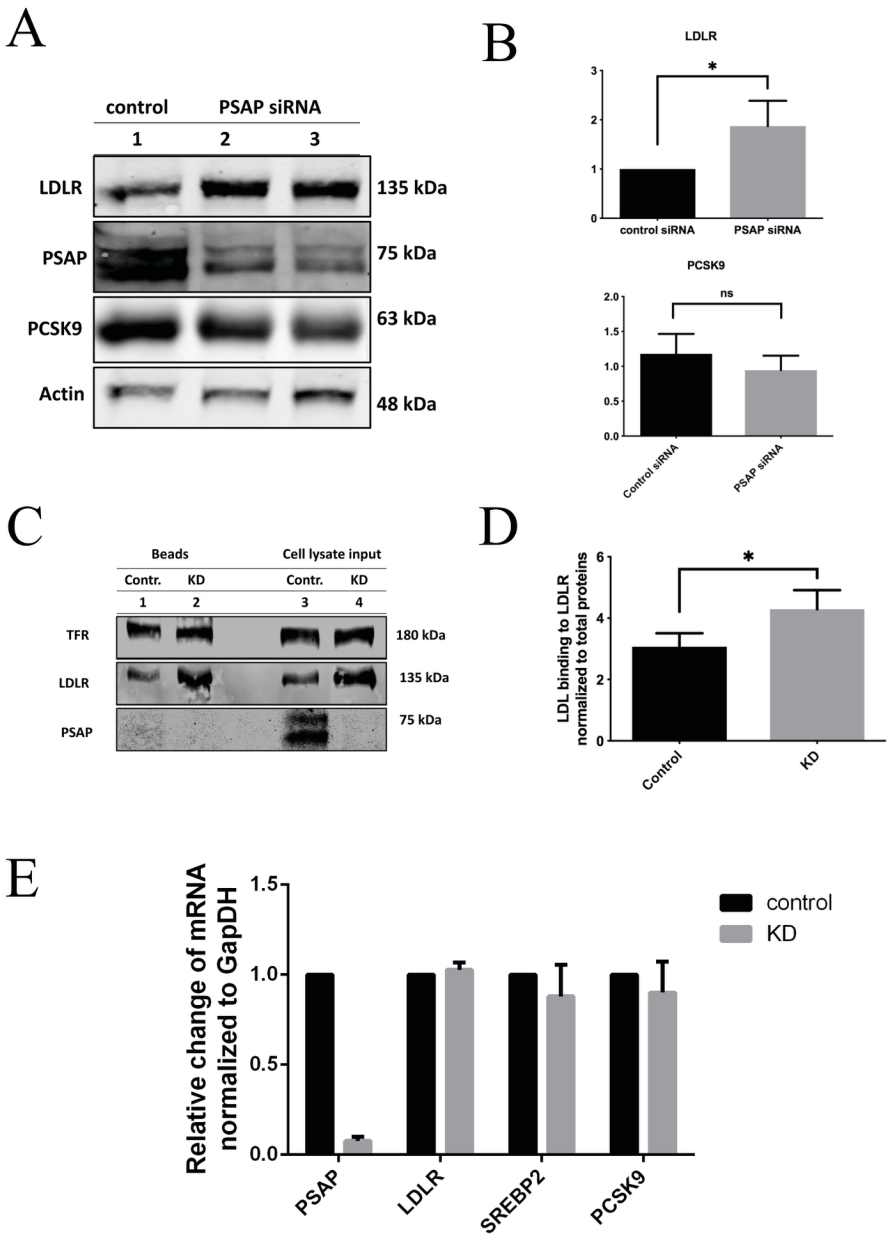

Figure 5.1 Effect of PSAP KD in cultured hepatoma-derived cells. ***A and B. Knockdown of PSAP increased LDLR in HepG2.*** Two different PSAP-specific siRNAs were used to knock down PSAP expression in HepG2 cells. After 48 h, whole cell lysate was prepared, followed by immunoblotting to detect LDLR and PCSK9 using a monoclonal anti-

LDLR (HL-1) and anti-PCSK9 (15A6) antibody, respectively. The figures in panel A showed representative protein levels. The densitometry was determined using a Licor Odyssey Infrared Imaging System. The relative densitometry was the ratio of the densitometry of LDLR to that of actin at the same condition. ***C. Biotinylation of LDLR***. Briefly, Huh7 cells were seed in a 6-well plate and transfected with control or PSAP siRNA (KD) as described above. After 48 h, cells were incubated with biotin in PBS (pH 8.0) for 20 mins at 4 °C with gentle shaking. After washed with ice-cold PBS three times and quenched in glycine for 30 mins, whole cell lysate was prepared and applied to NeutrAvidin agarose to pull down biotin-labelled cell surface proteins. Equal amount of whole-cell lysate (Inputs) and cell surface proteins (Beads) that were eluted from NeutrAvidin Beads were applied to immunoblotting using antibodies as described in the legend to panel A. ***D. Cellular Dil-LDL uptake.*** Briefly, Huh7 cells were set up in a 96-well plate and transfected with control or one of the two different PSAP siRNAs for 48 h, followed by incubation of Dil-LDL (10 μg/ml) in the presence or absence of unlabeled LDL (600 μg/ml) for 2 h. After washing three times, the cells were lysed, and the fluorescence signal was measured using a SYNERGY plate reader at an excitation wavelength of 520 nm and an emission wavelength of 580 nm. Total cellular proteins in each well were measured using the BCA protein assay kit. The relative fluorescence units (RFU) were the fluorescence signal normalized to total proteins. ***E. Relative changes of mRNA levels***. Huh7 cells were transfected with control and PSAP siRNA (KD). Total RNAs were isolated from cells using RNA isolation kits following the manufacturer's protocol (Qiagen). The cDNA was synthesized from same amount of total RNA (2 μg) using High Capacity cDNA Reverse Transcription Kit. qRT-PCR was performed on a SteponePlus

Real-Time PCR machine using SYBRGreen Master Mix, and relative mRNA levels were normalized to the *GAPDH*.

5.2.2 Knockdown of hepatic PSAP increased LDLR *in vivo*

Considering the effects of PSAP on LDLR expression in cultured cells and the critical role of hepatic LDLR in cholesterol metabolism *in vivo*, I further sought to understand the regulatory role of PSAP in cholesterol metabolism in mice. Given that PSAP-null mice die at an early age, we decided to use adeno-associated virus carrying PSAP shRNA (AAV-PSAP shRNA) to knock down PSAP expression in mouse liver. Equal amount of AAV-DJ/8-PSAP shRNA or scrambled shRNA was injected to C57BL/6 mice (8–10 weeks of age, 5 x 10^{10} gc/mouse, 6 mice/group). Mice were fed western-type diet and sacrificed 30 days after transduction. Liver and plasma samples were collected for further analysis.

qRT-PCR results revealed that mRNA levels of *PSAP* were dramatically reduced in the liver of mice injected with AAV-PSAP shRNA when compared with those treated with AAV-scrambled shRNA (Fig 5.2A). These mice were active, healthy and indistinguishable, and did not display a significant difference in H&E staining of liver sections (Fig S5.3A). Bodyweight and plasma ALT levels were also comparable in mice injected with AAV-scrambled or PSAP shRNA (Fig S5.3 C& D). Further, the mRNA levels of *Ldlr*, *Pcsk9*, *Hmgcr*, *Pcsk9*, and *Srebpf2* in the mouse liver were not affected by the reduction of PSAP (Fig 5.2A).

On the other hand, PSAP knockdown mice displayed a mild but significant increase in LDLR levels in the liver (Fig 5.2B and C) without any significant change in plasma PCSK9 levels (Fig 5.2D). We observed that knockdown of PSAP significantly reduced plasma levels of total cholesterol (Fig 5.2E). Fast protein liquid chromatography (FPLC) data showed a marked reduction of cholesterol content in both LDL and HDL fractions (Fig 5.3A). Consistently, the plasma levels of both HDL and non-HDL cholesterol wer significantly decreased as measured by the commercial Cholesterol Assay Kit (Cell Biolabs, INC) (Fig 5.3B and 5.3C). Further, plasma levels of apoE and apoB48 were decreased in the PSAP-

knockdown mice when compared with those in mice injected with scrambled shRNA (Fig 5.3D and 5.3E). These data suggest that reduction of PSAP might be sufficient to increase LDLR levels in the liver and indicate the important role of PSAP in the regulation of hepatic LDLR and plasma cholesterol.

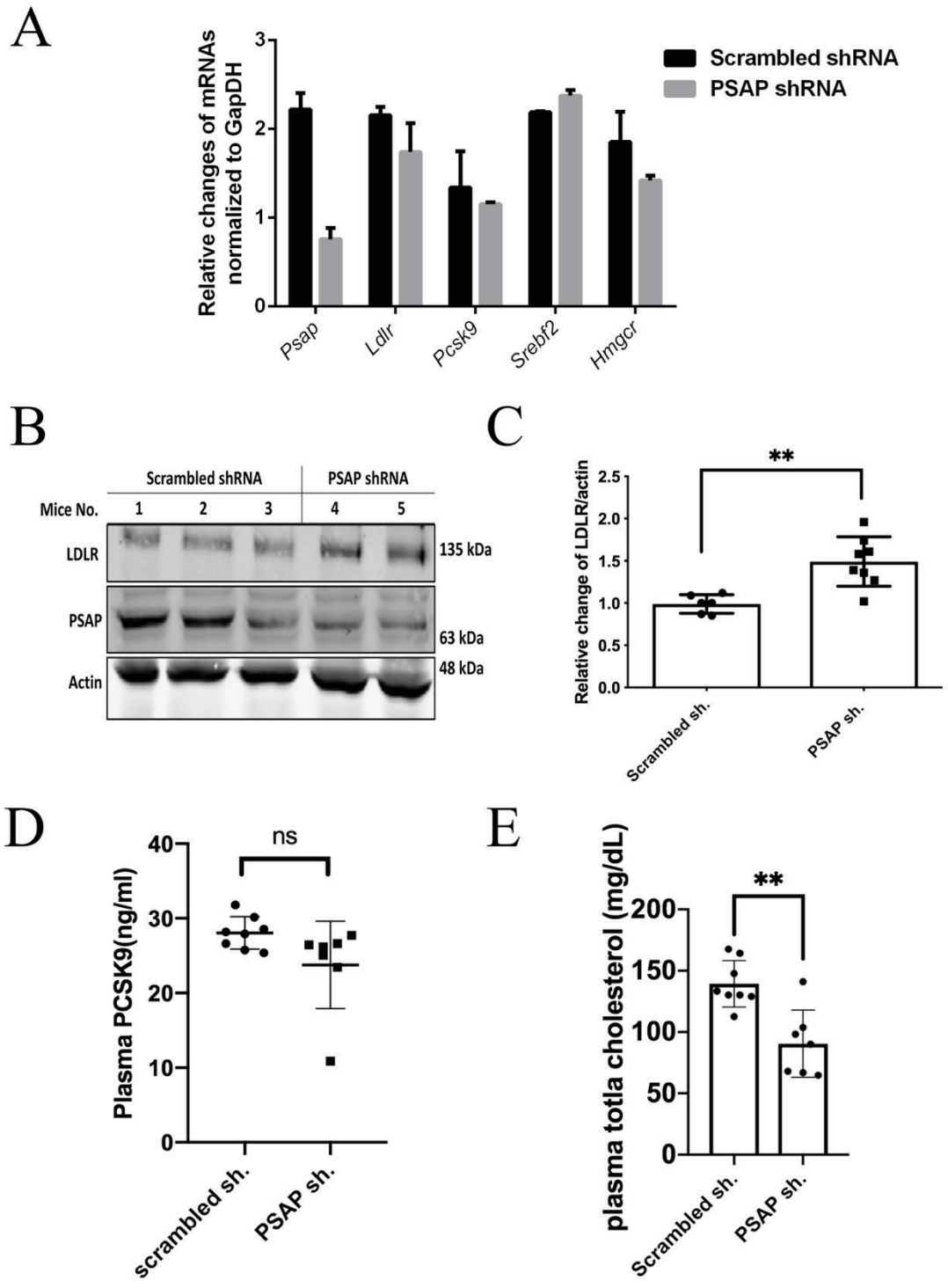

Figure 5.2 Effect of PSAP KD in mouse liver on LDLR and plasma PCSK9. ***A. mRNA levels of Ldlr and other Srebpf2 target genes.*** Total RNAs were extracted from

the liver from mice injected with AAV-scrambled or PSAP-shRNA with TRIzol, followed with qRT-PCR measurement of mRNA levels. The relative mRNA levels were the ratio of the mRNA levels of *target genes* to that of *Gapdh* in the same tissue. ***B. Hepatic LDLR levels.*** Same amount of liver homogenates from each mouse (90 μg/well) was subjected to immunoblotting. Relative densitometry was the ratio of the densitometry of LDLR of different mice to that of actin of the same mouse. ***C. Plasma PCSK9 level.*** Same amount of plasma from each mouse in the same group was applied to commercial ELISA kit for PCSK9 protein concentration. ***D. Plasma levels of total cholesterol.*** 20 μl of plasma from each mouse were applied to the measurement using a commercial kit in accordance with the manufacturer's instructions.

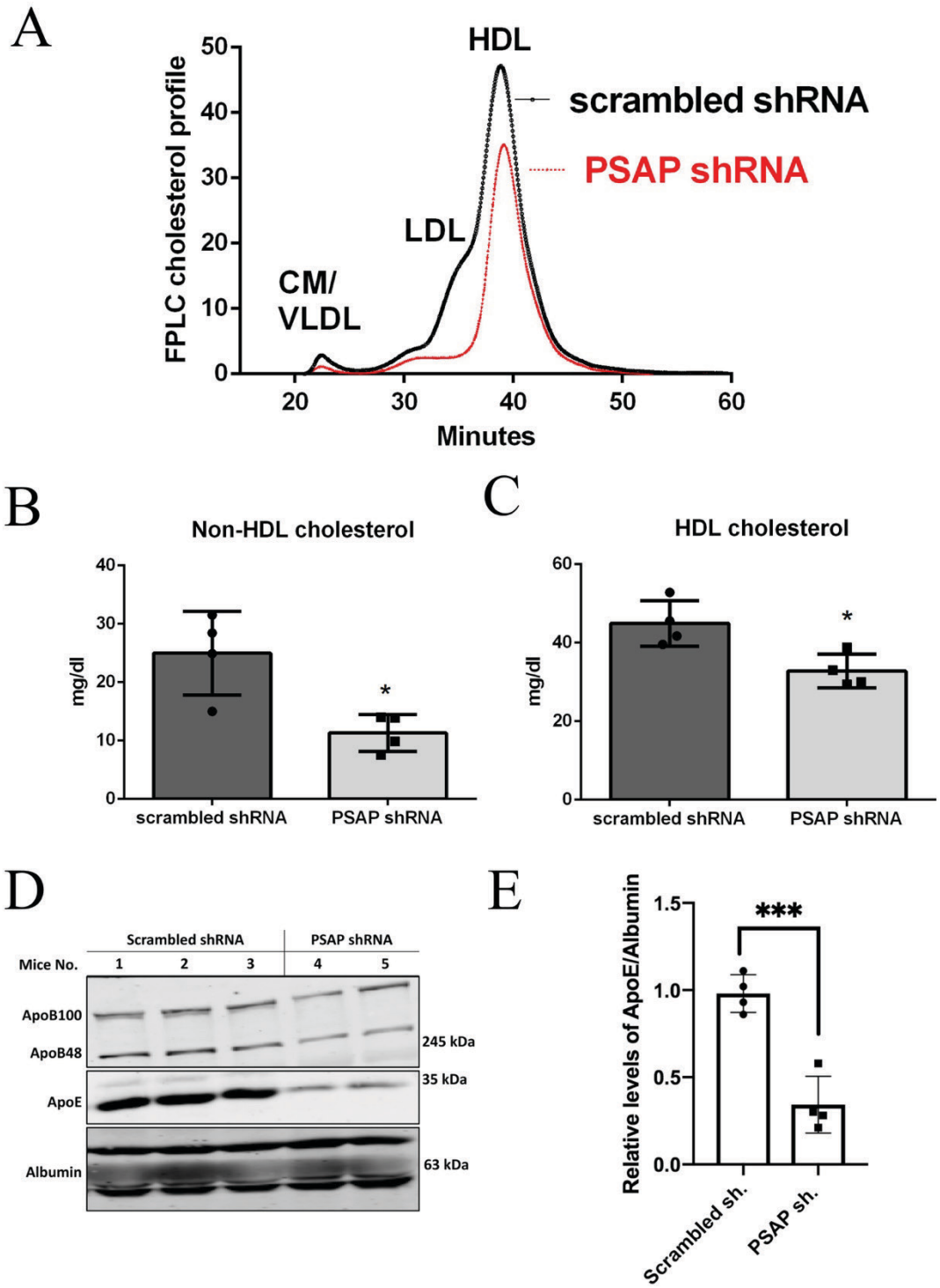

Figure 5.3 Effect of KD PSAP in mouse liver on plasma cholesterol and apolipoproteins. ***A. Plasma cholesterol profile.*** Same amount of plasma from each mouse in

the same group was pooled and applied to FPLC analysis of plasma cholesterol. ***B and C. Plasma levels of HDL and non-HDL cholesterol.*** 20 μl of plasma from each mouse were applied to the measurement using a commercial kit in accordance with manufacturer's instructions. ***D and E. Plasma levels of apolipoproteins.*** Same amount of plasma samples from each mouse was diluted with water and subjected to immunoblotting. Relative densitometry was the ratio of the densitometry of LDLR of different mice to that of albumin of the same mouse. The values of all data unless otherwise indicated were mean ± S.E.M of at least 6 mice in each group. *, $p<0.05$. **, $p<0.01$.

5.2.3 Effect of knocking down PSAP in *Ldlr*$^{-/-}$ mice on plasma cholesterol

To evaluate the dependence of the regulatory role of PSAP in plasma cholesterol on LDLR, we knocked down the expression of PSAP in *Ldlr*$^{-/-}$ mice (8-10 weeks of age, 5 x 10^{10} gc/mouse, 6 mice/group) using AAV-DJ/8-PSAP shRNA or scrambled shRNA. Mice were fed western-type diet and sacrificed 30 days after transduction for the collection of the liver and plasma samples. qRT-PCR results revealed that mRNA levels of *Psap* were dramatically reduced in the liver of mice injected with AAV-PSAP shRNA when compared with mice treated with AAV-scrambled shRNA (Fig 5.4A). The plasma levels of total cholesterol, apoE, and apoB were comparable between the two groups (Fig 5.4B, C, D and E). These results indicate that the impact of PSAP knockdown in plasma levels of cholesterol appears to depend on hepatic LDLR in mice.

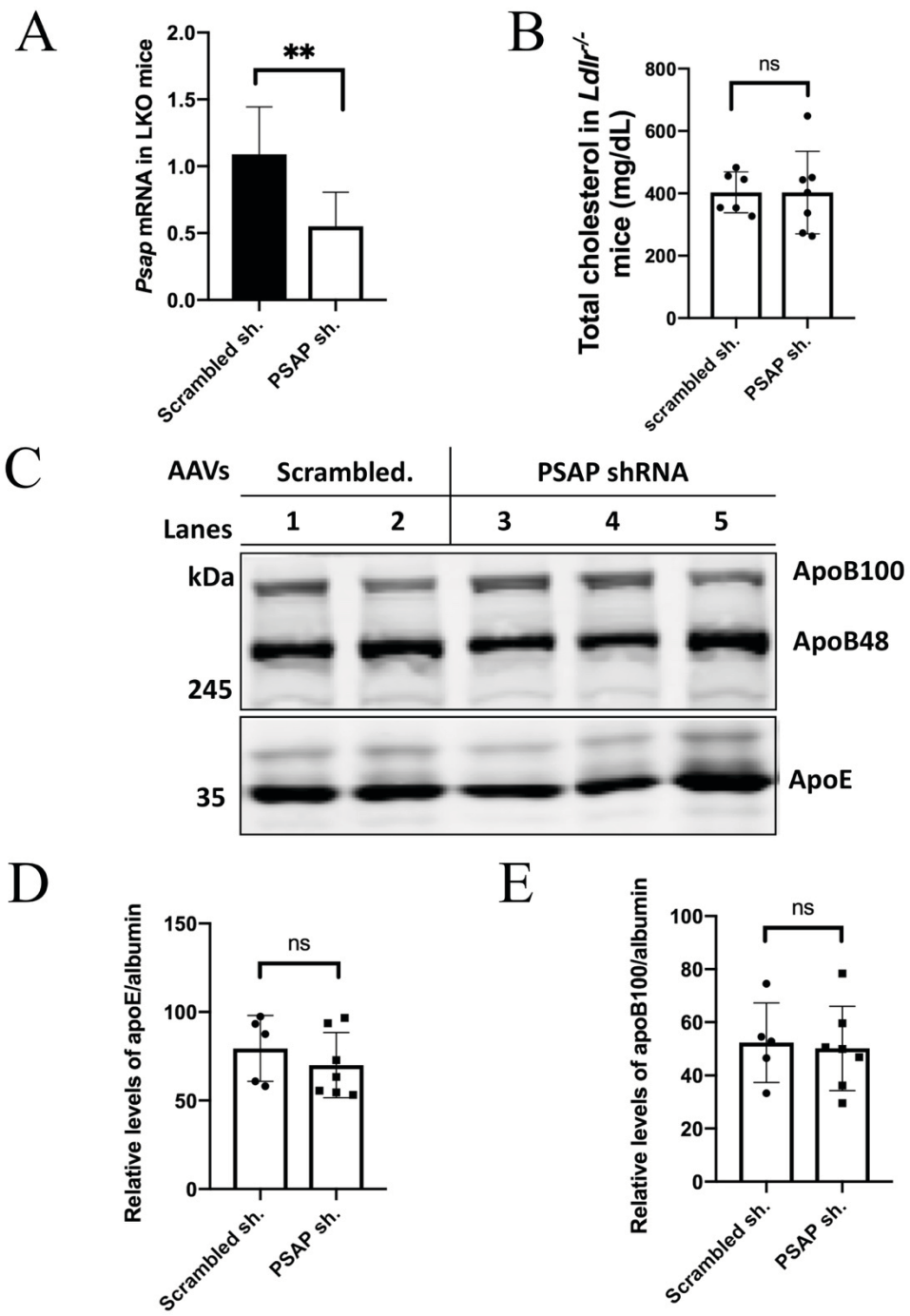

Figure 5.4 Effect of KD PSAP in *Ldlr-/-* mice on plasma cholesterol and apolipoproteins. ***A. Psap mRNA levels.*** Same amount of liver from each mouse (25 mg/mice) were homogenized using TRIZOL. Total RNAs were extracted and used for the synthesis of cDNA, followed by qRT-PCR. The relative mRNA levels were the ratio of the mRNA levels

of the target genes to that of *Gapdh* at the same condition. ***B. Plasma levels of total cholesterol.*** 20 μl of plasma from each mouse were applied to the measurement using a commercial kit in accordance with manufacturer's instructions. ***C, D and E. Plasma levels of apoE and apoB.*** Same amount of plasma samples from each mouse was diluted with water and subjected to immunoblotting. Relative densitometry was the ratio of the densitometry of LDLR of different mice to that of albumin of the same mouse. The values of all data unless otherwise indicated were mean ± S.E.M of at least 6 mice in each group. *, $p<0.05$. **, $p<0.01$.

5.2.4 Effect of knockdown PSAP on lysosomal function

Given that PSAP siRNAs efficiently reduced mRNA levels of *PSAP* but did not affect that of *LDLR, PCSK9, SREBP2* or *HMGCR* (Fig 5.1E), it appeared that PSAP had no dramatic effect on *LDLR* transcription. The complete loss of PSAP or one of the individual saposins causes lysosomal storage disorders (192). Thus, reducing PSAP expression in cultured cells might alter lysosomal function which, in turn, influence LDLR levels. We applied LysoBrite™ Green to monitor the acidification of lysosomes, an indication of the integrity of the lysosomal function. As shown in Figure 5.5A and 5.5B, the fluorescent signals were comparable between cells transfected with control or PSAP siRNAs, indicating that a negligible deleterious effect of knockdown of PSAP on the lysosomal acidification. LDLR is mainly degraded in the lysosomes. If the PSAP knockdown-induced increase in LDLR was caused by the impaired lysosomal function, LDLR levels should not be further increaseed when combined PSAP knockdown and inhibition of lysosome function. To test this hypothesis, we transfected Huh7 cells with scrambled or PSAP siRNA, and then treated the cells with chloroquine (CQ) that can accumulate in lysosome, raise pH in the lysosomes and consequently damage lysosomal function. As shown in Figure 5.5C and D, indeed, treatment with CQ and knockdown of PSAP significantly increased the levels of LDLR in the cells transfected with the scrambled siRNA (lane 4 vs 1) and in cells without addition of CQ (lane 2 vs 1), respectively. We also observed that combination of PSAP knockdown and CQ treatment further increased LDLR levels as compared to either treatment alone (lane 5 vs 4 or 2), indicating that the lysosome could efficiently degrade LDLR when the expression of PSAP was reduced. Next, we treated cells with cycoloheximide to inhibit newly LDLR synthesis and then monitored the levels of LDLR. As shown in Figure 5.5E and F, the biosynthesis of LDLR was inhibited, the newly made

proteins could be degraded in both scrambled and PSAP siRNA-transfected cells. We observed a sharp reduction in LDLR levels with 6 h in PSAP knockdown cells as compared to the control. Together, these findings indicated that knockdown of PSAP at least did not grossly impair lysosomal function, and the increase in LDLR induced by knockdown of PSAP was not mainly contributed by the potential deficiency of lysosome-dependent degradation of LDLR.

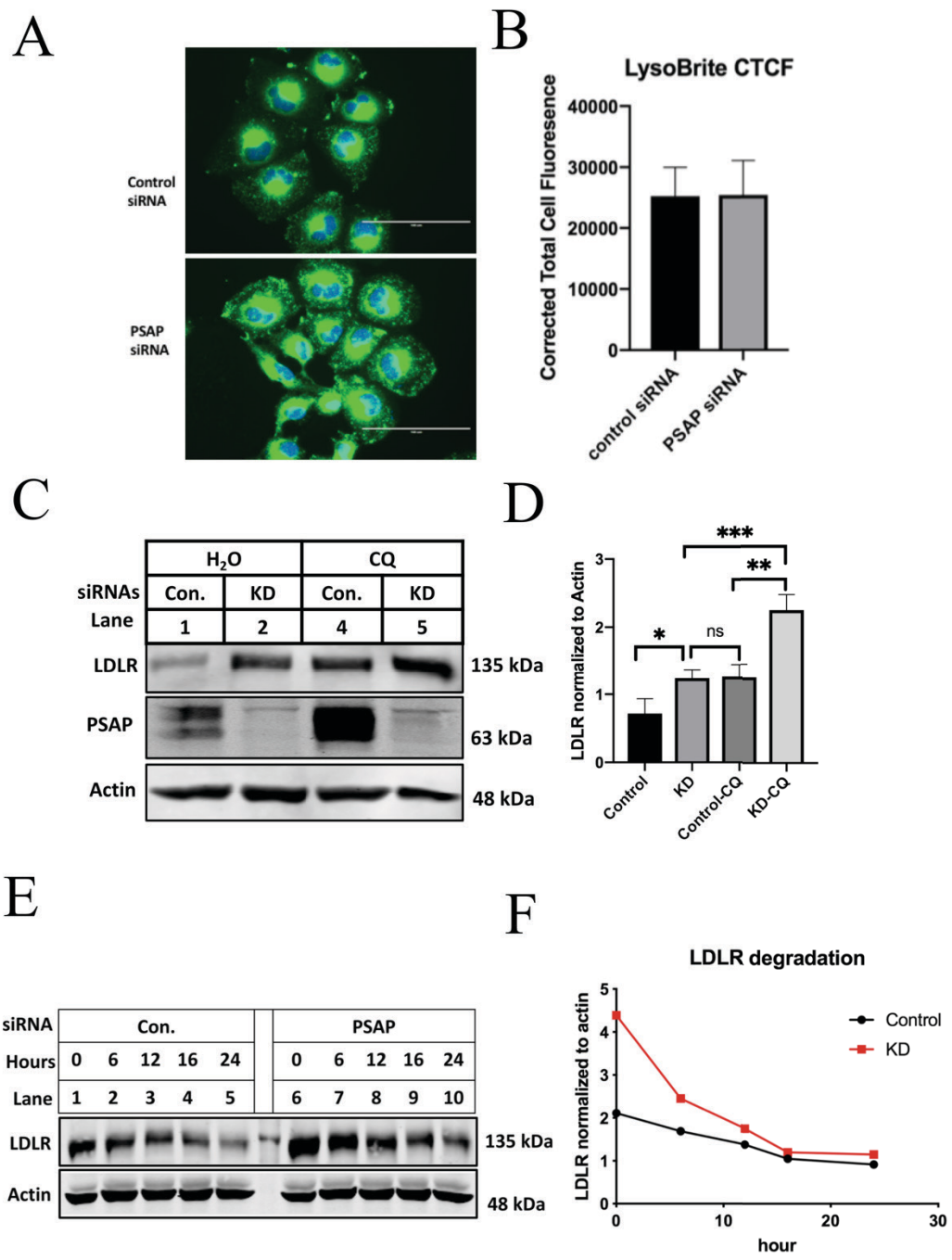

Figure 5.5 Effect of KD PSAP on lysosome function. ***A, lysosome acidification.*** Huh7 cells were transfected with control or PSAP siRNA. After 48 h, cells were incubated with LysoBrite™ (green) and DAPI (blue) for 30 min and then rinsed with PBS for 3 times. Representative images for each treatment were shown at panel A. ***B, Quantification of***

fluorescence signal. Fluorescence signal were measured by Image J. Corrected total cell fluorescence (CTCF) = integrated density – (the area of selected cell x background readings). ***C&D, Effect of KD PSAP on lysosomal LDLR degradation.*** 48 h after transfection, cells were incubated with CQ overnight and whole cell lysate was prepared, followed by immunoblotting to detect LDLR and PSAP using a monoclonal anti-LDLR (HL-1) antibody and anti-PSAP polyclonal antibody, respectively. The figures in panel C showed representative protein levels. The densitometry was determined using a Licor Odyssey Infrared Imaging System. The relative densitometry was the ratio of the densitometry of LDLR to that of actin at the same condition. ***E&F, Effect of KD PSAP on LDLR degradation.*** 48 h after transfection, cells were incubated with cycloheximide at 37 °C, and whole cell lysate was prepared at time points of 0, 6, 12, 16 and 24 h, followed by immunoblotting using a monoclonal anti-LDLR (HL-1) antibody and anti-actin monoclonal antibody, respectively. The figures in panel E showed representative protein levels. The densitometry was determined using a Licor Odyssey Infrared Imaging System. The relative densitometry was the ratio of the densitometry of LDLR to that of actin at the same condition.

5.2.5 PSAP-regulated LDLR was independent of PCSK9

Next, we investigated the role of PCSK9 in PSAP's action on LDLR. First, we incubated cells transfected with scrambled or PSAP siRNA with purified PCSK9 protein (DY). As shown in Figure 5.6A and B, addition of purified PCSK9 proteins efficiently promoted LDLR degradation in PSAP knockdown cells, indicating that PSAP is not required for PCSK9-promoted LDLR degradation. Next, we defined if PCSK9 was required for PSAP-induced degradation of LDLR. We treated HEK293 cells with new-born calf lipoprotein deficient serum (NCLPPS) to increase expression of LDLR and found that knockdown of PSAP increased LDLR levels even though the expression of PCSK9 was undetectable under this condition (Fig 5.6C). We also knocked down the expression of both PCSK9 and PSAP in Huh7 cells. As shown in Fig 5.7D and E, reducing expression of either PSAP or PCSK9 significantly increased LDLR levels. Knockdown of both PCSK9 and PSAP exihibited an additive increase in the levels of LDLR, suggesting that PCSK9 and PSAP might regulate LDLR via different pathways. Together, these findings indicate that the action of PCSK9 and PSAP on LDLR appears to be independent of each other.

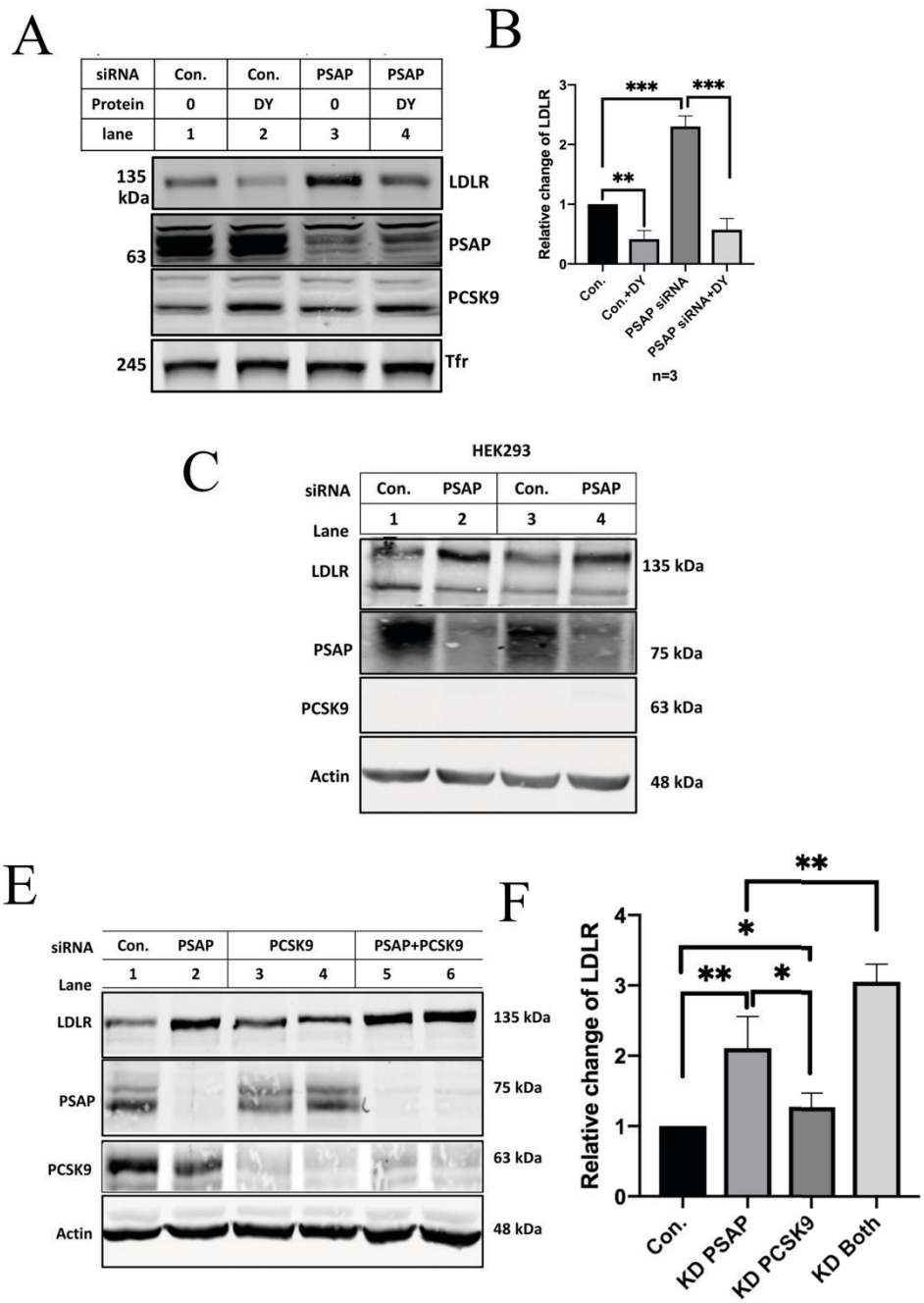

Figure 5.6 Role of PCSK9 in PSAP-regulated LDLR. ***A&B, Effect of KD PSAP on PCSK9-mediated LDLR degradation*.** PSAP-specific siRNAs were used to knock down PSAP expression in Huh7 cells. 48 h after transfection, cells were incubated with 4 μg/ml PCSK9-DY at 37 °C for 6 h, and whole cell lysate was prepared, followed by immunoblotting to detect LDLR, PSAP and PCSK9 using a monoclonal anti-LDLR (HL-1) antibody, anti-PSAP

polyclonal antibody, and anti-PCSK9 (15A6) monoclonal antibody, respectively. The figures in panel A showed representative protein levels. The densitometry was determined using a Licor Odyssey Infrared Imaging System. The relative densitometry was the ratio of the densitometry of LDLR to that of TFR at the same condition. ***C, Effect of KD PSAP on LDLR in HEK293.*** PSAP-specific siRNAs were used to knock down PSAP expression in HEK293 cells. 24 h after transfection, cells were incubated with 5% NCLPPS overnight, and whole cell lysate was prepared, followed by immunoblotting to detect LDLR, PSAP and PCSK9, respectively. The figure in panel C showed representative protein levels. ***D&E, Effect of KD PSAP and PCSK9 on LDLR.*** PSAP- or PCSK9- specific siRNAs were used to knock down their expression in Huh7 cells. After 48 h, whole cell lysate was prepared, followed by immunoblotting to detect LDLR, PSAP and PCSK9, respectively. The figures in panel D showed representative protein levels. The densitometry was determined using a Licor Odyssey Infrared Imaging System. The relative densitometry was the ratio of the densitometry of LDLR to that of actin at the same condition.

5.2.6 PSAP directly interacted LDLR

We then tried to dissect how PSAP induced LDLR degradation. First, we investigated if PSAP co-localized with LDLR using confocal microscopy. We found that PSAP (green fluorescence) and LDLR (red fluorescence) could be detected intracellularly and partially co-localized in Huh7 cells (yellow color, Fig 5.7A). Next, we performed immunoprecipitation using whole cell lysate isolated from Huh7 cells. As shown in Fig 5.7B, HL-1, a mouse anti-LDLR antibody, but not 9E10, a mouse anti-Myc tag antibody could efficiently pull down endogenous LDLR from the whole cell lysate. PSAP was present only in the LDLR-precipitated sample. The transferrin receptor (TFR) was not detectable in the

immunoprecipitated sample. We then generated a mutant LDLR in which the EGF domain was removed (LDLRΔEGF). PSAP and the wild-type (WT) or mutant LDLR were co-expressed in HEK293 cells. PSAP co-immunoprecipitated with the WT LDLR but not the LDLRΔEGF (Fig 5.7C), indicating that the EGF domain is required for the interaction between LDLR and PSAP. These data suggest that PSAP directly associates with LDLR and may induce the intracellular degradation of the receptor.

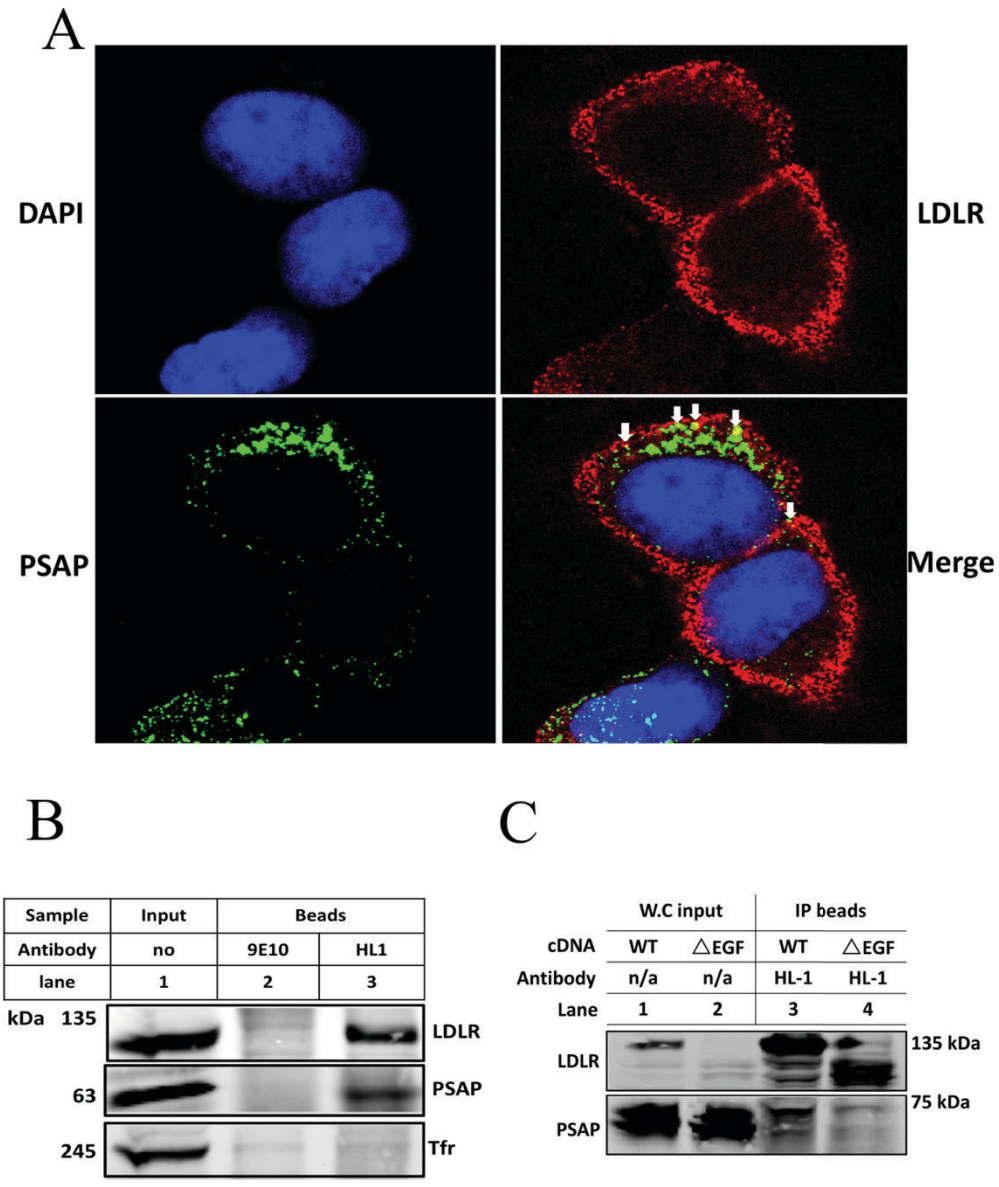

Figure 5.7 Interaction between PSAP and LDLR. ***A, Intracellular localization of LDLR***

and PSAP. Huh7 cells were cultured on coverslips with DMEM containing 5% NCLPPS for 16 h. After washing with PBS 3 times, cells were fixed with paraformaldehyde and permeabilized with ice-cold methanol. The monoclonal anti-LDLR antibody was used to detect LDLR and visualized with Alexa 568-conjugated goat anti-mouse IgG and shown in red. The polyclonal anti-PSAP antibody was visualized with Alexa 488-conjugated goat anti-rabbit IgG and shown in green. Nuclei were visualized with DAPI and shown in blue. ***B, Co-immunoprecipitation of PSAP with LDLR.*** Whole cell lysate was prepared from Huh7 cells (one 100 mm dish) and applied to an anti-LDLR antibody HL-1 and protein-G beads for 48 h. Beads were washed with ice-cold lysis buffer B for 3 times. Same amount of whole cell lysate (Inputs) and eluted proteins from beads (Beads) were applied to immunoblotting using antibodies as indicated. ***C, Interaction between PSAP and WT- and mutant LDLR.*** HEK293 cells were transfected with the WT or LDLRΔEGF. 48 h later, whole cell lysate was prepared, and same amount of total proteins were subjected to immunoprecipitation using the anti-LDLR antibody HL-1 as described above.

5.3 Discussion

Given the protective role of LDLR in atherosclerosis, identifying proteins or compounds that can increase LDLR levels is a key therapeutic avenue for reducing the risk of CVD. In this study, we identified PSAP as a novel regulator of LDLR most likely through a post-translational mechanism. Using *in vitro* and *in vivo* models, we found that 1) knockdown of PSAP expression increased cellular levels of LDLR but not PCSK9 in different types of cells including HepG2 and Huh7, as well as human primary hepatocytes; 2) knockdown of hepatic PSAP in mice increased LDLR in the liver and reduced plasma levels of total cholesterol; 3) knockdown of PSAP had no effect on the mRNA levels of *LDLR* and other *SREBP2* target genes including *PCSK9*, *SREBP2*, and *HMGCR*; and 4) lysosomal inhibition with chloroquine had no effect on PSAP-mediated increment of LDLR; 5) Despite the fact that we initially identified PSAP as a potential binding partner of PCSK9 using the yeast two-hybrid system, our data clearly showed that PCSK9 was not required for PSAP-induced LDLR degradation and vice versa. Studies of the potential interaction between PSAP and PCSK9 and its relevant physiological roles are ongoing in the lab. Nevertheless, our findings indicate that PSAP is a potential LDLR binding partner and regulates hepatic LDLR levels and plasma cholesterol metabolism.

Hepatic LDLR is critical for the clearance of circulating apoB100 and apoE containing lipoproteins. Knockdown of PSAP in cultured cells indeed enhanced cellular LDL uptake. Further, PSAP-KD mice fed Western-type diet showed an increase in hepatic LDLR levels and a significant reduction in plasma levels of total cholesterol, HDL and non-HDL cholesterol. This reduction is likely caused by enhanced LDLR-mediated clearance of LDL, chylomicron remnants, as well as apoE containing HDL particles as reported in PCSK9 knockout mice (56). For example, knockout of PCSK9 in mice dramatically reduces plasma

levels of LDL and HDL due to enhanced LDLR-mediated clearance of LDL and apoE-HDL. Taken together, our findings uncover a novel function of PSAP as a regulator of lipid metabolism.

Previous milestone discoveries in human genetics have established a clear link between PCSK9 function and plasma LDL-C concentrations. Mechanistic analysis reveals that secreted PCSK9 binds to LDLR at the hepatocyte cell surface and promotes its lysosomal degradation, increasing plasma levels of LDL-C and the risk of CVD. Molecular mapping of the PCSK9-LDLR binding interface showed that the EGF-A of LDLR is the main binding site of PCSK9 on the receptor. A blockage of the association between PCSK9 and LDLR reduces plasma levels of LDL-C and CVD (116). Here, we identified the main contribution of the EGF domain of LDLR to the binding between PSAP and LDLR. Removal of the whole EGF domain virtually eliminated the interaction between PSAP and LDLR. Given that knockdown of both PCSK9 and PSAP increased LDLR more significantly compared to knockdown of either PCSK9 or PSAP alone, it is possible that an inhibitor targeting the EGF domain could block the association of LDLR with PCSK9 and PSAP, leading to an additive effect on the increase in LDLR.

How does the binding of PSAP to LDLR cause the degradation of the receptor? We have found that addition of purified recombinant PSAP to the cultured cells did not affect the levels of LDLR, indicating that PSAP unlikely promoted LDLR degradation via the extracellular pathway (Fig 5.8). Sortilin and mannose-6-phosphate receptor can recognize and bind to the C-terminal region of PSAP and direct PSAP to the lysosome. Variants in *SORT1* locus have been shown to have a strong correlation with plasma levels of LDL-C and the risk of coronary heart disease. However, the underlying mechanism is unclear. Conflicting data on the role of sortilin in PCSK9 secretion have been reported in the literature. Studies from

Gustafsen et al. have showed that sortilin facilitated PCSK9 secretion probably at the trans-Golgi network, thereby reducing hepatic LDLR levels and increasing plasma levels of LDL cholesterol (92). On the other hand, Butkinaree et al. have reported that PCSK9 secretion was not affected by silence of sortilin in cultured cells or knockout of sortilin in mice (94). Our findings showed that PSAP interacted with LDLR in cells, and sortilin can bind to PSAP. Is it possible that sortilin directs PSAP/LDLR complex to the lysosome for degradation during the secretory pathway? Experiments are ongoing in the lab to investigate this possibility.

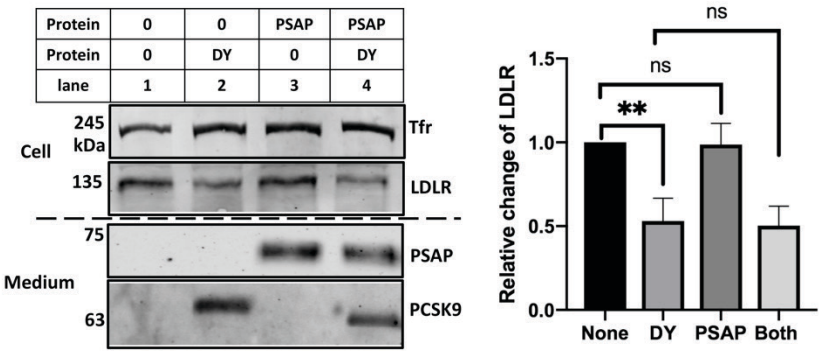

Figure 5.8 Effect of extracellular PSAP on LDLR. Huh7 cells were incubated with 4 μg/ml purified PSAP or PCSK9-DY at 37 °C for 6 h, and whole cell lysate was prepared, followed by immunoblotting to detect LDLR and PSAP using a monoclonal anti-LDLR (HL-1), anti-PSAP polyclonal antibody, and anti-PCSK9 (15A6) monoclonal antibodies, respectively. The figures on the left showed representative protein levels. The densitometry was determined using a Licor Odyssey Infrared Imaging System. The relative densitometry was the ratio of the densitometry of LDLR to that of tfr at the same condition.

Supplementary figures

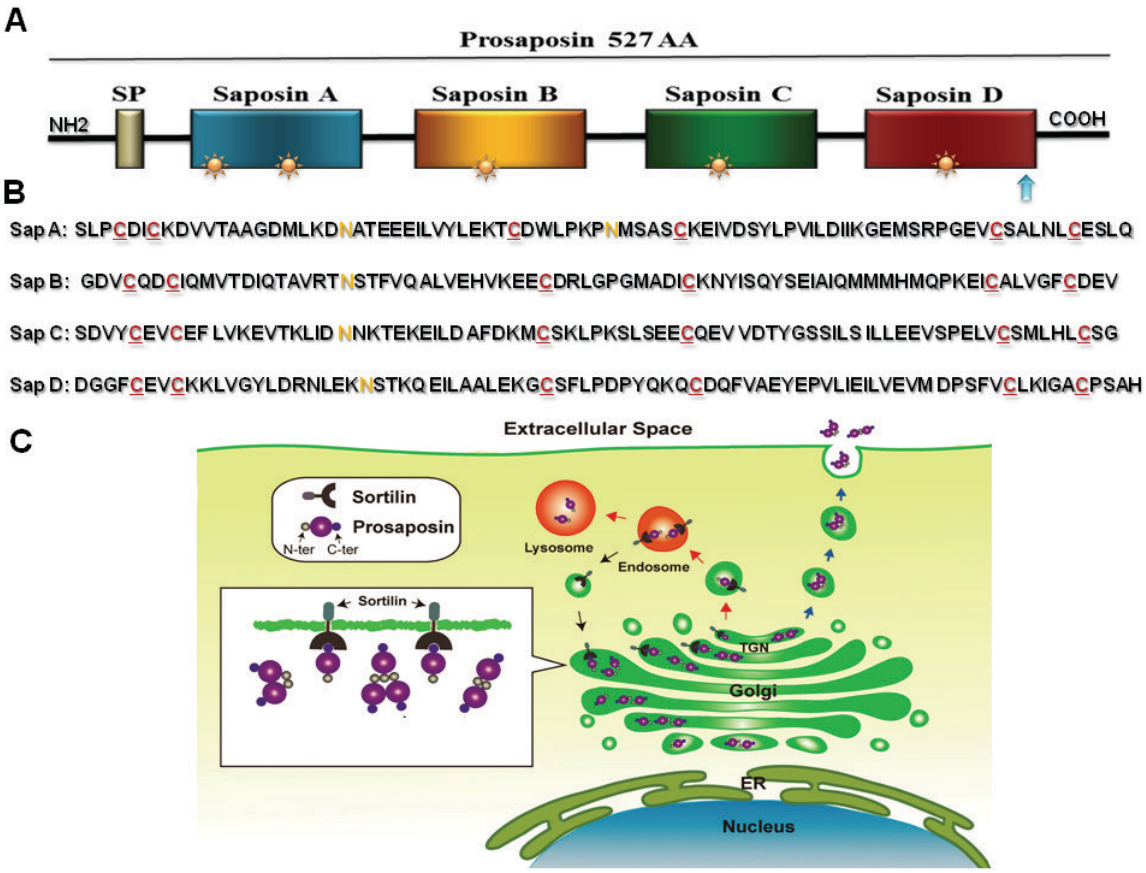

Figure 5.1S PSAP structure, and its intracellular trafficking and secretion. ***A, Organization of human PSAP protein.*** Structurally, PSAP contains a 16 amino acids signal peptide followed by four saposins. PSAP is proteolytically cleaved in the lysosome to generate saposin A, B, C, and D. Individual saposin domains and signal peptide are indicated; yellow stars represent the glycosylation sites in each saposin (modified from (188)); blue arrow points to the lysosomal targeting motif of PSAP. ***B, Amino acid sequence of human saposin A-D.*** Saposins are highly homologous molecules, each with approximately 80 amino acids containing six cysteine residues and N-glycosylated carbohydrate chains that are highly conserved. Potential N-glycosylation type carbohydrate side chains linked to asparagine are indicated with the yellow "N." As indicated, each saposin molecule also contains six cysteines

(red) positioned at almost similar locations. ***C, Working model of PSAP secretion and lysosomal trafficking pathway*** (modified from (198)). PSAP is a multifunctional protein that plays various physiological roles intracellularly and extracellularly (188,189). PSAP is synthesized in the ER as a 53 kDa protein and is post-translationally modified to a 62-65 kDa form after addition of high mannose. In the trans-Golgi network (TGN), this protein is further glycosylated to a 68-70 kDa secretory form.

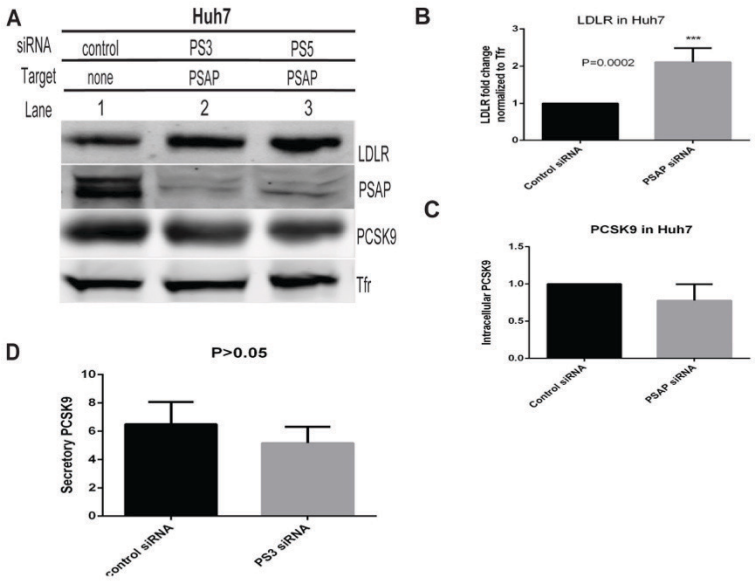

Figure 5.2S Effects of knocking down PSAP on LDLR and PCSK9 in huh7. Huh7 (**panel A, B, C&D**) cells were transfected with scrambled siRNA (control) or PSAP specific siRNA (PS3 and PS5) (20 μM) using Lipofectamine RNAiMax according to the manufacturer's protocol. After 24 hours, the culture medium was changed into DMEM plus 5% NCLPPS for overnight. Cells were lysed, and protein concentrations were measured by BCA protein assay. Same amount of total proteins was subjected to SDS-PAGE (8%) and transferred to nitrocellulose membranes by electroblotting. Immunoblotting was performed using an anti-LDLR rabbit polyclonal antibody 3143, an anti-PCSK9 polyclonal antibody (15A6), or a monoclonal anti-transferrin receptor antibody (TFR). Antibody binding was detected by IRDye-labeled goat anti-mouse or goat anti-rabbit IgG. The signal was detected by a Li-Cor Odyssey Infrared Imaging System (Li-Cor). The relative protein level was calculated by normalized to the densitometry of LDLR or PCSK9 to that of transferrin receptor (TFR). Normalized relative densitometry was the ratio of the relative densitometry to that of control group that was defined as 1. Similar results were obtained from at least three independent

experiments.

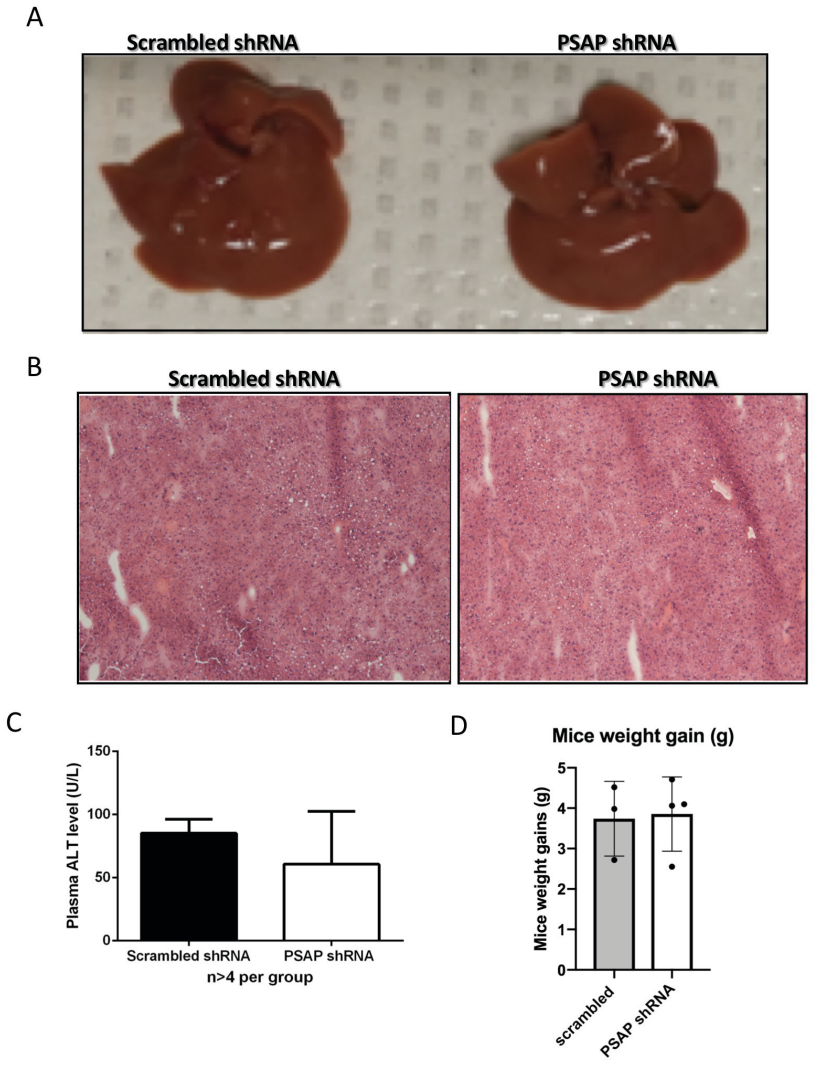

Figure 5.3S Effects of knocking down PSAP on mouse liver health. ***A. Liver morphology. B. Liver section staining.*** Representative figures of H&E staining of cross-sections of liver tissues. ***C. Plasma ALT activity.*** Each sample was assayed in triplicate as described previously. ***D. Bodyweight gain of Scrambled and PSAP-shRNA injected mice.***

Chapter 6

Discussion and Future Perspectives

Previous milestone discoveries in human genetics have established a clear link between PCSK9 function and plasma LDL-C concentrations. GOF mutations in the *PCSK9* gene cause autosomal dominant familial hypercholesterolemia. Conversely, LOF mutations are associated with hypocholesterolemia and protect against CVD. Mechanistic analysis reveals that circulating PCSK9 binds to LDLR at the cell surface of hepatocytes and promotes the degradation of LDLR in the lysosome. In this thesis, I sought to further explore the detailed molecular mechanisms, by which PCSK9 is secreted from hepatocytes and interacts with the LDLR, and directs the receptor for lysosomal degradation.

6.1 The role of PCSK9 CTD in its maturation and secretion

6.1.1 The length of CTD is important for PCSK9 maturation and secretion

Plasma PCSK9 is mainly secreted from hepatocytes, and its levels are positively associated with LDL-C concentrations. However, the molecular machinery that mediates PCSK9 secretion is unclear. The PCSK9 C-terminus is essential for PCSK9-promoted LDLR degradation. It has been reported that deletion of all three CMs, or only CM2 and CM3, does not affect PCSK9 secretion. Here, I have demonstrated that mutant $PCSK9^{1-528}$ that lacks CM2 and CM3 displayed no significant difference in PCSK9 secretion compared to the WT full-length PCSK9. However, I did find that mutant $PCSK9^{1-453}$, but not $PCSK9^{1-528}$, significantly impairs PCSK9 maturation, indicating a potential role of CM1 in the self-cleavage of PCSK9. Furthermore, we were the first to define the role of the hinge region in PCSK9 secretion. We found that full or partial deletion of the hinge region markedly impaired PCSK9 maturation to a similar extent. Conversely, mutant $PCSK9^{1-445}$ significantly reduced PCSK9 secretion but still could be fairly secreted to culture medium, whereas mutants $PCSK9^{1-444}$, $PCSK9^{1-443}$, and $PCSK9^{1-425}$ all essentially eliminated PCSK9 secretion. Considering that the hinge region is

exposed on the surface and close to amino acids Ile161 to Arg167 in the N-terminal CAT (83,105,109,139), removal of the hinge region might interfere with the structural integrity of the CAT, thereby affecting PCSK9 self-cleavage and maturation. In addition, deletion of Pro^{445} in mutant $PCSK9^{1-444}$ was processed as efficiently as mutants $PCSK9^{1-445}$ and $PCSK9^{1-446}$ that included Pro^{445}, but $PCSK9^{1-444}$ markedly reduced PCSK9 secretion compared to the other two mutations. Interestingly, Pro^{445} resides inside a pocket that is surrounded by Leu^{444}, Pro^{163}, Ala^{402}, Met^{398}, Ala^{402}, *etc.* (83,105,109). It would be of interest to see if this pocket is involved in the binding of cofactors that contribute to PCSK9 secretion and/or PCSK9-promoted LDLR degradation.

6.1.2 SEC24 isoforms play a role in PCSK9 ER exit

Recently, it has been reported that knockout of SEC24A, and reduced expression of SEC24B but not SEC24D in mice, decrease PCSK9 secretion (88). Consistently, we found that knockdown of SEC24A and SEC24B but not SEC24D impaired PCSK9 secretion in cultured human hepatocytes. Chen et al. also found that, unlike SEC24A and SEC24B, overexpression of SEC24C together with SEC23A did not enhance secretion of PCSK9 expressed in 293T cells (88). However, we observed that knockdown of SEC24C in cultured human hepatoma-derived Huh7 cells, significantly reduced PCSK9 secretion. Nevertheless, these findings demonstrate that SEC24 plays an important role in facilitating the ER-to-Golgi transport of PCSK9. The detailed molecular mechanism by which PCSK9 exits the ER, however, has yet to be determined.

6.1.3 Conclusion

In summary, Chapter 3 has demonstrated the important role of the hinge region of PCSK9 in its secretion and processing. We also found that both loss-of-function mutations

(S462P and A522T) and gain-of-function mutations (S465L and E482G) impair PCSK9 secretion. Further, we have shown that SEC24A, B and C, but not SEC24D, facilitate PCSK9 secretion in cultured human hepatoma-derived cells. Together, these findings shed some light on our understanding of PCSK9 secretion.

6.2 The binding motif between LDLR and PCSK9

6.2.1 The role of Asp203 of LDLR in PCSK9 binding

It has been reported that the side chain of Asp203 forms hydrogen bonds with the backbone amide of the LR5 of LDLR (170), thereby playing an important role in maintaining the structural stability of the LDLR. Indeed, mutations on Asp203 including D203N, D203G, D203A, and D203V, have been identified in FH patients (171-173). However, we did observe the mature form and cell surface expression of D203N, indicating that the mutant LDLR could be delivered to the plasma membrane. However, this mutation of LDLR significantly reduced binding of PCSK9 and LDL to the receptor, as well as PCSK9-promoted LDLR degradation. It is of note that patients carrying the D203N mutation display FH. Thus, the effect of D203N on LDL binding must be dominant over its effect on PCSK9 binding. In addition, mutations D203N, D154N and D172N of the LDLR all introduced a novel N-glycosylation site to the receptor. D203N and double mutation E153QD154N but not D172N seemed to cause a minor electrophoretic mobility shift of the LDLR on SDS-PAGE. However, E153QD154N, unlike D172N and D203N, had no detectable effect on PCSK9 binding. It would be of interest to determine if and how these mutations affect N-glycosylation of LDLR and the related functional consequences.

6.2.2 The role of Asp172 of LDLR in PCSK9 binding

Asp172 resides in the highly flexible C-terminal half of the linker between the LR4

and the LR5 (167). No FH mutation has been reported at this position except for a frameshift mutation that deletes three amino acid residues (172 to 174) and causes a premature stop (174). Mutation D172N appeared to have no marked effect on LDLR trafficking, LDL binding at pH 7.4 or PCSK9 binding at pH 6.0, but significantly reduced PCSK9 binding at pH 7.4.

PCSK9 mainly binds to the EGF-A domain of the LDLR. How did mutations D172N and D203N in the LR region of LDLR impair PCSK9 binding? We previously found that at least three ligand binding repeats were required for PCSK9-promoted LDLR degradation (97). Tyeten et al. also reported that binding of PCSK9 to mutant LDLR without the LRs was significantly lower at a neutral or acidic pH value than its binding to the full-length receptor (104). Yamamoto et al. further demonstrated that the LRs of LDLR bound to C-terminal PCSK9 in a pH-dependent manner with much stronger binding in the acidic endosomal environment (141). In addition, studies from Holla et al. indicated that the positively charged C-terminus of PCSK9 might interact with the negatively charged LRs of LDLR (112). Similarly, Cunningham et al. employed the surface plasmon resonance (SPR) assay and revealed that C-terminus of PCSK9 purified from Chinese Hamster Ovary (CHO) cells was important for PCSK9 binding to the LDLR (105). These findings indicate that the negatively charged LRs of LDLR may interact with the positively charged C-terminus of PCSK9. In this situation, D203N might affect the structural stability of the LR5 of LDLR and consequently impair PCSK9 binding. On the other hand, Asp172 that only affected PCSK9 binding at neutral pH might involve the interaction with PCSK9. Alternatively, the flexibility of the loops between the LRs might allow a possible intermodular crosstalk between different LRs. Thus, it is possible that the structural alteration in the LR5 caused by D203N may affect the structural stability of the LR7, eventually impairing the integrity of the EGF-A and interfering the PCSK9 binding to the receptor. In addition, several PCSK9 potential binding partners have

been reported (113,178,179). It will be of interest to investigate if the LRs of LDLR, especially D172 and D203, are involved in the interaction with these potential partners.

6.2.3 Conclusion

In Chapter 4, I have demonstrated the important role of negatively charged amino acids in the LRs of the LDLR in the binding of PCSK9 at the cell surface. We showed that the mutation D172N in the linker between the LR4 and the LR5, and the mutation D203N in the LR5 of the full-length LDLR, significantly reduced PCSK9 binding to the receptor at pH 7.4. Further, D203N but not D172N reduced PCSK9 binding at pH 6.0 and LDLR-mediated LDL uptake. Together, these findings indicate that Asp residues at specific positions in the LRs regulate the binding of PCSK9 to LDLR.

6.3 PSAP regulated LDLR degradation

6.3.1 PSAP versus PCSK9

In Chapter 5, we sought to identify the unknown cofactor(s) that binds to the CTD of PCSK9 and directs the PCSK9/LDLR complex to the lysosome for degradation. PSAP was one of the candidate proteins we obtained from the yeast two hybrid system. Our initial hypothesis was that extracellular PSAP bound to the CTD of PCSK9, while the CAT of PCSK9 interacted with the EGF-A domain of LDLR. After endocytosis, the PCSK9/LDLR complex would be delivered to the endosome, where the C-terminal domain of PSAP would provide a lysosomal targeting signal and direct PCSK9/LDLR to the lysosome for degradation. However, our results demonstrated that PSAP-regulated LDLR levels was independent of PCSK9 and vice versa. First, Huh7 cells incubated with purified PCSK9 protein displayed a reduction in LDLR levels, whereas incubation of purified PSAP protein

had no significant effect on LDLR abundance (Fig 5.8). Second, knockdown of PSAP increased LDLR levels in HEK293 cells that did not express PCSK9. These results suggested that PSAP regulates LDLR in a pathway different from that of PCSK9.

6.3.2 Intracellular PSAP-promoted LDLR degradation

PSAP is ubiquitously expressed in tissues at a high level, probably due to its main physiological role in facilitating glycosphingolipid degradation in the lysosome. However, PSAP is also secreted from many organs, including kidneys, heart, and liver, and is present in many body fluids such as plasma, at a high concentration (1.5 μg/ml). In this study, we used AAV-shRNA that reduce *PSAP* mRNA levels in the mouse liver and found that knockdown of PSAP increased hepatic LDLR and reduced plasma levels of total cholesterol. On the other hand, incubation of purified PSAP protein in cultured hepatoma-derived cells had no effect on LDLR levels (Fig 5.8). These results suggest that PSAP induces LDLR degradation mainly through an intracellular pathway. Furthermore, we found that PSAP bound to LDLR probably on its EGF domain. PSAP is transported to the lysosome by binding to a sorting receptor in the trans-Golgi network. It is possible that some of the LDLR is transported to the lysosome for degradation within the secretory pathway via interaction with PSAP.

6.4 Future directions

6.4.1 To uncover the binding motif in PSAP for its interaction with LDLR

In Figure 5.7B and 5.7C, I have demonstrated that PSAP interacted with LDLR via the EGF domain of the LDLR, however the binding motifs in PSAP remain unclear. Since the binding of the C-terminal domain of PSAP (aa 524-540) to a sorting receptor occurs in the trans-Golgi network, which is responsible for its lysosomal trafficking, I speculate that the N-

terminal domain of PSAP may interact with the EGF domain of LDLR. To characterize the structural requirement for PSAP's binding to the LDLR, I propose the following study. A recombinant expression vector containing the full-length human PSAP cDNA will be used as the template to generate a mutant form of PSAP, in which the N-terminal domain of PSAP is deleted (PSAPΔNTD) using the QuickChange^{TM} site-directed mutagenesis kit. Co-immunoprecipitation experiments will be performed as previously described in Figure 5.7C. I expect that LDLR will be pulled down with the WT PSAP but not with the PSAPΔNTD. This result will indicate the critical requirement of the N-terminal domain for PSAP for its interaction with LDLR.

6.4.2 To investigate the role of sortilin in PSAP-induced LDLR degradation

We have demonstrated that the intracellular PSAP bound to LDLR and regulated LDLR degradation. However, how this intracellular pathway functions is yet to be investigated. The sorting of PSAP to the lysosome occurs in the TGN by sortilin. Given the role of sortilin in regulation of lipid metabolism, I hypothesize that sortilin plays a role in the PSAP-induced LDLR degradation. To test this hypothesis, first, we will study the effect of knocking down sortilin expression on LDLR levels in human hepatocyte-derived cells. If reduction of sortilin expression increased LDLR levels, we would overexpress sortilin or PSAP alone, or together to study their collective effect on LDLR degradation in the presence or absence of the lysosome inhibitor chloroquine (CQ). I speculate that overexpression of both sortilin and PSAP will reduce LDLR levels in the absence of CQ. This result would indicate that sortilin plays a role in directing the PSAP/LDLR complex to lysosome for degradation. Furthermore, it has been reported that compared to the WT mice, sortilin$^{-/-}$ mice have higher hepatic LDLR levels and lower plasma levels of total cholesterol (92). We will characterize

the effect of PSAP knockdown in sortilin$^{-/-}$ mice. It would be interesting to see if knockdown of PSAP in these mice could modulate the levels of hepatic LDLR and plasma LDL-C.

6.4.3 To study the effect of PSAP knockdown in atherosclerosis

Our above findings have demonstrated that knockdown of PSAP in cultured cells enhanced cellular LDL uptake. Further, PSAP-KD mice fed the Western-type diet showed increased hepatic LDLR levels and a significant reduction in plasma levels of total cholesterol, HDL and non-HDL cholesterol. This reduction is likely caused by enhanced LDLR-mediated clearance of LDL, as well as chylomicron remnants and apoE containing HDL particles, as reported in PCSK9-KO mice. Considering that plasma levels of LDL-C are positively correlated with the risk of atherosclerosis, it is possible that knockdown of hepatic PSAP would prevent the development of atherosclerosis. *ApoE*$^{-/-}$ mice fed the Western-type diet would spontaneously develop atherosclerosis. Foam cell lesions are observed in these mice as early as 10 weeks of age. To investigate the role of PSAP in early lesion formation, we will inject *apoE*$^{-/-}$ mice fed the Western-type diet, with AAV-scrambled or PSAP-shRNA at 4 weeks of age when lesions are undetectable, and subsequently determine the effect of PSAP on the development of lesions. To assess the LDLR dependence, *Ldlr*$^{-/-}$ mice will be fed the Western-type diet for 12 weeks to develop atherosclerosis and we will then inject them with AAVs. At the end of the study, animals will be sacrificed, and blood and tissues will be harvested and analyzed as described in Figure 5.2 and 5.3. The aorta between the aortic root and iliac bifurcation will be collected, stained with oil red O and analyzed using Image-Pro Plus software to assess the atherosclerotic lesions. Given that many factors have both pro- and anti-atherogenic effects depending on the stages of atherosclerotic plaque, it is difficult to anticipate the outcome of PSAP knockdown on the development of atherosclerosis.

6.5 Concluding remarks

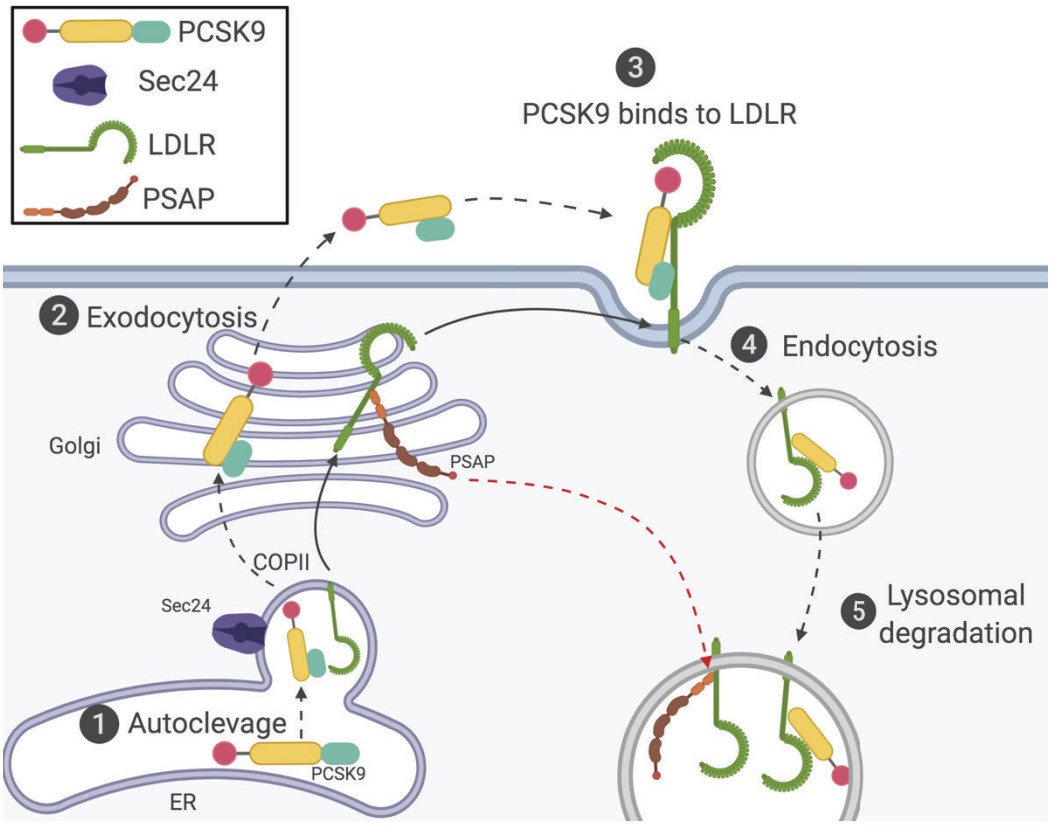

Figure 6.1 Final working model.

In summary, studies in my thesis have demonstrated the important role of PCSK9 C-terminus in PCSK9 secretion and function. In Chapter 3, I found that the hinge region of PCSK9 is critical for its processing and secretion, and SEC24A, B and C but not SEC24D facilitate PCSK9 secretion in cultured human hepatoma-derived cells. In Chapter 4, I showed the important role of negatively charged amino acids (D172N and D203N) in the LRs of LDLR in PCSK9 binding at the cell surface. In Chapter 5, using *in vitro* and *in vivo* models, I found that 1) knockdown of hepatic PSAP increased LDLR abundance *in vitro* and *in vivo* and reduced plasma levels of total cholesterol in mice; 2) knockdown of PSAP had no effect on the mRNA levels of *LDLR* and other *SREBP2* target genes including *PCSK9*, *SREBP2*, and *HMGCR*; 3) lysosomal inhibition with chloroquine had no effect on PSAP-mediated increase

of LDLR; 4) PCSK9 was not required for PSAP-induced LDLR degradation and vice versa. These findings indicate that PSAP is a potential LDLR binding partner and regulates hepatic LDLR levels and plasma cholesterol metabolism.

In conclusion, since the discovery of PCSK9 in 2003, it has garnered a staggering amount of attention from both the scientific community and pharmaceutical companies. Secreted into plasma by the liver, PCSK9 binds to the LDLR at the surface of hepatocytes, thereby preventing LDLR recycling and enhancing its degradation in the lysosome, resulting in reduced LDL-C clearance. It takes 9 years to elaborate powerful new PCSK9-based therapeutic approaches for reducing circulating levels of LDL-C. PCSK9 is now common parlance among scientists and clinicians interested in the prevention and treatment of atherosclerotic CVD. What makes this story so special is not only its recent discovery, and the fact that it uncovers previously unknown biology, but also that these important scientific insights have been translated into an effective medical therapy in a record short time. However, the PCSK9 saga is far from complete. PCSK9 mAbs that dramatically reduce LDL-C and incrementally reduce atherosclerotic CVD events, with additional therapeutic antagonists of PCSK9 are likely on the way. The work demonstrated in this thesis will shed light on the molecular mechanism of PCSK9-promoted LDLR degradation. Yet, continued research promises to provide further progress in the development of PCSK9 inhibitors.

References

1. Fan, J., Song, Y., Chen, Y., Hui, R., and Zhang, W. (2013) Combined effect of obesity and cardio-metabolic abnormality on the risk of cardiovascular disease: a meta-analysis of prospective cohort studies. *International journal of cardiology* **168**, 4761-4768
2. Ference, B. A., Ginsberg, H. N., Graham, I., Ray, K. K., Packard, C. J., Bruckert, E., Hegele, R. A., Krauss, R. M., Raal, F. J., Schunkert, H., Watts, G. F., Boren, J., Fazio, S., Horton, J. D., Masana, L., Nicholls, S. J., Nordestgaard, B. G., van de Sluis, B., Taskinen, M. R., Tokgozoglu, L., Landmesser, U., Laufs, U., Wiklund, O., Stock, J. K., Chapman, M. J., and Catapano, A. L. (2017) Low-density lipoproteins cause atherosclerotic cardiovascular disease. 1. Evidence from genetic, epidemiologic, and clinical studies. A consensus statement from the European Atherosclerosis Society Consensus Panel. *European heart journal* **38**, 2459-2472
3. Moore, K. J., and Tabas, I. (2011) Macrophages in the pathogenesis of atherosclerosis. *Cell* **145**, 341-355
4. Kwon, G. P., Schroeder, J. L., Amar, M. J., Remaley, A. T., and Balaban, R. S. (2008) Contribution of macromolecular structure to the retention of low-density lipoprotein at arterial branch points. *Circulation* **117**, 2919-2927
5. Libby, P. (2000) Changing concepts of atherogenesis. *Journal of internal medicine* **247**, 349-358
6. Libby, P., Buring, J. E., Badimon, L., Hansson, G. K., Deanfield, J., Bittencourt, M. S., Tokgozoglu, L., and Lewis, E. F. (2019) Atherosclerosis. *Nat Rev Dis Primers* **5**, 56
7. Fenske, D. B., Chana, R. S., Parmar, Y. I., Treleaven, W. D., and Cushley, R. J. (1990) Structure and motion of phospholipids in human plasma lipoproteins. A 31P NMR study. *Biochemistry* **29**, 3973-3981
8. Seman, L. J., DeLuca, C., Jenner, J. L., Cupples, L. A., McNamara, J. R., Wilson, P. W., Castelli, W. P., Ordovas, J. M., and Schaefer, E. J. (1999) Lipoprotein(a)-cholesterol and coronary heart disease in the Framingham Heart Study. *Clinical chemistry* **45**, 1039-1046
9. Mahley, R. W., Innerarity, T. L., Rall, S. C., Jr., and Weisgraber, K. H. (1984) Plasma lipoproteins: apolipoprotein structure and function. *Journal of lipid research* **25**, 1277-1294
10. Taggart, H. M., Applebaum-Bowden, D., Haffner, S., Warnick, G. R., Cheung, M. C., Albers, J. J., Chestnut, C. H., 3rd, and Hazzard, W. R. (1982) Reduction in high density lipoproteins by anabolic steroid (stanozolol) therapy for postmenopausal osteoporosis. *Metabolism: clinical and experimental* **31**, 1147-1152
11. Smith, L. C., Pownall, H. J., and Gotto, A. M., Jr. (1978) The plasma lipoproteins: structure and metabolism. *Annual review of biochemistry* **47**, 751-757
12. Clifton, P. M., Noakes, M., and Nestel, P. J. (1998) LDL particle size and LDL and HDL cholesterol changes with dietary fat and cholesterol in healthy subjects. *Journal of lipid research* **39**, 1799-1804
13. Goldstein, J. L., and Brown, M. S. (2015) A century of cholesterol and coronaries: from plaques to genes to statins. *Cell* **161**, 161-172

14. Kwiterovich, P. O., Jr. (2000) The metabolic pathways of high-density lipoprotein, low-density lipoprotein, and triglycerides: a current review. *The American journal of cardiology* **86**, 5L-10L
15. Gibbons, G. F. (1990) Assembly and secretion of hepatic very-low-density lipoprotein. *The Biochemical journal* **268**, 1-13
16. Garuti, R., Jones, C., Li, W. P., Michaely, P., Herz, J., Gerard, R. D., Cohen, J. C., and Hobbs, H. H. (2005) The modular adaptor protein autosomal recessive hypercholesterolemia (ARH) promotes low density lipoprotein receptor clustering into clathrin-coated pits. *The Journal of biological chemistry* **280**, 40996-41004
17. Rudenko, G., Henry, L., Henderson, K., Ichtchenko, K., Brown, M. S., Goldstein, J. L., and Deisenhofer, J. (2002) Structure of the LDL receptor extracellular domain at endosomal pH. *Science* **298**, 2353-2358
18. Brown, M. S., Anderson, R. G., and Goldstein, J. L. (1983) Recycling receptors: the round-trip itinerary of migrant membrane proteins. *Cell* **32**, 663-667
19. Basu, S. K., Goldstein, J. L., Anderson, R. G., and Brown, M. S. (1981) Monensin interrupts the recycling of low density lipoprotein receptors in human fibroblasts. *Cell* **24**, 493-502
20. Blacklow, S. C. (2007) Versatility in ligand recognition by LDL receptor family proteins: advances and frontiers. *Curr Opin Struct Biol* **17**, 419-426
21. Sudhof, T. C., Goldstein, J. L., Brown, M. S., and Russell, D. W. (1985) The LDL receptor gene: a mosaic of exons shared with different proteins. *Science* **228**, 815-822
22. Brown, M. S., and Goldstein, J. L. (1986) A receptor-mediated pathway for cholesterol homeostasis. *Science* **232**, 34-47
23. Zhang, D. W., Lagace, T. A., Garuti, R., Zhao, Z., McDonald, M., Horton, J. D., Cohen, J. C., and Hobbs, H. H. (2007) Binding of proprotein convertase subtilisin/kexin type 9 to epidermal growth factor-like repeat A of low density lipoprotein receptor decreases receptor recycling and increases degradation. *The Journal of biological chemistry* **282**, 18602-18612
24. Hua, X., Yokoyama, C., Wu, J., Briggs, M. R., Brown, M. S., Goldstein, J. L., and Wang, X. (1993) SREBP-2, a second basic-helix-loop-helix-leucine zipper protein that stimulates transcription by binding to a sterol regulatory element. *Proceedings of the National Academy of Sciences of the United States of America* **90**, 11603-11607
25. Magana, M. M., and Osborne, T. F. (1996) Two tandem binding sites for sterol regulatory element binding proteins are required for sterol regulation of fatty-acid synthase promoter. *The Journal of biological chemistry* **271**, 32689-32694
26. Hua, X., Sakai, J., Ho, Y. K., Goldstein, J. L., and Brown, M. S. (1995) Hairpin orientation of sterol regulatory element-binding protein-2 in cell membranes as determined by protease protection. *The Journal of biological chemistry* **270**, 29422-29427
27. Peng, Y., Schwarz, E. J., Lazar, M. A., Genin, A., Spinner, N. B., and Taub, R. (1997) Cloning, human chromosomal assignment, and adipose and hepatic expression of the CL-6/INSIG1 gene. *Genomics* **43**, 278-284
28. Sakai, J., Duncan, E. A., Rawson, R. B., Hua, X., Brown, M. S., and Goldstein, J. L. (1996) Sterol-regulated release of SREBP-2 from cell membranes requires two sequential cleavages, one within a transmembrane segment. *Cell* **85**, 1037-1046
29. Hua, X., Sakai, J., Brown, M. S., and Goldstein, J. L. (1996) Regulated cleavage of sterol regulatory element binding proteins requires sequences on both sides of the

endoplasmic reticulum membrane. *The Journal of biological chemistry* **271**, 10379-10384

30. Wang, X., Zelenski, N. G., Yang, J., Sakai, J., Brown, M. S., and Goldstein, J. L. (1996) Cleavage of sterol regulatory element binding proteins (SREBPs) by CPP32 during apoptosis. *The EMBO journal* **15**, 1012-1020
31. Yokoyama, C., Wang, X., Briggs, M. R., Admon, A., Wu, J., Hua, X., Goldstein, J. L., and Brown, M. S. (1993) SREBP-1, a basic-helix-loop-helix-leucine zipper protein that controls transcription of the low density lipoprotein receptor gene. *Cell* **75**, 187-197
32. Cholesterol Treatment Trialists, C., Baigent, C., Blackwell, L., Emberson, J., Holland, L. E., Reith, C., Bhala, N., Peto, R., Barnes, E. H., Keech, A., Simes, J., and Collins, R. (2010) Efficacy and safety of more intensive lowering of LDL cholesterol: a meta-analysis of data from 170,000 participants in 26 randomised trials. *Lancet* **376**, 1670-1681
33. Ahmad, Z. (2014) Statin intolerance. *The American journal of cardiology* **113**, 1765-1771
34. Ference, B. A., Robinson, J. G., Brook, R. D., Catapano, A. L., Chapman, M. J., Neff, D. R., Voros, S., Giugliano, R. P., Davey Smith, G., Fazio, S., and Sabatine, M. S. (2016) Variation in PCSK9 and HMGCR and Risk of Cardiovascular Disease and Diabetes. *The New England journal of medicine* **375**, 2144-2153
35. Swerdlow, D. I., Preiss, D., Kuchenbaecker, K. B., Holmes, M. V., Engmann, J. E., Shah, T., Sofat, R., Stender, S., Johnson, P. C., Scott, R. A., Leusink, M., Verweij, N., Sharp, S. J., Guo, Y., Giambartolomei, C., Chung, C., Peasey, A., Amuzu, A., Li, K., Palmen, J., Howard, P., Cooper, J. A., Drenos, F., Li, Y. R., Lowe, G., Gallacher, J., Stewart, M. C., Tzoulaki, I., Buxbaum, S. G., van der, A. D., Forouhi, N. G., Onland-Moret, N. C., van der Schouw, Y. T., Schnabel, R. B., Hubacek, J. A., Kubinova, R., Baceviciene, M., Tamosiunas, A., Pajak, A., Topor-Madry, R., Stepaniak, U., Malyutina, S., Baldassarre, D., Sennblad, B., Tremoli, E., de Faire, U., Veglia, F., Ford, I., Jukema, J. W., Westendorp, R. G., de Borst, G. J., de Jong, P. A., Algra, A., Spiering, W., Maitland-van der Zee, A. H., Klungel, O. H., de Boer, A., Doevendans, P. A., Eaton, C. B., Robinson, J. G., Duggan, D., Consortium, D., Consortium, M., InterAct, C., Kjekshus, J., Downs, J. R., Gotto, A. M., Keech, A. C., Marchioli, R., Tognoni, G., Sever, P. S., Poulter, N. R., Waters, D. D., Pedersen, T. R., Amarenco, P., Nakamura, H., McMurray, J. J., Lewsey, J. D., Chasman, D. I., Ridker, P. M., Maggioni, A. P., Tavazzi, L., Ray, K. K., Seshasai, S. R., Manson, J. E., Price, J. F., Whincup, P. H., Morris, R. W., Lawlor, D. A., Smith, G. D., Ben-Shlomo, Y., Schreiner, P. J., Fornage, M., Siscovick, D. S., Cushman, M., Kumari, M., Wareham, N. J., Verschuren, W. M., Redline, S., Patel, S. R., Whittaker, J. C., Hamsten, A., Delaney, J. A., Dale, C., Gaunt, T. R., Wong, A., Kuh, D., Hardy, R., Kathiresan, S., Castillo, B. A., van der Harst, P., Brunner, E. J., Tybjaerg-Hansen, A., Marmot, M. G., Krauss, R. M., Tsai, M., Coresh, J., Hoogeveen, R. C., Psaty, B. M., Lange, L. A., Hakonarson, H., Dudbridge, F., Humphries, S. E., Talmud, P. J., Kivimaki, M., Timpson, N. J., Langenberg, C., Asselbergs, F. W., Voevoda, M., Bobak, M., Pikhart, H., Wilson, J. G., Reiner, A. P., Keating, B. J., Hingorani, A. D., and Sattar, N. (2015) HMG-coenzyme A reductase inhibition, type 2 diabetes, and bodyweight: evidence from genetic analysis and randomised trials. *Lancet* **385**, 351-361
36. Seidah, N. G., Benjannet, S., Wickham, L., Marcinkiewicz, J., Jasmin, S. B., Stifani, S., Basak, A., Prat, A., and Chretien, M. (2003) The secretory proprotein convertase

neural apoptosis-regulated convertase 1 (NARC-1): liver regeneration and neuronal differentiation. *Proceedings of the National Academy of Sciences of the United States of America* **100**, 928-933
37. Seidah, N. G., Mayer, G., Zaid, A., Rousselet, E., Nassoury, N., Poirier, S., Essalmani, R., and Prat, A. (2008) The activation and physiological functions of the proprotein convertases. *The international journal of biochemistry & cell biology* **40**, 1111-1125
38. Seidah, N. G., and Prat, A. (2002) Precursor convertases in the secretory pathway, cytosol and extracellular milieu. *Essays in biochemistry* **38**, 79-94
39. Leren, T. P. (2004) Mutations in the PCSK9 gene in Norwegian subjects with autosomal dominant hypercholesterolemia. *Clinical genetics* **65**, 419-422
40. Naoumova, R. P., Tosi, I., Patel, D., Neuwirth, C., Horswell, S. D., Marais, A. D., van Heyningen, C., and Soutar, A. K. (2005) Severe hypercholesterolemia in four British families with the D374Y mutation in the PCSK9 gene: long-term follow-up and treatment response. *Arteriosclerosis, thrombosis, and vascular biology* **25**, 2654-2660
41. Timms, K. M., Wagner, S., Samuels, M. E., Forbey, K., Goldfine, H., Jammulapati, S., Skolnick, M. H., Hopkins, P. N., Hunt, S. C., and Shattuck, D. M. (2004) A mutation in PCSK9 causing autosomal-dominant hypercholesterolemia in a Utah pedigree. *Human genetics* **114**, 349-353
42. Abifadel, M., Varret, M., Rabes, J. P., Allard, D., Ouguerram, K., Devillers, M., Cruaud, C., Benjannet, S., Wickham, L., Erlich, D., Derre, A., Villeger, L., Farnier, M., Beucler, I., Bruckert, E., Chambaz, J., Chanu, B., Lecerf, J. M., Luc, G., Moulin, P., Weissenbach, J., Prat, A., Krempf, M., Junien, C., Seidah, N. G., and Boileau, C. (2003) Mutations in PCSK9 cause autosomal dominant hypercholesterolemia. *Nature genetics* **34**, 154-156
43. Bordicchia, M., Spannella, F., Ferretti, G., Bacchetti, T., Vignini, A., Di Pentima, C., Mazzanti, L., and Sarzani, R. (2019) PCSK9 is Expressed in Human Visceral Adipose Tissue and Regulated by Insulin and Cardiac Natriuretic Peptides. *International journal of molecular sciences* **20**
44. Seidah, N. G. (2017) The PCSK9 revolution and the potential of PCSK9-based therapies to reduce LDL-cholesterol. *Glob Cardiol Sci Pract* **2017**, e201702
45. Seidah, N. G., Awan, Z., Chretien, M., and Mbikay, M. (2014) PCSK9: a key modulator of cardiovascular health. *Circulation research* **114**, 1022-1036
46. Kaya, E., Kayikcioglu, M., Tetik Vardarli, A., Eroglu, Z., Payzin, S., and Can, L. (2017) PCSK 9 gain-of-function mutations (R496W and D374Y) and clinical cardiovascular characteristics in a cohort of Turkish patients with familial hypercholesterolemia. *Anatolian journal of cardiology* **18**, 266-272
47. Holla, O. L., Cameron, J., Berge, K. E., Kulseth, M. A., Ranheim, T., and Leren, T. P. (2006) Low-density lipoprotein receptor activity in Epstein-Barr virus-transformed lymphocytes from heterozygotes for the D374Y mutation in the PCSK9 gene. *Scand J Clin Lab Invest* **66**, 317-328
48. Sanchez-Hernandez, R. M., Di Taranto, M. D., Benito-Vicente, A., Uribe, K. B., Lamiquiz-Moneo, I., Larrea-Sebal, A., Jebari, S., Galicia-Garcia, U., Novoa, F. J., Boronat, M., Wagner, A. M., Civeira, F., Martin, C., and Fortunato, G. (2019) The Arg499His gain-of-function mutation in the C-terminal domain of PCSK9. *Atherosclerosis* **289**, 162-172
49. Di Taranto, M. D., Benito-Vicente, A., Giacobbe, C., Uribe, K. B., Rubba, P., Etxebarria, A., Guardamagna, O., Gentile, M., Martin, C., and Fortunato, G. (2017)

Identification and in vitro characterization of two new PCSK9 Gain of Function variants found in patients with Familial Hypercholesterolemia. *Scientific reports* **7**, 15282

50. Abifadel, M., Guerin, M., Benjannet, S., Rabes, J. P., Le Goff, W., Julia, Z., Hamelin, J., Carreau, V., Varret, M., Bruckert, E., Tosolini, L., Meilhac, O., Couvert, P., Bonnefont-Rousselot, D., Chapman, J., Carrie, A., Michel, J. B., Prat, A., Seidah, N. G., and Boileau, C. (2012) Identification and characterization of new gain-of-function mutations in the PCSK9 gene responsible for autosomal dominant hypercholesterolemia. *Atherosclerosis* **223**, 394-400
51. Cohen, J., Pertsemlidis, A., Kotowski, I. K., Graham, R., Garcia, C. K., and Hobbs, H. H. (2005) Low LDL cholesterol in individuals of African descent resulting from frequent nonsense mutations in PCSK9. *Nat Genet* **37**, 161-165
52. Benjannet, S., Hamelin, J., Chretien, M., and Seidah, N. G. (2012) Loss- and gain-of-function PCSK9 variants: cleavage specificity, dominant negative effects, and low density lipoprotein receptor (LDLR) degradation. *J Biol Chem* **287**, 33745-33755
53. Zhao, Z., Tuakli-Wosornu, Y., Lagace, T. A., Kinch, L., Grishin, N. V., Horton, J. D., Cohen, J. C., and Hobbs, H. H. (2006) Molecular characterization of loss-of-function mutations in PCSK9 and identification of a compound heterozygote. *American journal of human genetics* **79**, 514-523
54. Hooper, A. J., Marais, A. D., Tanyanyiwa, D. M., and Burnett, J. R. (2007) The C679X mutation in PCSK9 is present and lowers blood cholesterol in a Southern African population. *Atherosclerosis* **193**, 445-448
55. Huang, C. C., Fornage, M., Lloyd-Jones, D. M., Wei, G. S., Boerwinkle, E., and Liu, K. (2009) Longitudinal association of PCSK9 sequence variations with low-density lipoprotein cholesterol levels: the Coronary Artery Risk Development in Young Adults Study. *Circulation. Cardiovascular genetics* **2**, 354-361
56. Rashid, S., Curtis, D. E., Garuti, R., Anderson, N. N., Bashmakov, Y., Ho, Y. K., Hammer, R. E., Moon, Y. A., and Horton, J. D. (2005) Decreased plasma cholesterol and hypersensitivity to statins in mice lacking Pcsk9. *Proceedings of the National Academy of Sciences of the United States of America* **102**, 5374-5379
57. Zaid, A., Roubtsova, A., Essalmani, R., Marcinkiewicz, J., Chamberland, A., Hamelin, J., Tremblay, M., Jacques, H., Jin, W., Davignon, J., Seidah, N. G., and Prat, A. (2008) Proprotein convertase subtilisin/kexin type 9 (PCSK9): hepatocyte-specific low-density lipoprotein receptor degradation and critical role in mouse liver regeneration. *Hepatology* **48**, 646-654
58. Denis, M., Marcinkiewicz, J., Zaid, A., Gauthier, D., Poirier, S., Lazure, C., Seidah, N. G., and Prat, A. (2012) Gene inactivation of proprotein convertase subtilisin/kexin type 9 reduces atherosclerosis in mice. *Circulation* **125**, 894-901
59. Horton, J. D., Goldstein, J. L., and Brown, M. S. (2002) SREBPs: activators of the complete program of cholesterol and fatty acid synthesis in the liver. *The Journal of clinical investigation* **109**, 1125-1131
60. Dubuc, G., Chamberland, A., Wassef, H., Davignon, J., Seidah, N. G., Bernier, L., and Prat, A. (2004) Statins upregulate PCSK9, the gene encoding the proprotein convertase neural apoptosis-regulated convertase-1 implicated in familial hypercholesterolemia. *Arteriosclerosis, thrombosis, and vascular biology* **24**, 1454-1459

61. Davignon, J., and Dubuc, G. (2009) Statins and ezetimibe modulate plasma proprotein convertase subtilisin kexin-9 (PCSK9) levels. *Transactions of the American Clinical and Climatological Association* **120**, 163-173
62. Awan, Z., Seidah, N. G., MacFadyen, J. G., Benjannet, S., Chasman, D. I., Ridker, P. M., and Genest, J. (2012) Rosuvastatin, proprotein convertase subtilisin/kexin type 9 concentrations, and LDL cholesterol response: the JUPITER trial. *Clinical chemistry* **58**, 183-189
63. Karlson, B. W., Palmer, M. K., Nicholls, S. J., Lundman, P., and Barter, P. J. (2016) Doses of rosuvastatin, atorvastatin and simvastatin that induce equal reductions in LDL-C and non-HDL-C: Results from the VOYAGER meta-analysis. *European journal of preventive cardiology* **23**, 744-747
64. Nicholls, S. J., Brandrup-Wognsen, G., Palmer, M., and Barter, P. J. (2010) Meta-analysis of comparative efficacy of increasing dose of Atorvastatin versus Rosuvastatin versus Simvastatin on lowering levels of atherogenic lipids (from VOYAGER). *The American journal of cardiology* **105**, 69-76
65. Li, H., Dong, B., Park, S. W., Lee, H. S., Chen, W., and Liu, J. (2009) Hepatocyte nuclear factor 1alpha plays a critical role in PCSK9 gene transcription and regulation by the natural hypocholesterolemic compound berberine. *The Journal of biological chemistry* **284**, 28885-28895
66. Ai, D., Chen, C., Han, S., Ganda, A., Murphy, A. J., Haeusler, R., Thorp, E., Accili, D., Horton, J. D., and Tall, A. R. (2012) Regulation of hepatic LDL receptors by mTORC1 and PCSK9 in mice. *The Journal of clinical investigation* **122**, 1262-1270
67. Lai, Q., Giralt, A., Le May, C., Zhang, L., Cariou, B., Denechaud, P. D., and Fajas, L. (2017) E2F1 inhibits circulating cholesterol clearance by regulating Pcsk9 expression in the liver. *JCI Insight* **2**
68. Gong, Y., Ma, Y., Ye, Z., Fu, Z., Yang, P., Gao, B., Guo, W., Hu, D., Ye, J., Ma, S., Zhang, F., Zhou, L., Xu, X., Li, Z., Yang, T., and Zhou, H. (2017) Thyroid stimulating hormone exhibits the impact on LDLR/LDL-c via up-regulating hepatic PCSK9 expression. *Metabolism: clinical and experimental* **76**, 32-41
69. Cao, S., Xu, P., Yan, J., Liu, H., Liu, L., Cheng, L., Qiu, F., and Kang, N. (2018) Berberrubine and its analog, hydroxypropyl-berberrubine, regulate LDLR and PCSK9 expression via the ERK signal pathway to exert cholesterol-lowering effects in human hepatoma HepG2 cells. *Journal of cellular biochemistry*
70. Naeli, P., Mirzadeh Azad, F., Malakootian, M., Seidah, N. G., and Mowla, S. J. (2017) Post-transcriptional Regulation of PCSK9 by miR-191, miR-222, and miR-224. *Front Genet* **8**, 189
71. Wang, Y., Huang, Y., Hobbs, H. H., and Cohen, J. C. (2012) Molecular characterization of proprotein convertase subtilisin/kexin type 9-mediated degradation of the LDLR. *Journal of lipid research* **53**, 1932-1943
72. Li, H., Zhao, L., Singh, R., Ham, J. N., Fadoju, D. O., Bean, L. J. H., Zhang, Y., Xu, Y., Xu, H. E., and Gambello, M. J. (2018) The first pediatric case of glucagon receptor defect due to biallelic mutations in GCGR is identified by newborn screening of elevated arginine. *Molecular genetics and metabolism reports* **17**, 46-52
73. Spolitu, S., Okamoto, H., Dai, W., Zadroga, J. A., Wittchen, E. S., Gromada, J., and Ozcan, L. (2019) Hepatic Glucagon Signaling Regulates PCSK9 and Low-Density Lipoprotein Cholesterol. *Circulation research* **124**, 38-51

74. Benjannet, S., Rhainds, D., Hamelin, J., Nassoury, N., and Seidah, N. G. (2006) The proprotein convertase (PC) PCSK9 is inactivated by furin and/or PC5/6A: functional consequences of natural mutations and post-translational modifications. *The Journal of biological chemistry* **281**, 30561-30572
75. Gauthier, M. S., Awan, Z., Bouchard, A., Champagne, J., Tessier, S., Faubert, D., Chabot, K., Garneau, P. Y., Rabasa-Lhoret, R., Seidah, N. G., Ridker, P. M., Genest, J., and Coulombe, B. (2018) Posttranslational modification of proprotein convertase subtilisin/kexin type 9 is differentially regulated in response to distinct cardiometabolic treatments as revealed by targeted proteomics. *Journal of clinical lipidology* **12**, 1027-1038
76. Persson, L., Cao, G., Stahle, L., Sjoberg, B. G., Troutt, J. S., Konrad, R. J., Galman, C., Wallen, H., Eriksson, M., Hafstrom, I., Lind, S., Dahlin, M., Amark, P., Angelin, B., and Rudling, M. (2010) Circulating proprotein convertase subtilisin kexin type 9 has a diurnal rhythm synchronous with cholesterol synthesis and is reduced by fasting in humans. *Arteriosclerosis, thrombosis, and vascular biology* **30**, 2666-2672
77. Persson, L., Galman, C., Angelin, B., and Rudling, M. (2009) Importance of proprotein convertase subtilisin/kexin type 9 in the hormonal and dietary regulation of rat liver low-density lipoprotein receptors. *Endocrinology* **150**, 1140-1146
78. Baass, A., Dubuc, G., Tremblay, M., Delvin, E. E., O'Loughlin, J., Levy, E., Davignon, J., and Lambert, M. (2009) Plasma PCSK9 is associated with age, sex, and multiple metabolic markers in a population-based sample of children and adolescents. *Clinical chemistry* **55**, 1637-1645
79. Chan, D. C., Lambert, G., Barrett, P. H., Rye, K. A., Ooi, E. M., and Watts, G. F. (2009) Plasma proprotein convertase subtilisin/kexin type 9: a marker of LDL apolipoprotein B-100 catabolism? *Clinical chemistry* **55**, 2049-2052
80. Kappelle, P. J., Lambert, G., and Dullaart, R. P. (2011) Plasma proprotein convertase subtilisin-kexin type 9 does not change during 24h insulin infusion in healthy subjects and type 2 diabetic patients. *Atherosclerosis* **214**, 432-435
81. Maxwell, K. N., and Breslow, J. L. (2005) Proprotein convertase subtilisin kexin 9: the third locus implicated in autosomal dominant hypercholesterolemia. *Current opinion in lipidology* **16**, 167-172
82. Benjannet, S., Rhainds, D., Essalmani, R., Mayne, J., Wickham, L., Jin, W., Asselin, M. C., Hamelin, J., Varret, M., Allard, D., Trillard, M., Abifadel, M., Tebon, A., Attie, A. D., Rader, D. J., Boileau, C., Brissette, L., Chretien, M., Prat, A., and Seidah, N. G. (2004) NARC-1/PCSK9 and its natural mutants: zymogen cleavage and effects on the low density lipoprotein (LDL) receptor and LDL cholesterol. *The Journal of biological chemistry* **279**, 48865-48875
83. Piper, D. E., Jackson, S., Liu, Q., Romanow, W. G., Shetterly, S., Thibault, S. T., Shan, B., and Walker, N. P. (2007) The crystal structure of PCSK9: a regulator of plasma LDL-cholesterol. *Structure* **15**, 545-552
84. Lebeau, P., Al-Hashimi, A., Sood, S., Lhotak, S., Yu, P., Gyulay, G., Pare, G., Chen, S. R., Trigatti, B., Prat, A., Seidah, N. G., and Austin, R. C. (2017) Endoplasmic Reticulum Stress and Ca2+ Depletion Differentially Modulate the Sterol Regulatory Protein PCSK9 to Control Lipid Metabolism. *The Journal of biological chemistry* **292**, 1510-1523
85. Lebeau, P., Platko, K., Al-Hashimi, A. A., Byun, J. H., Lhotak, S., Holzapfel, N., Gyulay, G., Igdoura, S. A., Cool, D. R., Trigatti, B., Seidah, N. G., and Austin, R. C.

(2018) Loss-of-function PCSK9 mutants evade the unfolded protein response sensor GRP78 and fail to induce endoplasmic reticulum stress when retained. *The Journal of biological chemistry* **293**, 7329-7343

86. Zanetti, G., Pahuja, K. B., Studer, S., Shim, S., and Schekman, R. (2011) COPII and the regulation of protein sorting in mammals. *Nat Cell Biol* **14**, 20-28
87. Barlowe, C., and Helenius, A. (2016) Cargo Capture and Bulk Flow in the Early Secretory Pathway. *Annu Rev Cell Dev Biol* **32**, 197-222
88. Chen, X. W., Wang, H., Bajaj, K., Zhang, P., Meng, Z. X., Ma, D., Bai, Y., Liu, H. H., Adams, E., Baines, A., Yu, G., Sartor, M. A., Zhang, B., Yi, Z., Lin, J., Young, S. G., Schekman, R., and Ginsburg, D. (2013) SEC24A deficiency lowers plasma cholesterol through reduced PCSK9 secretion. *eLife* **2**, e00444
89. Emmer, B. T., Hesketh, G. G., Kotnik, E., Tang, V. T., Lascuna, P. J., Xiang, J., Gingras, A. C., Chen, X. W., and Ginsburg, D. (2018) The cargo receptor SURF4 promotes the efficient cellular secretion of PCSK9. *Elife* **7**
90. Shen, Y., Wang, B., Deng, S., Zhai, L., Gu, H. M., Alabi, A., Xia, X., Zhao, Y., Chang, X., Qin, S., and Zhang, D. W. (2019) Surf4 regulates expression of proprotein convertase subtilisin/kexin type 9 (PCSK9) but is not required for PCSK9 secretion in cultured human hepatocytes. *Biochim Biophys Acta Mol Cell Biol Lipids*, 158555
91. Debose-Boyd, R. A., and Horton, J. D. (2013) Opening up new fronts in the fight against cholesterol. *eLife* **2**, e00663
92. Gustafsen, C., Kjolby, M., Nyegaard, M., Mattheisen, M., Lundhede, J., Buttenschon, H., Mors, O., Bentzon, J. F., Madsen, P., Nykjaer, A., and Glerup, S. (2014) The Hypercholesterolemia-Risk Gene SORT1 Facilitates PCSK9 Secretion. *Cell Metab* **19**, 310-318
93. Hermey, G., Sjogaard, S. S., Petersen, C. M., Nykjaer, A., and Gliemann, J. (2006) Tumour necrosis factor alpha-converting enzyme mediates ectodomain shedding of Vps10p-domain receptor family members. *The Biochemical journal* **395**, 285-293
94. Butkinaree, C., Canuel, M., Essalmani, R., Poirier, S., Benjannet, S., Asselin, M. C., Roubtsova, A., Hamelin, J., Marcinkiewicz, J., Chamberland, A., Guillemot, J., Mayer, G., Sisodia, S. S., Jacob, Y., Prat, A., and Seidah, N. G. (2015) Amyloid Precursor-like Protein 2 and Sortilin Do Not Regulate the PCSK9 Convertase-mediated Low Density Lipoprotein Receptor Degradation but Interact with Each Other. *J Biol Chem* **290**, 18609-18620
95. McNutt, M. C., Lagace, T. A., and Horton, J. D. (2007) Catalytic activity is not required for secreted PCSK9 to reduce low density lipoprotein receptors in HepG2 cells. *The Journal of biological chemistry* **282**, 20799-20803
96. Gu, H. M., Adijiang, A., Mah, M., and Zhang, D. W. (2013) Characterization of the role of EGF-A of low density lipoprotein receptor in PCSK9 binding. *Journal of lipid research* **54**, 3345-3357
97. Zhang, D. W., Garuti, R., Tang, W. J., Cohen, J. C., and Hobbs, H. H. (2008) Structural requirements for PCSK9-mediated degradation of the low-density lipoprotein receptor. *Proc Natl Acad Sci U S A* **105**, 13045-13050
98. Zhang, Y., Zhou, L., Kong-Beltran, M., Li, W., Moran, P., Wang, J., Quan, C., Tom, J., Kolumam, G., Elliott, J. M., Skelton, N. J., Peterson, A. S., and Kirchhofer, D. (2012) Calcium-independent inhibition of PCSK9 by affinity-improved variants of the LDL receptor EGF(A) domain. *Journal of molecular biology* **422**, 685-696

99. Deng, S. J., Alabi, A., Gu, H. M., Adijiang, A., Qin, S., and Zhang, D. W. (2019) Identification of amino acid residues in the ligand binding repeats of LDL receptor important for PCSK9 binding. *Journal of lipid research* **60**, 516-527
100. Gustafsen, C., Olsen, D., Vilstrup, J., Lund, S., Reinhardt, A., Wellner, N., Larsen, T., Andersen, C. B. F., Weyer, K., Li, J. P., Seeberger, P. H., Thirup, S., Madsen, P., and Glerup, S. (2017) Heparan sulfate proteoglycans present PCSK9 to the LDL receptor. *Nature communications* **8**, 503
101. Galvan, A. M., and Chorba, J. S. (2019) Cell-associated heparin-like molecules modulate the ability of LDL to regulate PCSK9 uptake. *Journal of lipid research* **60**, 71-84
102. Nassoury, N., Blasiole, D. A., Tebon Oler, A., Benjannet, S., Hamelin, J., Poupon, V., McPherson, P. S., Attie, A. D., Prat, A., and Seidah, N. G. (2007) The cellular trafficking of the secretory proprotein convertase PCSK9 and its dependence on the LDLR. *Traffic* **8**, 718-732
103. Jang, H. D., Lee, S. E., Yang, J., Lee, H. C., Shin, D., Lee, H., Lee, J., Jin, S., Kim, S., Lee, S. J., You, J., Park, H. W., Nam, K. Y., Lee, S. H., Park, S. W., Kim, J. S., Kim, S. Y., Kwon, Y. W., Kwak, S. H., Yang, H. M., and Kim, H. S. (2019) Cyclase-associated protein 1 is a binding partner of proprotein convertase subtilisin/kexin type-9 and is required for the degradation of low-density lipoprotein receptors by proprotein convertase subtilisin/kexin type-9. *European heart journal*
104. Tveten, K., Holla, O. L., Cameron, J., Strom, T. B., Berge, K. E., Laerdahl, J. K., and Leren, T. P. (2012) Interaction between the ligand-binding domain of the LDL receptor and the C-terminal domain of PCSK9 is required for PCSK9 to remain bound to the LDL receptor during endosomal acidification. *Human molecular genetics* **21**, 1402-1409
105. Cunningham, D., Danley, D. E., Geoghegan, K. F., Griffor, M. C., Hawkins, J. L., Subashi, T. A., Varghese, A. H., Ammirati, M. J., Culp, J. S., Hoth, L. R., Mansour, M. N., McGrath, K. M., Seddon, A. P., Shenolikar, S., Stutzman-Engwall, K. J., Warren, L. C., Xia, D., and Qiu, X. (2007) Structural and biophysical studies of PCSK9 and its mutants linked to familial hypercholesterolemia. *Nature structural & molecular biology* **14**, 413-419
106. Lo Surdo, P., Bottomley, M. J., Calzetta, A., Settembre, E. C., Cirillo, A., Pandit, S., Ni, Y. G., Hubbard, B., Sitlani, A., and Carfi, A. (2011) Mechanistic implications for LDL receptor degradation from the PCSK9/LDLR structure at neutral pH. *EMBO reports* **12**, 1300-1305
107. Qian, Y. W., Schmidt, R. J., Zhang, Y., Chu, S., Lin, A., Wang, H., Wang, X., Beyer, T. P., Bensch, W. R., Li, W., Ehsani, M. E., Lu, D., Konrad, R. J., Eacho, P. I., Moller, D. E., Karathanasis, S. K., and Cao, G. (2007) Secreted PCSK9 downregulates low density lipoprotein receptor through receptor-mediated endocytosis. *Journal of lipid research* **48**, 1488-1498
108. Saavedra, Y. G., Day, R., and Seidah, N. G. (2012) The M2 module of the Cys-His-rich domain (CHRD) of PCSK9 protein is needed for the extracellular low-density lipoprotein receptor (LDLR) degradation pathway. *The Journal of biological chemistry* **287**, 43492-43501
109. Hampton, E. N., Knuth, M. W., Li, J., Harris, J. L., Lesley, S. A., and Spraggon, G. (2007) The self-inhibited structure of full-length PCSK9 at 1.9 A reveals structural

homology with resistin within the C-terminal domain. *Proc Natl Acad Sci U S A* **104**, 14604-14609
110. Kotowski, I. K., Pertsemlidis, A., Luke, A., Cooper, R. S., Vega, G. L., Cohen, J. C., and Hobbs, H. H. (2006) A spectrum of PCSK9 alleles contributes to plasma levels of low-density lipoprotein cholesterol. *American journal of human genetics* **78**, 410-422
111. Poirier, S., Hamouda, H. A., Villeneuve, L., Demers, A., and Mayer, G. (2016) Trafficking Dynamics of PCSK9-Induced LDLR Degradation: Focus on Human PCSK9 Mutations and C-Terminal Domain. *PloS one* **11**, e0157230
112. Holla, O. L., Cameron, J., Tveten, K., Strom, T. B., Berge, K. E., Laerdahl, J. K., and Leren, T. P. (2011) Role of the C-terminal domain of PCSK9 in degradation of the LDL receptors. *Journal of lipid research* **52**, 1787-1794
113. Poirier, S., Mamarbachi, M., Chen, W. T., Lee, A. S., and Mayer, G. (2015) GRP94 Regulates Circulating Cholesterol Levels through Blockade of PCSK9-Induced LDLR Degradation. *Cell reports* **13**, 2064-2071
114. Poirier, S., Mayer, G., Poupon, V., McPherson, P. S., Desjardins, R., Ly, K., Asselin, M. C., Day, R., Duclos, F. J., Witmer, M., Parker, R., Prat, A., and Seidah, N. G. (2009) Dissection of the endogenous cellular pathways of PCSK9-induced low density lipoprotein receptor degradation: evidence for an intracellular route. *The Journal of biological chemistry* **284**, 28856-28864
115. Sabatine, M. S., Giugliano, R. P., Keech, A. C., Honarpour, N., Wiviott, S. D., Murphy, S. A., Kuder, J. F., Wang, H., Liu, T., Wasserman, S. M., Sever, P. S., Pedersen, T. R., Committee, F. S., and Investigators. (2017) Evolocumab and Clinical Outcomes in Patients with Cardiovascular Disease. *The New England journal of medicine* **376**, 1713-1722
116. Schwartz, G. G., Steg, P. G., Szarek, M., Bhatt, D. L., Bittner, V. A., Diaz, R., Edelberg, J. M., Goodman, S. G., Hanotin, C., Harrington, R. A., Jukema, J. W., Lecorps, G., Mahaffey, K. W., Moryusef, A., Pordy, R., Quintero, K., Roe, M. T., Sasiela, W. J., Tamby, J. F., Tricoci, P., White, H. D., Zeiher, A. M., Committees, O. O., and Investigators. (2018) Alirocumab and Cardiovascular Outcomes after Acute Coronary Syndrome. *The New England journal of medicine* **379**, 2097-2107
117. Raal, F. J., Honarpour, N., Blom, D. J., Hovingh, G. K., Xu, F., Scott, R., Wasserman, S. M., Stein, E. A., and Investigators, T. (2015) Inhibition of PCSK9 with evolocumab in homozygous familial hypercholesterolaemia (TESLA Part B): a randomised, double-blind, placebo-controlled trial. *Lancet* **385**, 341-350
118. Giugliano, R. P., Pedersen, T. R., Park, J. G., De Ferrari, G. M., Gaciong, Z. A., Ceska, R., Toth, K., Gouni-Berthold, I., Lopez-Miranda, J., Schiele, F., Mach, F., Ott, B. R., Kanevsky, E., Pineda, A. L., Somaratne, R., Wasserman, S. M., Keech, A. C., Sever, P. S., Sabatine, M. S., and Investigators, F. (2017) Clinical efficacy and safety of achieving very low LDL-cholesterol concentrations with the PCSK9 inhibitor evolocumab: a prespecified secondary analysis of the FOURIER trial. *Lancet* **390**, 1962-1971
119. Fitzgerald, K., White, S., Borodovsky, A., Bettencourt, B. R., Strahs, A., Clausen, V., Wijngaard, P., Horton, J. D., Taubel, J., Brooks, A., Fernando, C., Kauffman, R. S., Kallend, D., Vaishnaw, A., and Simon, A. (2017) A Highly Durable RNAi Therapeutic Inhibitor of PCSK9. *The New England journal of medicine* **376**, 41-51
120. Ray, K. K., Landmesser, U., Leiter, L. A., Kallend, D., Dufour, R., Karakas, M., Hall, T., Troquay, R. P., Turner, T., Visseren, F. L., Wijngaard, P., Wright, R. S., and

Kastelein, J. J. (2017) Inclisiran in Patients at High Cardiovascular Risk with Elevated LDL Cholesterol. *The New England journal of medicine* **376**, 1430-1440
121. Chadwick, A. C., Wang, X., and Musunuru, K. (2017) In Vivo Base Editing of PCSK9 (Proprotein Convertase Subtilisin/Kexin Type 9) as a Therapeutic Alternative to Genome Editing. *Arteriosclerosis, thrombosis, and vascular biology* **37**, 1741-1747
122. Kawakami, R., Nozato, Y., Nakagami, H., Ikeda, Y., Shimamura, M., Yoshida, S., Sun, J., Kawano, T., Takami, Y., Noma, T., Rakugi, H., Minamino, T., and Morishita, R. (2018) Development of vaccine for dyslipidemia targeted to a proprotein convertase subtilisin/kexin type 9 (PCSK9) epitope in mice. *PloS one* **13**, e0191895
123. Cameron, J., Holla, O. L., Laerdahl, J. K., Kulseth, M. A., Berge, K. E., and Leren, T. P. (2009) Mutation S462P in the PCSK9 gene reduces secretion of mutant PCSK9 without affecting the autocatalytic cleavage. *Atherosclerosis* **203**, 161-165
124. Chorba, J. S., Galvan, A. M., and Shokat, K. M. (2018) Stepwise processing analyses of the single-turnover PCSK9 protease reveal its substrate sequence specificity and link clinical genotype to lipid phenotype. *J Biol Chem* **293**, 1875-1886
125. Du, F., Hui, Y., Zhang, M., Linton, M. F., Fazio, S., and Fan, D. (2011) Novel domain interaction regulates secretion of proprotein convertase subtilisin/kexin type 9 (PCSK9) protein. *The Journal of biological chemistry* **286**, 43054-43061
126. Lagace, T. A., Curtis, D. E., Garuti, R., McNutt, M. C., Park, S. W., Prather, H. B., Anderson, N. N., Ho, Y. K., Hammer, R. E., and Horton, J. D. (2006) Secreted PCSK9 decreases the number of LDL receptors in hepatocytes and in livers of parabiotic mice. *The Journal of clinical investigation* **116**, 2995-3005
127. Gu, H. M., Adijiang, A., Mah, M., and Zhang, D. W. (2013) Characterization of the role of EGF-A of low-density lipoprotein receptor in PCSK9 binding. *J Lipid Res* **54**, 3345-3357
128. Gu, H. M., Li, G., Gao, X., Berthiaume, L. G., and Zhang, D. W. (2013) Characterization of palmitoylation of ATP binding cassette transporter G1: effect on protein trafficking and function. *Biochim Biophys Acta* **1831**, 1067-1078
129. Gu, H. M., Wang, F., Alabi, A., Deng, S., Qin, S., and Zhang, D. W. (2016) Identification of an Amino Acid Residue Critical for Plasma Membrane Localization of ATP-Binding Cassette Transporter G1. *Arterioscler Thromb Vasc Biol* **36**, 253-255
130. Stephan, Z. F., and Yurachek, E. C. (1993) Rapid fluorometric assay of LDL receptor activity by DiI-labeled LDL. *J Lipid Res* **34**, 325-330
131. Fisher, T. S., Lo Surdo, P., Pandit, S., Mattu, M., Santoro, J. C., Wisniewski, D., Cummings, R. T., Calzetta, A., Cubbon, R. M., Fischer, P. A., Tarachandani, A., De Francesco, R., Wright, S. D., Sparrow, C. P., Carfi, A., and Sitlani, A. (2007) Effects of pH and low density lipoprotein (LDL) on PCSK9-dependent LDL receptor regulation. *The Journal of biological chemistry* **282**, 20502-20512
132. Koornneef, A., Maczuga, P., van Logtenstein, R., Borel, F., Blits, B., Ritsema, T., van Deventer, S., Petry, H., and Konstantinova, P. (2011) Apolipoprotein B knockdown by AAV-delivered shRNA lowers plasma cholesterol in mice. *Mol Ther* **19**, 731-740
133. Borel, F., Kay, M. A., and Mueller, C. (2014) Recombinant AAV as a platform for translating the therapeutic potential of RNA interference. *Molecular therapy : the journal of the American Society of Gene Therapy* **22**, 692-701
134. Folsom, A. R., Peacock, J. M., and Boerwinkle, E. (2009) Variation in PCSK9, low LDL cholesterol, and risk of peripheral arterial disease. *Atherosclerosis* **202**, 211-215

135. Ray, K. K., Stoekenbroek, R. M., Kallend, D., Leiter, L. A., Landmesser, U., Wright, R. S., Wijngaard, P., and Kastelein, J. J. P. (2018) Effect of an siRNA Therapeutic Targeting PCSK9 on Atherogenic Lipoproteins. *Circulation* **138**, 1304-1316
136. Szarek, M., White, H. D., Schwartz, G. G., Alings, M., Bhatt, D. L., Bittner, V. A., Chiang, C. E., Diaz, R., Edelberg, J. M., Goodman, S. G., Hanotin, C., Harrington, R. A., Jukema, J. W., Kimura, T., Kiss, R. G., Lecorps, G., Mahaffey, K. W., Moryusef, A., Pordy, R., Roe, M. T., Tricoci, P., Xavier, D., Zeiher, A. M., Steg, P. G., Committees, O. O., and Investigators. (2018) Alirocumab Reduces Total Nonfatal Cardiovascular and Fatal Events in the ODYSSEY OUTCOMES Trial. *J Am Coll Cardiol*
137. Sabatine, M. S., De Ferrari, G. M., Giugliano, R. P., Huber, K., Lewis, B. S., Ferreira, J., Kuder, J. F., Murphy, S. A., Wiviott, S. D., Kurtz, C. E., Honarpour, N., Keech, A. C., Sever, P. S., and Pedersen, T. R. (2018) Clinical Benefit of Evolocumab by Severity and Extent of Coronary Artery Disease: An Analysis from FOURIER. *Circulation*
138. McNutt, M. C., Kwon, H. J., Chen, C., Chen, J. R., Horton, J. D., and Lagace, T. A. (2009) Antagonism of secreted PCSK9 increases low-density lipoprotein receptor expression in HEPG2 cells. *J Biol Chem* **284**, 10561-10570
139. Kwon, H. J., Lagace, T. A., McNutt, M. C., Horton, J. D., and Deisenhofer, J. (2008) Molecular basis for LDL receptor recognition by PCSK9. *Proceedings of the National Academy of Sciences of the United States of America* **105**, 1820-1825
140. Bottomley, M. J., Cirillo, A., Orsatti, L., Ruggeri, L., Fisher, T. S., Santoro, J. C., Cummings, R. T., Cubbon, R. M., Lo Surdo, P., Calzetta, A., Noto, A., Baysarowich, J., Mattu, M., Talamo, F., De Francesco, R., Sparrow, C. P., Sitlani, A., and Carfi, A. (2009) Structural and biochemical characterization of the wild type PCSK9-EGF(AB) complex and natural familial hypercholesterolemia mutants. *J Biol Chem* **284**, 1313-1323
141. Yamamoto, T., Lu, C., and Ryan, R. O. (2011) A two-step binding model of PCSK9 interaction with the low density lipoprotein receptor. *J Biol Chem* **286**, 5464-5470
142. Surdo, P. L., Bottomley, M. J., Calzetta, A., Settembre, E. C., Cirillo, A., Pandit, S., Ni, Y. G., Hubbard, B., Sitlani, A., and Carfi, A. (2011) Mechanistic implications for LDL receptor degradation from the PCSK9/LDLR structure at neutral pH. *EMBO Rep* **12**, 1300-1305
143. Seidah, N. G. (2016) New developments in proprotein convertase subtilisin-kexin 9's biology and clinical implications. *Curr Opin Lipidol* **27**, 274-281
144. Lagace, T. A. (2014) PCSK9 and LDLR degradation: regulatory mechanisms in circulation and in cells. *Curr Opin Lipidol* **25**, 387-393
145. Grefhorst, A., McNutt, M. C., Lagace, T. A., and Horton, J. D. (2008) Plasma PCSK9 preferentially reduces liver LDL receptors in mice. *J Lipid Res* **49**, 1303-1311
146. Miller, E., Antonny, B., Hamamoto, S., and Schekman, R. (2002) Cargo selection into COPII vesicles is driven by the Sec24p subunit. *The EMBO journal* **21**, 6105-6113
147. Wendeler, M. W., Paccaud, J. P., and Hauri, H. P. (2007) Role of Sec24 isoforms in selective export of membrane proteins from the endoplasmic reticulum. *EMBO Rep* **8**, 258-264
148. Lipari, M. T., Li, W., Moran, P., Kong-Beltran, M., Sai, T., Lai, J., Lin, S. J., Kolumam, G., Zavala-Solorio, J., Izrael-Tomasevic, A., Arnott, D., Wang, J., Peterson, A. S., and Kirchhofer, D. (2012) Furin-cleaved proprotein convertase subtilisin/kexin

type 9 (PCSK9) is active and modulates low density lipoprotein receptor and serum cholesterol levels. *J Biol Chem* **287**, 43482-43491
149. Lambert, G., Ancellin, N., Charlton, F., Comas, D., Pilot, J., Keech, A., Patel, S., Sullivan, D. R., Cohn, J. S., Rye, K. A., and Barter, P. J. (2008) Plasma PCSK9 concentrations correlate with LDL and total cholesterol in diabetic patients and are decreased by fenofibrate treatment. *Clin Chem* **54**, 1038-1045
150. Mayne, J., Raymond, A., Chaplin, A., Cousins, M., Kaefer, N., Gyamera-Acheampong, C., Seidah, N. G., Mbikay, M., Chretien, M., and Ooi, T. C. (2007) Plasma PCSK9 levels correlate with cholesterol in men but not in women. *Biochem Biophys Res Commun* **361**, 451-456
151. Huijgen, R., Fouchier, S. W., Denoun, M., Hutten, B. A., Vissers, M. N., Lambert, G., and Kastelein, J. J. (2012) Plasma levels of PCSK9 and phenotypic variability in familial hypercholesterolemia. *J Lipid Res* **53**, 979-983
152. Cameron, J., Holla, O. L., Ranheim, T., Kulseth, M. A., Berge, K. E., and Leren, T. P. (2006) Effect of mutations in the PCSK9 gene on the cell surface LDL receptors. *Hum Mol Genet* **15**, 1551-1558
153. Fasano, T., Cefalu, A. B., Di Leo, E., Noto, D., Pollaccia, D., Bocchi, L., Valenti, V., Bonardi, R., Guardamagna, O., Averna, M., and Tarugi, P. (2007) A novel loss of function mutation of PCSK9 gene in white subjects with low-plasma low-density lipoprotein cholesterol. *Arterioscler Thromb Vasc Biol* **27**, 677-681
154. Ruotolo, A., Di Taranto, M. D., D'Agostino, M. N., Marotta, G., Gentile, M., Nunziata, M., Sodano, M., Di Noto, R., Del Vecchio, L., Rubba, P., and Fortunato, G. (2014) The novel variant p.Ser465Leu in the PCSK9 gene does not account for the decreased LDLR activity in members of a FH family. *Clin Chem Lab Med* **52**, e175-178
155. Homer, V. M., Marais, A. D., Charlton, F., Laurie, A. D., Hurndell, N., Scott, R., Mangili, F., Sullivan, D. R., Barter, P. J., Rye, K. A., George, P. M., and Lambert, G. (2008) Identification and characterization of two non-secreted PCSK9 mutants associated with familial hypercholesterolemia in cohorts from New Zealand and South Africa. *Atherosclerosis* **196**, 659-666
156. Lakoski, S. G., Lagace, T. A., Cohen, J. C., Horton, J. D., and Hobbs, H. H. (2009) Genetic and metabolic determinants of plasma PCSK9 levels. *J Clin Endocrinol Metab* **94**, 2537-2543
157. Martinez-Menarguez, J. A., Geuze, H. J., Slot, J. W., and Klumperman, J. (1999) Vesicular tubular clusters between the ER and Golgi mediate concentration of soluble secretory proteins by exclusion from COPI-coated vesicles. *Cell* **98**, 81-90
158. Szul, T., and Sztul, E. (2011) COPII and COPI traffic at the ER-Golgi interface. *Physiology (Bethesda)* **26**, 348-364
159. Nyfeler, B., Reiterer, V., Wendeler, M. W., Stefan, E., Zhang, B., Michnick, S. W., and Hauri, H. P. (2008) Identification of ERGIC-53 as an intracellular transport receptor of alpha1-antitrypsin. *J Cell Biol* **180**, 705-712
160. Strating, J. R., Hafmans, T. G., and Martens, G. J. (2009) Functional diversity among p24 subfamily members. *Biol Cell* **101**, 207-219
161. Neve, E. P., Svensson, K., Fuxe, J., and Pettersson, R. F. (2003) VIPL, a VIP36-like membrane protein with a putative function in the export of glycoproteins from the endoplasmic reticulum. *Exp Cell Res* **288**, 70-83

162. Lloyd-Jones, D. M., Wilson, P. W., Larson, M. G., Leip, E., Beiser, A., D'Agostino, R. B., Cleeman, J. I., and Levy, D. (2003) Lifetime risk of coronary heart disease by cholesterol levels at selected ages. *Arch Intern Med* **163**, 1966-1972
163. Goldstein, J. L., and Brown, M. S. (2015) A century of cholesterol and coronaries: from plaques to genes to statins. *Cell* **161**, 161-172
164. Goldstein, J. L., and Brown, M. S. (2009) The LDL receptor. *Arteriosclerosis, thrombosis, and vascular biology* **29**, 431-438
165. Russell, D. W., Brown, M. S., and Goldstein, J. L. (1989) Different combinations of cysteine-rich repeats mediate binding of low density lipoprotein receptor to two different proteins. *J Biol Chem* **264**, 21682-21688
166. Ishibashi, S., Brown, M. S., Goldstein, J. L., Gerard, R. D., Hammer, R. E., and Herz, J. (1993) Hypercholesterolemia in low density lipoprotein receptor knockout mice and its reversal by adenovirus-mediated gene delivery. *J Clin Invest* **92**, 883-893
167. Guttman, M., and Komives, E. A. (2011) The structure, dynamics, and binding of the LA45 module pair of the low-density lipoprotein receptor suggest an important role for LA4 in ligand release. *Biochemistry* **50**, 11001-11008
168. Cummings, R. D., Kornfeld, S., Schneider, W. J., Hobgood, K. K., Tolleshaug, H., Brown, M. S., and Goldstein, J. L. (1983) Biosynthesis of N- and O-linked oligosaccharides of the low density lipoprotein receptor. *The Journal of biological chemistry* **258**, 15261-15273
169. Filipovic, I. (1989) Effect of inhibiting N-glycosylation on the stability and binding activity of the low density lipoprotein receptor. *J Biol Chem* **264**, 8815-8820
170. Fass, D., Blacklow, S., Kim, P. S., and Berger, J. M. (1997) Molecular basis of familial hypercholesterolaemia from structure of LDL receptor module. *Nature* **388**, 691-693
171. Hobbs, H. H., Brown, M. S., and Goldstein, J. L. (1992) Molecular genetics of the LDL receptor gene in familial hypercholesterolemia. *Human mutation* **1**, 445-466
172. Loubser, O., Marais, A. D., Kotze, M. J., Godenir, N., Thiart, R., Scholtz, C. L., de Villiers, J. N., Hillermann, R., Firth, J. C., Weich, H. F., Maritz, F., Jones, S., and van der Westhuyzen, D. R. (1999) Founder mutations in the LDL receptor gene contribute significantly to the familial hypercholesterolemia phenotype in the indigenous South African population of mixed ancestry. *Clin Genet* **55**, 340-345
173. Fouchier, S. W., Defesche, J. C., Umans-Eckenhausen, M. W., and Kastelein, J. P. (2001) The molecular basis of familial hypercholesterolemia in The Netherlands. *Hum Genet* **109**, 602-615
174. Hattori, H., Hirayama, T., Nobe, Y., Nagano, M., Kujiraoka, T., Egashira, T., Ishii, J., Tsuji, M., and Emi, M. (2002) Eight novel mutations and functional impairments of the LDL receptor in familial hypercholesterolemia in the north of Japan. *J Hum Genet* **47**, 80-87
175. Beglova, N., Jeon, H., Fisher, C., and Blacklow, S. C. (2004) Cooperation between fixed and low pH-inducible interfaces controls lipoprotein release by the LDL receptor. *Mol Cell* **16**, 281-292
176. Leigh, S., Futema, M., Whittall, R., Taylor-Beadling, A., Williams, M., den Dunnen, J. T., and Humphries, S. E. (2017) The UCL low-density lipoprotein receptor gene variant database: pathogenicity update. *J Med Genet* **54**, 217-223
177. Pena, F., Jansens, A., van Zadelhoff, G., and Braakman, I. (2010) Calcium as a crucial cofactor for low density lipoprotein receptor folding in the endoplasmic reticulum. *J Biol Chem* **285**, 8656-8664

178. Ly, K., Essalmani, R., Desjardins, R., Seidah, N. G., and Day, R. (2016) An Unbiased Mass Spectrometry Approach Identifies Glypican-3 as an Interactor of Proprotein Convertase Subtilisin/Kexin Type 9 (PCSK9) and LDL Receptor in Hepatocellular Carcinoma Cells. *J Biol Chem*
179. Ly, K., Saavedra, Y. G., Canuel, M., Routhier, S., Desjardins, R., Hamelin, J., Mayne, J., Lazure, C., Seidah, N. G., and Day, R. (2014) Annexin A2 reduces PCSK9 protein levels via a translational mechanism and interacts with the M1 and M2 domains of PCSK9. *J Biol Chem* **289**, 17732-17746
180. Tada, H., Kawashiri, M. A., Yoshida, T., Teramoto, R., Nohara, A., Konno, T., Inazu, A., Mabuchi, H., Yamagishi, M., and Hayashi, K. (2016) Lipoprotein(a) in Familial Hypercholesterolemia With Proprotein Convertase Subtilisin/Kexin Type 9 (PCSK9) Gain-of-Function Mutations. *Circulation journal : official journal of the Japanese Circulation Society* **80**, 512-518
181. Hopkins, P. N., Defesche, J., Fouchier, S. W., Bruckert, E., Luc, G., Cariou, B., Sjouke, B., Leren, T. P., Harada-Shiba, M., Mabuchi, H., Rabes, J. P., Carrie, A., van Heyningen, C., Carreau, V., Farnier, M., Teoh, Y. P., Bourbon, M., Kawashiri, M. A., Nohara, A., Soran, H., Marais, A. D., Tada, H., Abifadel, M., Boileau, C., Chanu, B., Katsuda, S., Kishimoto, I., Lambert, G., Makino, H., Miyamoto, Y., Pichelin, M., Yagi, K., Yamagishi, M., Zair, Y., Mellis, S., Yancopoulos, G. D., Stahl, N., Mendoza, J., Du, Y., Hamon, S., Krempf, M., and Swergold, G. D. (2015) Characterization of Autosomal Dominant Hypercholesterolemia Caused by PCSK9 Gain of Function Mutations and Its Specific Treatment With Alirocumab, a PCSK9 Monoclonal Antibody. *Circulation. Cardiovascular genetics* **8**, 823-831
182. Cohen, J. C., Boerwinkle, E., Mosley, T. H., Jr., and Hobbs, H. H. (2006) Sequence variations in PCSK9, low LDL, and protection against coronary heart disease. *The New England journal of medicine* **354**, 1264-1272
183. Raal, F. J., Stein, E. A., Dufour, R., Turner, T., Civeira, F., Burgess, L., Langslet, G., Scott, R., Olsson, A. G., Sullivan, D., Hovingh, G. K., Cariou, B., Gouni-Berthold, I., Somaratne, R., Bridges, I., Scott, R., Wasserman, S. M., Gaudet, D., and Investigators, R.-. (2015) PCSK9 inhibition with evolocumab (AMG 145) in heterozygous familial hypercholesterolaemia (RUTHERFORD-2): a randomised, double-blind, placebo-controlled trial. *Lancet* **385**, 331-340
184. Stein, E. A., Giugliano, R. P., Koren, M. J., Raal, F. J., Roth, E. M., Weiss, R., Sullivan, D., Wasserman, S. M., Somaratne, R., Kim, J. B., Yang, J., Liu, T., Albizem, M., Scott, R., Sabatine, M. S., and Investigators, P. (2014) Efficacy and safety of evolocumab (AMG 145), a fully human monoclonal antibody to PCSK9, in hyperlipidaemic patients on various background lipid therapies: pooled analysis of 1359 patients in four phase 2 trials. *European heart journal* **35**, 2249-2259
185. Lambert, G., Chatelais, M., Petrides, F., Passard, M., Thedrez, A., Rye, K. A., Schwahn, U., Gusarova, V., Blom, D. J., Sasiela, W., and Marais, A. D. (2014) Normalization of low-density lipoprotein receptor expression in receptor defective homozygous familial hypercholesterolemia by inhibition of PCSK9 with alirocumab. *Journal of the American College of Cardiology* **64**, 2299-2300
186. Lefrancois, S., Zeng, J., Hassan, A. J., Canuel, M., and Morales, C. R. (2003) The lysosomal trafficking of sphingolipid activator proteins (SAPs) is mediated by sortilin. *The EMBO journal* **22**, 6430-6437

187. Hiraiwa, M., Martin, B. M., Kishimoto, Y., Conner, G. E., Tsuji, S., and O'Brien, J. S. (1997) Lysosomal proteolysis of prosaposin, the precursor of saposins (sphingolipid activator proteins): its mechanism and inhibition by ganglioside. *Archives of biochemistry and biophysics* **341**, 17-24
188. Meyer, R. C., Giddens, M. M., Coleman, B. M., and Hall, R. A. (2014) The protective role of prosaposin and its receptors in the nervous system. *Brain research* **1585**, 1-12
189. Azuma, N., Seo, H. C., Lie, O., Fu, Q., Gould, R. M., Hiraiwa, M., Burt, D. W., Paton, I. R., Morrice, D. R., O'Brien, J. S., and Kishimoto, Y. (1998) Cloning, expression and map assignment of chicken prosaposin. *The Biochemical journal* **330 (Pt 1)**, 321-327
190. Fujita, N., Suzuki, K., Vanier, M. T., Popko, B., Maeda, N., Klein, A., Henseler, M., Sandhoff, K., Nakayasu, H., and Suzuki, K. (1996) Targeted disruption of the mouse sphingolipid activator protein gene: a complex phenotype, including severe leukodystrophy and wide-spread storage of multiple sphingolipids. *Human molecular genetics* **5**, 711-725
191. Motta, M., Tatti, M., Furlan, F., Celato, A., Di Fruscio, G., Polo, G., Manara, R., Nigro, V., Tartaglia, M., Burlina, A., and Salvioli, R. (2016) Clinical, biochemical and molecular characterization of prosaposin deficiency. *Clinical genetics* **90**, 220-229
192. Kuchar, L., Ledvinova, J., Hrebicek, M., Myskova, H., Dvorakova, L., Berna, L., Chrastina, P., Asfaw, B., Elleder, M., Petermoller, M., Mayrhofer, H., Staudt, M., Krageloh-Mann, I., Paton, B. C., and Harzer, K. (2009) Prosaposin deficiency and saposin B deficiency (activator-deficient metachromatic leukodystrophy): report on two patients detected by analysis of urinary sphingolipids and carrying novel PSAP gene mutations. *American journal of medical genetics. Part A* **149A**, 613-621
193. Hiraiwa, M., Campana, W. M., Mizisin, A. P., Mohiuddin, L., and O'Brien, J. S. (1999) Prosaposin: A myelinotrophic protein that promotes expression of myelin constituents and is secreted after nerve injury. *Glia* **26**, 353-360
194. Meyer, R. C., Giddens, M. M., Schaefer, S. A., and Hall, R. A. (2013) GPR37 and GPR37L1 are receptors for the neuroprotective and glioprotective factors prosaptide and prosaposin. *Proceedings of the National Academy of Sciences of the United States of America* **110**, 9529-9534
195. Zhou, X., Sun, L., Bastos de Oliveira, F., Qi, X., Brown, W. J., Smolka, M. B., Sun, Y., and Hu, F. (2015) Prosaposin facilitates sortilin-independent lysosomal trafficking of progranulin. *The Journal of cell biology* **210**, 991-1002
196. Ly, K., Essalmani, R., Desjardins, R., Seidah, N. G., and Day, R. (2016) An Unbiased Mass Spectrometry Approach Identifies Glypican-3 as an Interactor of Proprotein Convertase Subtilisin/Kexin Type 9 (PCSK9) and Low Density Lipoprotein Receptor (LDLR) in Hepatocellular Carcinoma Cells. *The Journal of biological chemistry* **291**, 24676-24687
197. Bartz, F., Kern, L., Erz, D., Zhu, M., Gilbert, D., Meinhof, T., Wirkner, U., Erfle, H., Muckenthaler, M., Pepperkok, R., and Runz, H. (2009) Identification of cholesterol-regulating genes by targeted RNAi screening. *Cell metabolism* **10**, 63-75
198. Carvelli, L., Libin, Y., and Morales, C. R. (2015) Prosaposin: a protein with differential sorting and multiple functions. *Histology and histopathology* **30**, 647-660